

**ANALYSIS OF HISTORIC AERIAL PHOTOGRAPHS FOR ECOLOGICAL
MANAGEMENT USING OBJECT-BASED APPROACHES**

by

JESSICA LINDSAY MORGAN

B.Sc., University of Calgary, 2006

A THESIS SUBMITTED IN PARTIAL FULFILLMENT OF
THE REQUIREMENTS FOR THE DEGREE OF

MASTER OF SCIENCE

in

THE FACULTY OF GRADUATE STUDIES

(Forestry)

THE UNIVERSITY OF BRITISH COLUMBIA

(Vancouver)

September 2009

© Jessica Lindsay Morgan, 2009

ABSTRACT

Aerial photographs are a crucial tool for ecological monitoring and management. New approaches for aerial photograph analysis are needed because of several existing (and anticipated) challenges associated with traditional analysis techniques. The goal of this thesis is to provide a synthesis of the valuable, and often unique, ecological information available from aerial photographs, and to explore the utility of novel image analysis approaches to extract this information. This research is organized to reflect the future of aerial photography as a discipline. In chapter two, I review the benefits and challenges of using aerial photographs for ecological management. The traditional framework used to classify aerial photographs, as well as sources of error are described within the context of the diverse ecological questions that can be addressed using aerial photography. The need for new approaches to analyze aerial photographs is emphasized throughout this chapter. In chapter three, I compare manual interpretation to an automated approach (combining object-based analysis and classification tree modeling), for five classification schemes routinely used in British Columbia. Automated approaches hold potential for replicating certain aspects of the manual process (such as the delineation of polygons), as automated and manually-delineated objects display few statistical differences. Automated classification accuracy is highly variable, with individual class accuracies ranging from 0 – 74%; however the overall accuracy of several classification schemes exceeded 60%, suggesting certain schemes are well suited to automated analysis. In chapter four, object-based analysis is applied to historic aerial photographs to better quantify spatial heterogeneity, a concept fundamental to the field of landscape ecology. My results suggest sixteen independent factors are needed to describe baseline levels of landscape heterogeneity, including several factors not previously identified by the discipline of landscape ecology. Lastly, in Chapter five, the significance of this thesis for resource management, remote sensing, and landscape ecology is highlighted. Further avenues of research are also discussed.

TABLE OF CONTENTS

ABSTRACT	ii
TABLE OF CONTENTS	iii
LIST OF TABLES	v
LIST OF FIGURES	vii
ACKNOWLEDGEMENTS	ix
CO-AUTHORSHIP STATEMENT	x
1 INTRODUCTION	1
1.1 The Role of Aerial Photography within Ecology	1
1.2 Remote Sensing Challenges for Aerial Photograph Analysis	2
1.3 New Approaches for Aerial Photograph Analysis	3
1.4 Historic Landscape Heterogeneity	4
1.5 Research Objectives	6
1.6 References	7
2 AERIAL PHOTOGRAPHY: A RAPIDLY EVOLVING TOOL FOR ECOLOGICAL MANAGEMENT	11
2.1 Introduction	11
2.2 Aerial Photography Basics	14
2.3 Digitization of Aerial Photographs	17
2.4 Overview of Basic Photographic Errors	19
2.5 Error Correction	21
2.6 Aerial Photograph Interpretation	22
2.6.1 Tone/Color	26
2.6.2 Size	26
2.6.3 Shape	27
2.6.4 Texture	28
2.6.5 Pattern	28
2.6.6 Shadow	29
2.6.7 Site and Context	30
2.7 New Approaches for Aerial Photograph Analysis	31
2.8 Accuracy Assessment	34
2.9 Conclusions	37
2.10 References	39
3 A COMPARISON OF MANUAL AND AUTOMATED APPROACHES FOR CLASSIFICATION OF DIGITAL AERIAL PHOTOGRAPHS	46
3.1 Introduction	46
3.2 Methods	48
3.2.1 Study Area and Spatial Data	48
3.2.2 Manual Interpretation	50
3.2.3 Automated Object Creation	51
3.2.4 Comparison of Manually-delineated Polygons and Segmented Objects	55
3.2.5 Automated Object Classification	57
3.3 Results	58
3.3.1 Comparison of Object and Polygon Characteristics	58
3.3.2 Comparative Accuracy of the Five Classification Schemes	60
3.4 Discussion	67
3.4.1 Object Creation	67
3.4.2 Object Classification	68

3.5 Future Work and Conclusions	70
3.6 References	72
4 QUANTIFYING LANDSCAPE HETEROGENEITY FROM HISTORIC AERIAL PHOTOGRAPHS USING OBJECT-BASED ANALYSIS	77
4.1 Introduction	77
4.2 Methods	80
4.2.1 Study Area	80
4.2.2 Spatial Data	80
4.2.3 Object-based Analysis	84
4.2.4 Statistical Analysis	88
4.3 Results	90
4.4 Discussion	94
4.4.1 Quantitative description of spatial landscape heterogeneity	94
4.4.2 Heterogeneity over landscapes with different structure	96
4.4.3 Object-based analysis as a landscape analysis tool	97
4.5 Significance	99
4.6 References	101
5 CONCLUSION	106
5.1 Research Summary and Implications	106
5.2 Future Research	107
5.3 References	110
APPENDICES	112
Appendix A	112
Appendix B	113
Appendix C	114
Appendix D	118

LIST OF TABLES

Table 2.1 Comparative advantages and disadvantages associated with traditional film-based aerial photography, digital aerial photographs, and satellite imagery.	12
Table 2.2 Relationship between scanner resolution and ground resolution for multiple scales of aerial photography. Adapted from (Jensen 2000) p. 111. For example, a 1:20,000 photograph scanned at 1200dpi, will result in a digital image with a spatial resolution (pixel size) of 0.42m. A brief description of common mapping units and general uses of each scale is included.	18
Table 2.3 Common errors associated with the use of aerial photographs. Adapted from (Paine and Kiser 2003) p. 35.	20
Table 2.4 The eight primary aerial photograph characteristics used in manual interpretation, related ecological features, and examples of corresponding digital methods which may also be useful for analysis of these attributes.	24
Table 2.5 Comparative advantages and disadvantages of manual aerial photograph interpretation, conventional pixel-based analysis, and object-based classification methods.	32
Table 3.1 Five classification schemes as used within the Vegetation Resources Inventory in British Columbia (Province of British Columbia 2002). Note: For polygons marked none, the absence of forest cover, shadows or other interfering factors impeded classification.	52
Table 3.2 Comparison of 30 characteristics for objects derived from an automated segmentation and manual interpretation over three spatial scales. The percentage (%) of landscapes (N = 8) in which the segmented objects were statistically similar to the manually-delineated polygons are shown. Percentages less than 50% are shown in bold, indicating polygon characteristics not well mimicked by the automated approach.	59
Table 3.3 Totaled accuracy assessment results summarized over all eight landscapes for the Leading Species classification scheme (defined in Table 3.1).	61
Table 3.4 Totaled accuracy assessment results summarized over all eight landscapes for the Vertical Complexity classification scheme (defined in Table 3.1).	61
Table 3.5 Totaled accuracy assessment results summarized over all eight landscapes for the Site Productivity classification scheme (defined in Table 3.1).	62
Table 3.6 Totaled accuracy assessment results summarized over all eight landscapes for the Site Position classification scheme (defined in Table 3.1).	62
Table 3.7 Totaled accuracy assessment results summarized over all eight landscapes for the Surface Expression classification scheme (defined in Table 3.1).	63

Table 3.8 Variables of importance for class differentiation within the five classification schemes (as defined by models built using a combined dataset), and the overall accuracy of each model.	64
Table 4.1 Input layers used in the segmentation process to create objects and define landscape heterogeneity.	83
Table 4.2 The scale hierarchy selected for all eight landscapes based on the trends in minimum object size and number of objects (shown in Figure 4.3). Associated size statistics (averaged over all eight landscapes) and the biophysical features they are meant to represent are described. Examples of images segmented using this scale hierarchy are shown in Figure 4.2.	86
Table 4.3 The sixteen elements (clusters) identified as important for describing baseline landscape heterogeneity. The object-based metrics with the highest loadings for factors within each element and the potential ecological relevance of each element is included. ...	91
Table 4.4 The sixteen elements (clusters) identified over all landscapes, along with their universality (percentage the element is present over all landscapes), strength (average eigenvalue and % variance explained), and consistency (average Pearson’s absolute pair-wise correlation).	92
Table 4.5 Universal elements (clusters) identified for riparian and upland landscapes, listed in order of average % variance explained. Also shown is the consistency (average Pearson’s absolute pair-wise correlation) of the elements within each landscape type.	93

LIST OF FIGURES

- Figure 2.1 Aerial photograph subsets: a. Darker tree species near water are coniferous (*Tsuga heterophylla*); lighter tree species are deciduous (*Alnus rubra*). b. Yellow trees are trembling aspen (*Populus tremuloides*); green trees are Sitka spruce (*Picea sitchensis*). c. Larger trees on left side of photograph are mature western hemlock (*T. heterophylla*); on right side of photograph trees are smaller, immature western hemlock (*T. heterophylla*). d. The long, linear object is a road and the irregular geometric patches are cultivated areas. e. The rough texture in the top right corner of the photograph is indicative of a mature stand with high stand complexity; the smooth textured stands at the bottom are more uniform in height, indicating a younger stand. f. Various patterns indicating different agricultural uses (crops, vineyards, etc.) g. Tree shadows cast on the river help species identification (*T. heterophylla* and *Thuja plicata*). h. Lighter color of trees suggests presence of deciduous vegetation. i. Presence of river indicates riparian area. j. Shadow on left side of photograph suggests decrease in elevation towards right side of photograph.23**
- Figure 3.1 The Kennedy Lake watershed is located on the west coast of Vancouver Island, British Columbia, Canada.49**
- Figure 3.2 An illustrative example of manually-delineated polygons and segmented objects (shown in white) for a subset of an example landscape.54**
- Figure 3.3 The three spatial levels of statistical comparison between the manually-delineated polygons and segmented objects (shown in black) including a) a subset of one image showing paired locations (white dots); b) a subset of one image showing non-border polygons (shown in gray); and c) an example of two frequency distributions of objects and polygons shown in b.56**
- Figure 3.4 Pruned classification tree (Sherrod 2008) developed to model leading species (defined in Table 3.1) based on the combined dataset. Metric abbreviations are shown in Table 3.2. Target classes (terminal nodes) are shown in grey, along with the number of polygons correctly classified out of the total polygons identified by that split.65**
- Figure 3.5 Pruned classification tree (Sherrod 2008) developed to model surface expression (defined in Table 3.1) based on the combined dataset. Metric abbreviations are shown in Table 3.2. Target classes (terminal nodes) are shown in grey, along with the number of polygons correctly classified out of the total polygons identified by that split.65**
- Figure 4.1 The study area encompasses the entire Kennedy Lake watershed, from which eight photographs were selected to represent contrasting riparian and upland landscapes.81**
- Figure 4.2 Changes in the number of objects and the minimum object size for segmentations using different scale parameters. Panel a. Representative riparian landscape (as shown in Figure 4.3a); Panel b. Representative upland landscape (as shown in Figure 4.3b). The plateaus were used to guide selection of scale parameters suited to all eight landscapes. The resulting scale parameters selected were 280, 500 and 720 (shown with arrows).85**

Figure 4.3 An example photograph (landscape) and segmentation results shown on a subsection of each photograph for a. a representative riparian landscape, and b. a representative upland landscape. The scale hierarchy is nested, and object outlines are shown in white on the photographs and are described further in Table 4.2.87

Figure 4.4 Plot of hierarchical clustering results, displaying the distances at which factors (and clusters) are grouped/fused together. Fusion distances represent dissimilarity, and are based on the correlations between factors.89

ACKNOWLEDGEMENTS

Jessica Lindsay Morgan was funded by an NSERC PGS-M scholarship. This work was also supported by NSREC Discovery Grants to Dr. Sarah Gergel (and Dr. Nicholas Coops), and funding from the BC Ministry of Forests and Range (Coast Forest Region), and the Forest Science Program (No. Y082305). Additional support was provided by Environment Canada – Environmental Damages Fund. This research would not have been possible without the encouragement, guidance, and support of Dr. Sarah Gergel. I am particularly grateful to Dr. Nicholas Coops, Dr. Brett Eaton, and Dr. Valerie LeMay for methodological and editorial suggestions. Finally, I would like to thank Matt Tomlinson, Shanley Thompson, Trevor Lantz, Kate Kirby, Andy MacKinnon, all adopted Gergelites, as well as the members of the IRSS lab for filling the past three years with great memories.

CO-AUTHORSHIP STATEMENT

This thesis consists of three scientific manuscripts for which I am lead author. The objectives of this research were developed throughout the course of my degree with the help of Dr. Sarah Gergel and Dr. Nicholas Coops. The initial project ideas were proposed by Dr. Sarah Gergel, and refined by myself after recognizing the ecological importance of historic aerial photographs and the unexplored potential of object-based analysis as key areas of research. I performed all of the research, data analysis, and interpretation of results for the three journal articles, as well as preparation of the final manuscripts. Co-authors provided methodological guidance and editorial suggestions throughout the writing of these scientific journal articles.

1 INTRODUCTION

1.1 The Role of Aerial Photography within Ecology

Aerial photographs are a cornerstone of resource management and ecosystem planning. Used to map various land cover and land use systems, the classification objectives of aerial photograph analysis range from the identification of rare habitats, to production of geologic and soil maps for engineering purposes (Paine and Kiser 2003). First used as a military reconnaissance tool during World War I (Lillesand et al. 2004), aerial photographs have revolutionized the way humans view the world, particularly for exploring the interactions between human activities and Earth's ecosystems. An additional benefit of using aerial photographs is the significant reduction in associated mapping costs in comparison to alternative mapping methods, such as field data collection (Paine and Kiser 2003). As a result, aerial photographs are of enormous value to managers and researchers in many disciplines.

Over the course of the 20th century, rapid and extensive environmental changes have occurred on local, regional, and global scales, and aerial photographs are one of only a few spatial data sources recording these long-term changes. Collected since the 1930's, aerial photograph archives provide one of the largest records of temporally continuous, spatially complete landscape information (Paine and Kiser 2003). This long-term information is important because it fosters our comprehension of ecosystem patterns and processes, contributes to making informed management decisions, and provides reference data for evaluating management goals (Arcese and Sinclair 1997, Landres et al. 1999, Swetnam et al. 1999). Furthermore, as landscapes continue to change in the future, the past becomes increasingly important for evaluating the magnitude of recent changes, such as changes in the rates of catastrophic events (Peters et al.

2004). Due to the rarity of historic information, archival aerial photographs provide an invaluable resource for ecological monitoring.

1.2 Remote Sensing Challenges for Aerial Photograph Analysis

Traditionally, ecological information has been derived from aerial photographs through a process known as manual interpretation. As a result, manual interpretation is the standard method for production of ecosystem classification and inventory maps in many regions (Cohen et al. 1996, Hall 2003, Thompson et al. 2007). Manual interpretation consists of two primary steps: 1) polygon delineation from hard-copy or digitized photographs; and 2) classification of the created polygons. Both of these steps are achieved through human cognition, meaning an individual delineates polygons based on perceived boundaries, and then assigns a label representing their best estimate at what is actually on the ground. Interpreters use a convergence-of-evidence approach, accounting for tone, shape, size, texture, pattern, shadow, site (local characteristics), and context simultaneously (Avery and Berlin 1992, Paine and Kiser 2003).

Despite rigorous training of interpreters and thorough development of guidelines to attempt standardization of the manual process, there are numerous challenges inherent to this approach. Results are somewhat subjective, and inconsistent among interpreters (Fookes et al. 1991). As a result, the accuracy of interpretation relies greatly on the personal experience, knowledge, and expectations of the interpreter for a given location. Interpretation is also costly, in terms of the time, labor, and monetary requirements (Green 2000, MacMillan et al. 2007). Of particular concern to the future of manual interpretation is the current shortage of well-trained interpreters, whose skills have ideally been combined with years in the field. This lack of interpreters is especially troubling given the continued demand for maps derived from manual interpretation.

A recent shift in emphasis towards satellite imagery has contributed to this loss of trained interpreters for aerial photograph analysis. This shift has primarily been due to the greater spectral sensitivity, broader spatial coverage, and more regular re-visitation frequencies of many satellites. In addition, rapidly decreasing costs and the increasing availability of free imagery has provided cost-effective alternatives to aerial photographs. However, the spatial resolution of the most widely available and free satellite imagery is generally coarser than aerial photographs (Tuominen and Pekkarinen 2004). Furthermore, collection of satellite imagery began in the 1970's, limiting their use for analysis of longer-term landscape change. Given both the loss of expert interpreters, and the four additional decade's worth of information within aerial photograph archives, new approaches for analysis of aerial photographs are a research imperative.

1.3 New Approaches for Aerial Photograph Analysis

Object-based methods are one image analysis technique with great potential for improving and supplementing traditional aerial photograph analysis. The basic premise of the object-based approach employed in this research is that neighboring pixels of similar characteristics are merged into homogenous objects using a process called segmentation (Benz et al. 2004, Definiens 2007). Essentially, pixels are grouped through numerous iterations that combine similar (homogenous) regions of pixels while dissimilar (heterogeneous) regions are kept distinct. The end product is an image partitioned into homogeneous objects, which can then be classified. This approach used here employs a region merging algorithm for object creation; however many different object-based methods have been developed (Hay et al. 2003, Shankar 2007).

Object-based approaches have successfully aided a variety of mapping purposes including production of forest inventories (Chubey et al. 2006, Wulder et al. 2008), assessment of agricultural land use (Lucas et al. 2007, Watts et al. 2009), and analysis of change over time (Laliberte et al. 2004, Pringle et al. 2009). Particularly valuable for resource management, the products of object-based analysis could easily be adapted into frameworks of existing management strategies based upon aerial photograph interpretation. Furthermore, automated object-based methods could increase objectivity and repeatability of results, as compared to manual interpretation. The ability of object-based approaches to account for contextual information (relationships between neighboring objects) and represent landscape structure over multiple spatial scales (create objects of various sizes) is one of the primary benefits of this technique (Benz et al. 2004, Blaschke 2004). As a result, higher overall accuracies have been reported for maps made with object-based techniques over pixel-based approaches (Pringle et al. 2009, Wang et al. 2004, Yan et al. 2006).

1.4 Historic Landscape Heterogeneity

Of the many landscape characteristics and ecological indicators of interest to ecologists and managers (Dale and Beyeler 2001), none are more challenging to quantify than spatial heterogeneity. Heterogeneity can be related to species diversity, resilience, and ecosystem function (Huston 1999) and is highly influential to important biotic and abiotic processes such as landscape disturbance and movement of organisms (Turner 1989). Furthermore, despite the significance of historical dynamics in understanding spatial patterns and processes, there has been less research on quantifying historic spatial heterogeneity. Quantitative measures of historic heterogeneity provide reference conditions useful for conservation planning and are valuable for setting restoration targets (Sklenicka and Lhota 2002). An ideal source of information for defining historic heterogeneity is archival aerial photographs.

Landscape heterogeneity may be broadly defined as the degree of spatial variability of some property within a system (Li and Reynolds 1995). However, heterogeneity is highly dependent upon the spatial and temporal scales over which it is measured (Wiens 1989). The discipline of landscape ecology has made progress in quantifying landscape heterogeneity, but has generally approached this task using the patch mosaic paradigm (McGarigal et al. 2009). This patch mosaic paradigm uses categorical data (e.g. discrete land cover classes) to represent landscape heterogeneity via patch-based metrics (or landscape pattern indices) (Cushman et al. 2008, Gustafson 1998, Riitters et al. 1995). The major limitation of this approach is that the landscape is represented as discrete patches at one spatial scale, when in fact, heterogeneity occurs as gradients over a variety of spatial scales (McGarigal et al. 2009). Therefore, new approaches capable of characterizing the complexity of landscape heterogeneity are needed.

Object-based analysis may hold great potential for defining landscape heterogeneity. Object-based analysis is similar to the patch mosaic paradigm in that the landscape is represented through a series of 'objects' or 'patches'. For example, patch-based indices (e.g. mean patch size, patch shape) derived from categorical data are similar to the object-based metrics derived from the segmentation process (e.g. object size, object shape). The primary difference between these approaches is that the segmentation process utilizes continuous remotely-sensed data for calculation of object-based metrics, whereas the patch mosaic paradigm derives patch-based indices using discrete thematic data. A distinct advantage of using object-based metrics, is that variability contained within objects is accounted for, unlike in the patch mosaic perspective which ignores within-patch heterogeneity. The use of object-based analysis to define heterogeneity is completely novel, and may provide important insights into quantification of landscape structure. These themes provide the conceptual basis for the research presented here.

1.5 Research Objectives

This thesis is comprised of three studies that highlight the ecological potential of aerial photographs and the emerging role of object-based analysis for answering important ecological, management, and theoretical questions. With special emphasis on historic aerial photographs, I explore a variety of remote sensing tools and spatial statistics for quantitative analyses. I focus on the historic landscape of the Kennedy Lake watershed on Vancouver Island, British Columbia, Canada. The goals of each chapter are discussed below.

My focus in chapter two was to provide a general overview of aerial photographs, and emphasize their importance for ecological management. Technical and methodological challenges associated with their use are discussed, and new approaches for more objective, consistent, and efficient analysis of aerial photographs are presented. An anticipated impact of this chapter is a renewed interest in research using aerial photographs for ecological management. My goal in chapter three was to assess the ability of automated analysis techniques (object-based analysis and classification tree models) to mimic manual interpretation. The results of manual and automated approaches were compared for five different classification schemes related to forest and terrain attributes. This pilot comparison provides a compelling argument for further development of automated techniques for ecosystem mapping. My objective in chapter four was to quantify historic landscape heterogeneity from archival aerial photographs. Object-based segmentation was used as a novel method for defining spatial heterogeneity. A new quantitative definition was extracted using a multi-scale approach, which identifies several previously ignored components of landscape heterogeneity. The implications for the discipline of landscape ecology are discussed. Finally, in chapter five I provide a summary of the significance of this research and potential directions for future work.

1.6 References

- Arcese P, Sinclair ARE. 1997. The Role of Protected Areas as Ecological Baselines. *The Journal of Wildlife Management* 61: 587-602.
- Avery TA, Berlin GL. 1992. *Fundamentals of Remote Sensing and Air Photo Interpretation*. Upper Saddle River: Prentice Hall.
- Benz UC, Hofmann P, Willhauck G, Lingenfelder I, Heynen M. 2004. Multi-resolution, object-oriented fuzzy analysis of remote sensing data for GIS-ready information. *ISPRS Journal of Photogrammetry & Remote Sensing* 58: 239-258.
- Blaschke T. 2004. Object-based contextual image classification built on image segmentation. *IEEE TRANSACTIONS ON GEOSCIENCE AND REMOTE SENSING*: 113-119.
- Chubey MS, Franklin SE, Wulder MA. 2006. Object-based Analysis of Ikonos-2 Imagery for Extraction of Forest Inventory Parameters. *Photogrammetric Engineering & Remote Sensing* 72: 383-394.
- Cohen WB, Kushla JD, Ripple WJ, Garman SL. 1996. An introduction to digital methods in remote sensing of forested ecosystems: Focus on the Pacific Northwest, USA. *Environmental Management* 20: 1432-1009.
- Cushman SA, McGarigal K, Neel MC. 2008. Parsimony in landscape metrics: Strength, universality, and consistency. *Ecological Indicators* 8: 691-703.
- Dale VH, Beyeler SC. 2001. Challenges in the development and use of ecological indicators. *Ecological Indicators* 1: 3-10.
- Definiens. 2007. *Definiens Developer 7 User Guide*. Munchen, Germany. Report no.
- Fookes PG, Dale SG, Land JM. 1991. Some observations on a comparative aerial photography interpretation of a land slipped area. *Quarterly Journal of Engineering Geology* 24: 249-265.
- Green K. 2000. Selecting and Interpreting High-Resolution Images. *Journal of Forestry* 37-39.

- Gustafson EJ. 1998. Quantifying Landscape Spatial Pattern: What Is the State of the Art? *Ecosystems* 1: 143-156.
- Hall RJ. 2003. The roles of aerial photographs in forestry remote sensing image analysis. Pages 47-75 in Wulder M, Franklin SE, eds. *Remote Sensing of Forest Environments: Concepts and Case Studies*. Boston: Kluwer.
- Hay GJ, Blaschke T, Marceau DJ, Bouchard A. 2003. A comparison of three image-object methods for the multi-scale analysis of landscape structure. *ISPRS Journal of Photogrammetry & Remote Sensing* 57: 327-345.
- Huston MA. 1999. Local Processes and Regional Patterns: Appropriate Scales for Understanding Variation in the Diversity of Plants and Animals. *Oikos* 86: 393-401.
- Laliberte AS, Rango A, Havstad KM, Paris JF, Beck RF, McNeely R, Gonzalez AL. 2004. Object-oriented image analysis for mapping shrub encroachment from 1937 to 2003 in southern New Mexico. *Remote Sensing of Environment* 93: 198-210.
- Landres PB, Morgan P, Swanson FJ. 1999. Overview of the use of natural variability concepts in managing ecological systems. *Ecological Applications* 9: 1179-1188.
- Li H, Reynolds JF. 1995. On Definition and Quantification of Heterogeneity. *Oikos* 73: 280-284.
- Lillesand TM, Kiefer RW, Chipman JW. 2004. *Remote Sensing and Image Interpretation*. USA: John Wiley & Sons, Inc.
- Lucas R, Rowlands A, Brown A, Keyworth S, Bunting P. 2007. Rule-based classification of multi-temporal satellite imagery for habitat and agricultural land cover mapping. *ISPRS Journal of Photogrammetry & Remote Sensing* 62: 165-185.
- MacMillan RA, Moon DE, Coupe RA. 2007. Automated predictive ecological mapping in a Forest Region of B.C., Canada, 2001-2005. *Geoderma* 140: 353-373.
- McGarigal K, Tagil S, Cushman SA. 2009. Surface metrics: an alternative to patch metrics for the quantification of landscape structure. *Landscape Ecology* 24: 433-450.

- Paine DP, Kiser JD. 2003. *Aerial Photography and Image Interpretation*, 2nd Edn. Hoboken, New Jersey: John Wiley & Sons, Inc.
- Peters DPC, Pielke RA, Bestelmeyer BT, Allen CD, Munson-McGee S, Havstad KM. 2004. Cross-scale interactions, nonlinearities, and forecasting catastrophic events. *Proceedings of the National Academy of Science* 101: 15130-15135.
- Pringle RM, Syfert M, Webb JK, Shine R. 2009. Quantifying historical changes in habitat availability for endangered species: use of pixel- and object-based remote sensing. *Journal of Applied Ecology* 46: 544-553.
- Riitters KH, O'Neil RV, Hunsaker CT, Wickham JD, Yankee DH, Timmins SP, Jones KB, Jackson BL. 1995. A factor analysis of landscape pattern and structure metrics. *Landscape Ecology* 10: 23-39.
- Shankar BU. 2007. Novel Classification and Segmentation Techniques with Application to Remotely Sensed Images. Pages 295-380. *Transaction on Rough Sets VII*, vol. 4400/2007. Berlin / Heidelberg: Springer.
- Sklenicka P, Lhota T. 2002. Landscape heterogeneity- a quantitative criterion for landscape reconstruction. *Landscape and Urban Planning* 58: 147-156.
- Swetnam TW, Allen CD, Betancourt JL. 1999. Applied Historical Ecology: Using the Past to Manage for the Future. *Ecological Applications* 9: 1189-1206.
- Thompson ID, Maher SC, Rouillard DP, Fryxell JM, Baker JA. 2007. Accuracy of forest inventory mapping: Some implications for boreal forest management. *Forest Ecology and Management* 252.
- Tuominen S, Pekkarinen A. 2004. Local radiometric correction of digital aerial photographs for multi source forest inventory. *Remote Sensing of Environment* 89: 72-82.
- Turner MG. 1989. Landscape Ecology - the Effect of Pattern on Process. *Annual Review of Ecology and Systematics* 20: 171-197.

- Wang L, Sousa WP, Gong P. 2004. Integration of object-based and pixel-based classification for mapping mangroves with IKONOS imagery. *International Journal of Remote Sensing* 25: 5655-5668.
- Watts JD, Lawrence RL, Miller PR, Montagne C. 2009. Monitoring of cropland practices for carbon sequestration purposes in north central Montana by Landsat remote sensing. *Remote Sensing of Environment* 113: 1846-1852.
- Wiens JA. 1989. Spatial Scaling in Ecology. *Functional Ecology* 3: 385-397.
- Wulder M, White JC, Hay GJ, Castilla G. 2008. Towards automated segmentation of forest inventory polygons on high spatial resolution satellite imagery. *The Forestry Chronicle* 84: 221-230.
- Yan G, Mas J-F, Maathuis BHP, Xiangmin Z, Van Dijk PM. 2006. Comparison of pixel-based and object-oriented image classification approaches-a case study in a coal fire area, Wuda, Inner Mongolia, China. *International Journal of Remote Sensing* 27: 4039-4055.

2 AERIAL PHOTOGRAPHY: A RAPIDLY EVOLVING TOOL FOR ECOLOGICAL MANAGEMENT¹

2.1 Introduction

The use of aerial photography to assess and map landscape change is a crucial element of ecosystem management. Aerial photographs are ideal for mapping small ecosystems and fine-scale landscape features, such as riparian areas or individual trees (Fensham and Fairfax 2002, Tuominen and Pekkarinen 2005) because they often possess a high level of spatial and radiometric (tonal) detail. Aerial photographs also provide the longest available, temporally continuous, and spatially complete record of landscape change, dating from the early 1930's in some cases. As a result, aerial photographs are a source of valuable historical information on vegetation cover and condition (Cohen et al. 1996, Fensham and Fairfax 2002). Aerial photographs can reduce costs involved in mapping, inventorying, and planning (Paine and Kiser 2003), and as such are used for applications ranging from forest inventories, disturbance mapping, productivity estimates, and wildlife management (Avery and Berlin 1992). Thus, many important management decisions are routinely based on maps derived from aerial photographs (Cohen et al. 1996, Paine and Kiser 2003).

Proliferation of satellite imagery over the past few decades has influenced the use and perceived utility of aerial photography in several contrasting ways (Table 2.1). Satellite imagery, with its broad spatial coverage and regular re-visitation frequency, has provided researchers and managers with a cost-effective alternative to aerial photography. This has contributed to a shift in emphasis of university curricula, and the training of remote sensing specialists, away from aerial

¹ A version of this chapter has been accepted for publication. Morgan, J.L., Gergel, S.E., Coops, N.C. In Press. Aerial Photography: A Rapidly Evolving Tool for Ecological Management. BioScience.

Table 2.1 Comparative advantages and disadvantages associated with traditional film-based aerial photography, digital aerial photographs, and satellite imagery.

	Advantages	Disadvantages
Aerial Photography	<ul style="list-style-type: none"> • Long time series (1930's and onwards) • Often high spatial resolution • Primary basis for many maps used by agencies • Stereoscopic view capturing height and topography • Comparatively easy to capture • Can be collected at any time or place • Easy to tailor to specific needs (photograph scale, spatial, spectral, and temporal characteristics, etc.) • Less atmospheric interference (due to lower altitude) 	<ul style="list-style-type: none"> • Individual photographs have limited spatial coverage • Large time effort required for processing (film development and orthorectification) • Photographs often variable among flight lines (environmental and positional) • Difficulty in standardizing image contrast and rectification • Manual interpretation can be subjective • Quality of photograph dependent upon weather • Spatial coverage dependent on needs of original project • Limited/inconsistent metadata (mainly historic photographs)
Aerial Digital Photography	<ul style="list-style-type: none"> • Easy to tailor to specific needs (photograph scale, spatial, spectral, and temporal characteristics, etc.) • Image access is immediate (during flight) • Exposure conditions optimized in-flight • Digital storage is reusable (digital memory) • Can be copied repeatedly without data loss • Radiometric calibration procedures are extensive • Many digital cameras record positional data (GPS) 	<ul style="list-style-type: none"> • Individual photographs have limited spatial coverage • Quality of image dependent upon weather • Spatial coverage dependent on needs of original project • Shorter time series (1990's and onwards) • Often have coarser resolution than film-based photographs • Large amount of digital space required to store high resolution images
Satellite Imagery	<ul style="list-style-type: none"> • High temporal frequency • Systematic collection • Broad spatial coverage • Easily accessible (many images are free) • Many image analysis methods developed • Broader spectral range • Typically have more rigorous radiometric calibration • Metadata precise and easily obtained • Current high resolution data provides continuous land cover data (facilitates comparison to historic photos) 	<ul style="list-style-type: none"> • Shorter time series (1970's and onwards) • Often have coarser resolution than film-based photographs • Higher spatial resolution data are expensive • Large amount of digital space required to store high resolution images • Atmospheric correction usually needed (weather) • Sensors are not serviceable (due to their location in space) • Greater atmospheric influence (captured outside atmosphere)

photographs (Sader and Vermillion 2000) to digital platforms. However, a lack of long-term satellite imagery (prior to 1970s) limits the use of satellite data in change detection analyses to the past three decades, underscoring the value of longer-term aerial photographs. In addition, the spatial resolution of the most widely available and free satellite imagery is generally coarser than that of aerial photographs (Tuominen and Pekkarinen 2004). One important development associated with the recent emphasis on satellite imagery, however, has been the development of a wide range of digital image analysis techniques. While many of these techniques were originally developed for satellite imagery, they have also expanded upon the range of analysis techniques now available for aerial photographs.

Despite the many advantages of aerial photographs, there are challenges specific to using aerial photographs, especially with respect to manual aerial photograph interpretation. While manual interpretation by highly-trained individuals remains one of the most effective and commonly used approaches for classification of aerial photographs (Wulder 1998), this technique relies greatly on the personal experience, knowledge, and expectations of the interpreter for a given location. Thus, human interpretations are subjective, and vulnerable to inconsistency and error. In addition, resource management agencies are beginning to face a shortage of well-trained interpreters, especially those whose skills have ideally been combined with years spent in the field. As a result, there is a need for new approaches to reduce or eliminate these difficulties associated with traditional aerial photograph analysis, to help foster their continued and evolving use.

Motivated by the unique information available from aerial photographs, recent developments in digital analysis techniques, and what we believe is a need to reinvigorate training and research in ecological management using aerial photography, we review and develop several important

themes. First we provide an overview of aerial photographs, along with a generalized discussion of challenges inherent with their use, and highlight the ecological importance of the eight essential characteristics used in traditional, manual interpretation. Second, we examine how digitized aerial photographs may be analyzed using alternative analysis techniques to provide more consistent information using more efficient means. We end with several examples of emerging ecological management questions that may be best addressed through the use of aerial photographs. Our overall aim is to highlight the unique value that aerial photographs hold for ecosystem management, and explore possible synergies between new technologies and traditional approaches for using aerial photographs.

2.2 Aerial Photography Basics

Aerial photography is the collection of photographs using an airborne camera. Photographs are essentially a representation of the reflectance characteristics (relative brightness) of features recorded onto photographic film. More specifically, reflectance is recorded by the film's emulsion, which is a layer of light-sensitive silver halide crystals on backing material for black and white photographs, or a series of emulsions for color photographs (Wolf and Dewitt 2000, Lillesand et al. 2004). Filters also play an important role in determining the type of information recorded by the camera, and consist of a layer of dyes which selectively absorb and transmit target wavelengths. Like any camera, the film is protected until briefly exposed to light through a lens and filter(s), during which the silver halide crystals (and dyes) react based on the degree of reflectance from features on the ground which fall within the camera's frame, or field of view (Lillesand et al. 2004). Aerial photographs are captured most commonly as panchromatic (black and white), color, or false color infrared; however various types of electromagnetic radiation can also be recorded onto photographic film with the use of different emulsions and filters (Cohen et al. 1996).

Obtaining a photograph with an appropriate amount of contrast, or tonal variation, is paramount for accurate analysis or interpretation. Photographic contrast, or the range of values within the photograph, is a product of the film's emulsion type, the degree of exposure to light, and film development conditions (Wolf and Dewitt 2000). Contrast is also directly related to radiometric resolution, which is defined as the smallest detectable difference in exposure, or measurable difference in reflectance levels (Lillesand et al. 2004). Generally, when exposure and development conditions are ideal, any decreases in radiometric resolution (smaller detectable differences in tone) will result in greater contrast within the photograph.

Of fundamental importance to the quality of aerial photographs is the camera used to obtain the images. Two broad types of airborne cameras are used: film-based and digital cameras (Table 2.1). The most common type of cameras used in aerial photography are film-based, single-lens frame cameras, with lenses of high geometric quality to minimize distortion (Wolf and Dewitt 2000). Aerial cameras must take photographs of features from great distances; therefore the focal length of the lens (the distance from the lens to the film) is fixed to focus reflectance from effectively infinite distances away (Wolf and Dewitt 2000, Lillesand et al. 2004). The most common focal length for aerial cameras is 152 mm; however longer focal lengths may be used to capture imagery from higher altitudes, which are used primarily for aerial mosaics. Aerial digital cameras are quite similar in structure; however reflectance is recorded with electronic sensors and stored digitally as opposed to the use of film. Although images captured by airborne digital cameras are not technically photographs, such imagery will be referred to as digital photography in this paper.

The scale of an aerial photograph is a function of camera focal length and the flying height of the aircraft (Cohen et al. 1996) and most often refers to the conversion between a unit distance represented on the photograph and the number of equivalent units on the ground. Scale can also refer to the finest/highest spatial unit of resolution (grain), as well as the size of the entire scene (extent). The finest unit of resolution on a film-based photograph is not represented by uniform pixels (the smallest spatial unit of resolution within an image) as is the case with airborne digital imagery or satellite imagery, but is dependent upon the clusters of silver halide grains within the emulsion, which tend to be irregularly sized and unevenly distributed (Lillesand et al. 2004). As silver halide grains are smaller than most digital detectors, film camera resolution is often finer than digital camera resolution (Paine and Kiser 2003). However, the resolution of some current digital cameras can be comparable to film resolutions for systems with similar formatting and scale (Lillesand et al. 2004). Also of relevance to scale is consideration of the minimum mapping unit (MMU), which represents the size of the smallest entity to be mapped. This is often established as part of the classification system; however both the scale of the photographs and the grain will influence definition of the MMU.

Photographs can be grouped according to their geometry as either vertical or oblique. Vertical photographs are taken parallel to the ground with the optical axis of the camera situated directly downwards. Due to the variable conditions during photograph collection (wind, turbulence, etc.) true vertical orientation is rarely achieved and photographs almost always contain some degree of tilt. Tilted images are obtained on an oblique angle meaning that the optical axis of the camera diverges more than 3° from the vertical (Jensen 2000), shifting the normally central focus of a photograph to another location and thereby shifting the positions of certain features (Avery and Berlin 1992). In contrast, oblique photographs are acquired with a deliberate deviation from a vertical orientation. While oblique landscape photographs can predate aerial photographs by

decades (acquired from high points on the landscape such as land surveys or airborne) and often provide rare historical information, they are more challenging to analyze systematically.

Therefore, our discussion is limited to the use of vertical aerial photographs.

Two closely related disciplines involved in aerial photography: photogrammetry and aerial photograph interpretation; yet each are distinct in their end goals. Photogrammetry (also called metric photogrammetry) is concerned with obtaining exceptionally precise quantitative measurements from aerial photographs, whereas photographic interpretation (or interpretive photogrammetry) focuses more on the recognition, identification, and significance of features on photographs (Wolf and Dewitt 2000, Paine and Kiser 2003). Photogrammetric methods are highly precise and much of this discipline evolves around techniques to address and correct photographic errors. Interpretation methods have also been extensively developed and are relevant for understanding the types of ecological information which can be derived from aerial photographs. While principles of both disciplines are addressed here, we primarily focus on photograph interpretation and classification.

2.3 Digitization of Aerial Photographs

Film-based photographs may be converted into digital format through scanning (Wolf and Dewitt 2000). Photogrammetric scanners convert analog (or continuous tone photographs) into digital files represented as pixels (Wolf and Dewitt 2000). The cost of the highest quality scanners can be considerable, from \$25,000 - \$100,000 USD (Aronoff 2005); however scanners <\$10,000 USD produce digital products suitable for most interpretation needs, with the exception of precise photogrammetric work. An inherent drawback of scanning photographs is a potential loss of radiometric/tonal variation and spatial resolution from the photograph (Warner et al. 1996), and as a result, second or third generation products will not have the detail found in

the original. Thus, it is crucial that the scanning resolution (both spatial and radiometric), is sufficient to create a geometrically and visually accurate representation of the original aerial photograph. It is primarily the physical characteristics of the film and the scale of the aerial photograph which will limit the resolvable scanning resolution (dots per inch) (Jensen 2000) (Table 2.2); however, other factors such as atmospheric clarity and scene contrast can also impact resolution of photographs. Scanning at a resolution too low will result in loss of information, whereas a needlessly high scanning resolution will lead to digital files of enormous size and storage requirements. Scanning has the advantage that any subsequent interpretation can be assisted by software capable of providing systematic analyses (Fensham and Fairfax 2002).

Table 2.2 Relationship between scanner resolution and ground resolution for multiple scales of aerial photography. Adapted from (Jensen 2000) p. 111. For example, a 1:20,000 photograph scanned at 1200dpi, will result in a digital image with a spatial resolution (pixel size) of 0.42m. A brief description of common mapping units and general uses of each scale is included.

Digitizer Detector IFOV* (Scanner resolution: Spot size)		Pixel Ground Resolution as a function of Photographic Scale (meters)					
Dots per inch (dpi)	Micro-meters (μm)	1:40,000	1:20,000	1:9,600	1:4,800	1:2,400	1:1,200
200	127.00	5.08	2.54	1.22	0.61	0.30	0.15
600	42.34	1.69	0.85	0.41	0.20	0.10	0.05
800	31.75	1.27	0.64	0.30	0.15	0.08	0.04
1200	21.17	0.85	0.42	0.20	0.10	0.05	0.03
1500	16.94	0.67	0.34	0.16	0.08	0.04	0.02
2000	12.70	0.51	0.25	0.12	0.06	0.03	0.02
Common Minimum Mapping Units		General land cover: 2 - 4 ha	Natural disturbances	Forest stands, habitat patches		Individual trees, stream reaches	
Common uses		General resource assessment and planning.	Mapping of tree species, agricultural crops, vegetation communities, and soil surveys. Historic (archival) photographs are often captured at these scales.		Intensive mapping and monitoring of specific entities, such as damage surveys.		

* IFOV (Instantaneous Field of View)

2.4 Overview of Basic Photographic Errors

Despite the great utility of aerial photographs, it is important to note that errors often occur during the collection and digitization of photographs which can limit their use (Cohen et al. 1996, Tuominen and Pekkarinen 2004). While these inaccuracies rarely render aerial photographs useless (provided appropriate precautions were taken during photographic acquisition, storage, and digitization), an understanding of the major sources of error is crucial for accurate analysis. Typically, for many ecological management purposes, geometric errors and radiometric errors are most relevant, as they may inaccurately represent photographic features. Therefore, we examine the major sources and types of photographic errors in four main categories. Errors can be classified as either geometric or radiometric in origin, and either systematic or random in form (Table 2.3).

Geometric errors (or positional errors) alter the perceived location and size of features on a photograph. Geometric errors can occur due to problems with the equipment used to capture the photographs (Wolf and Dewitt 2000), stability of the air borne platform, flying and shutter speeds (Paine and Kiser 2003), and the location being photographed. Relief displacement, in particular, results in features at higher elevations appearing larger than similarly sized features located at lower elevations (Aronoff 2005). However, relief displacement is also what enables 3-dimensional viewing of overlapping stereo-pairs (called parallax), which aids manual photograph interpretation by allowing visualization of topographic relief (Jensen 2000, Paine and Kiser 2003, Aronoff 2005). A stereo-pair is defined as two adjacent photographs from the same flight line that possess some amount of image overlap, usually 60% (Paine and Kiser 2003). While geometric distortion is utilized in the manual interpretation process, geometric errors are often problematic for digital analyses.

Table 2.3 Common errors associated with the use of aerial photographs. Adapted from (Paine and Kiser 2003) p. 35.

Type of Error		Systematic	Random
Geometric	Distortion	Lens distortion* - More common on old photographs Image motion compensation - Typically occurs on high spatial resolution photographs	Film/print shrinkage* - Occurs on historic photographs/film Atmospheric refraction of light*
	Displacement	Earth curvature*	Topographic/relief displacement - More obvious in mountainous areas Tilt displacement - Especially problematic for oblique photographs Detector error (roll, crab/yaw, pitch)* - Typically affects older aerial photographs
Radiometric	Sensor	Exposure falloff Sensing geometry	Bidirectional reflectance - e.g. Hotspot effects and mutual shadowing
	Environment	Atmospheric (haze)	Clouds Sun angle - Worse for photographs taken off solar noon

* Errors generally considered to be negligible or accounted for during processing

Radiometric errors (errors in tone/color) can be caused by the vantage point, condition, and calibration of the camera, as well as the types of filter and film emulsion (Jensen 2000).

Environmental sources of radiometric variability include the hour and season of image capture (which affects the angle of the sun), and can cause shadow and/or glare. Atmospheric interference due to clouds and haze can also cause radiometric errors (Cohen et al. 1996). In addition, the geometry of the airborne platform (camera) can cause variability in brightness values, which can be further confounded by sun angle, platform position, and topographic variation (Cohen et al. 1996, Paine and Kiser 2003). Next, we present some basic methods for

addressing the most relevant geometric and radiometric errors, recognizing that additional errors can also affect aerial photographs (Table 2.3).

2.5 Error Correction

For most digital classification and mapping purposes, it is necessary to use orthorectification procedures to correct for geometric displacement errors and provide spatial reference.

Orthorectification involves the spatial manipulation of a digitized/digital photograph into an orthophoto, by adding vertical map (x , y , and z) coordinates to accurately represent distances, angles, and areas (Lillesand et al. 2004). This process is different than georeferencing, which solely assigns horizontal map (x , y) coordinates to an image. The most basic need for correcting these geometric errors is a reference dataset, or a set of reference coordinates, commonly derived from existing topographic maps, GIS datasets, satellite imagery, orthophotos or orthophoto mosaics. Highly accurate reference/control data is critical because the spatial accuracy of the corrected product is dependent upon the geometric quality of the reference layer. Reference data are used to orientate the photograph to its true position through the selection of ground control points (GCPs). GCPs are locations or features, easily identifiable on both the reference data and uncorrected photograph, ideally distributed evenly throughout the entire scene. The target aerial photograph (lacking spatial reference) is shifted or warped to its true spatial position by re-sampling the data using the GCPs as a guide. While various re-sampling algorithms exist, most common are the nearest neighbor (simplest and fastest), bilinear interpolation, and cubic convolution (yields the smoothest image, yet is computationally intensive), and are available within most standard orthorectification software. Of importance to note, is that orthorectification and georeferencing are time consuming, particularly for large sets of aerial photographs.

Geometric correction of historic photographs can be particularly challenging, because changes in land cover and feature position over time can make GCP identification difficult. In addition,

orthorectification procedures can distort spectral data, therefore spatial referencing is commonly applied post-classification.

The most common radiometric procedures applied to digitized aerial photographs typically involve manipulation of the image histogram (distribution of the tonal/radiometric values for the entire photograph/image). Contrast or histogram stretching, is often used to improve the visual appearance of aerial photographs, and alters the frequency distribution of original pixel values to allow for better differentiation among unclear or hazy regions. Contrast enhancement includes procedures such as image dodging (equalizes dark and light areas across an image for a monochromatically balanced product), saturation, and sharpening. Photographs acquired at various times within the day are particularly problematic as radiometric response is highly dependent upon sun angle and atmospheric conditions. Normalization techniques exist, which work to identify similar land cover types across photographs taken under various conditions and resample problematic photographs based on the tonal distributions of photographs with more ideal contrast. Histogram manipulation can be achieved using a variety of software, such as Adobe Photoshop and most standard image processing and analysis programs.

2.6 Aerial Photograph Interpretation

Traditionally, information has been obtained from aerial photographs through manual interpretation. Over the years, manual interpretation has evolved from plastic overlays on hard copy images, to soft-copy systems and digitized photographs (Avery and Berlin 1992, Wolf and Dewitt 2000). Regardless of the approach used, manual interpretation typically involves delineation of polygon boundaries (areas with similar properties) on a stereo-pair and the subsequent classification of those polygons by a trained specialist. A variety of key characteristics are used to delineate and classify polygons, including tone/color, shape, size,

pattern, texture, shadows, site, and context/association (Figure 2.1) (Avery and Berlin 1992, Lillesand et al. 2004). Interestingly, while these characteristics can help identify important ecological features, they can also be linked to various concepts in ecology (Table 2.4). While we discuss these eight characteristics separately, manual interpretation often requires some combination of these characteristics for feature identification.

Figure 2.1 Aerial photograph subsets: a. Darker tree species near water are coniferous (*Tsuga heterophylla*); lighter tree species are deciduous (*Alnus rubra*). b. Yellow trees are trembling aspen (*Populus tremuloides*); green trees are Sitka spruce (*Picea sitchensis*). c. Larger trees on left side of photograph are mature western hemlock (*T. heterophylla*); on right side of photograph trees are smaller, immature western hemlock (*T. heterophylla*). d. The long, linear object is a road and the irregular geometric patches are cultivated areas. e. The rough texture in the top right corner of the photograph is indicative of a mature stand with high stand complexity; the smooth textured stands at the bottom are more uniform in height, indicating a younger stand. f. Various patterns indicating different agricultural uses (crops, vineyards, etc.) g. Tree shadows cast on the river help species identification (*T. heterophylla* and *Thuja plicata*). h. Lighter color of trees suggests presence of deciduous vegetation. i. Presence of river indicates riparian area. j. Shadow on left side of photograph suggests decrease in elevation towards right side of photograph.

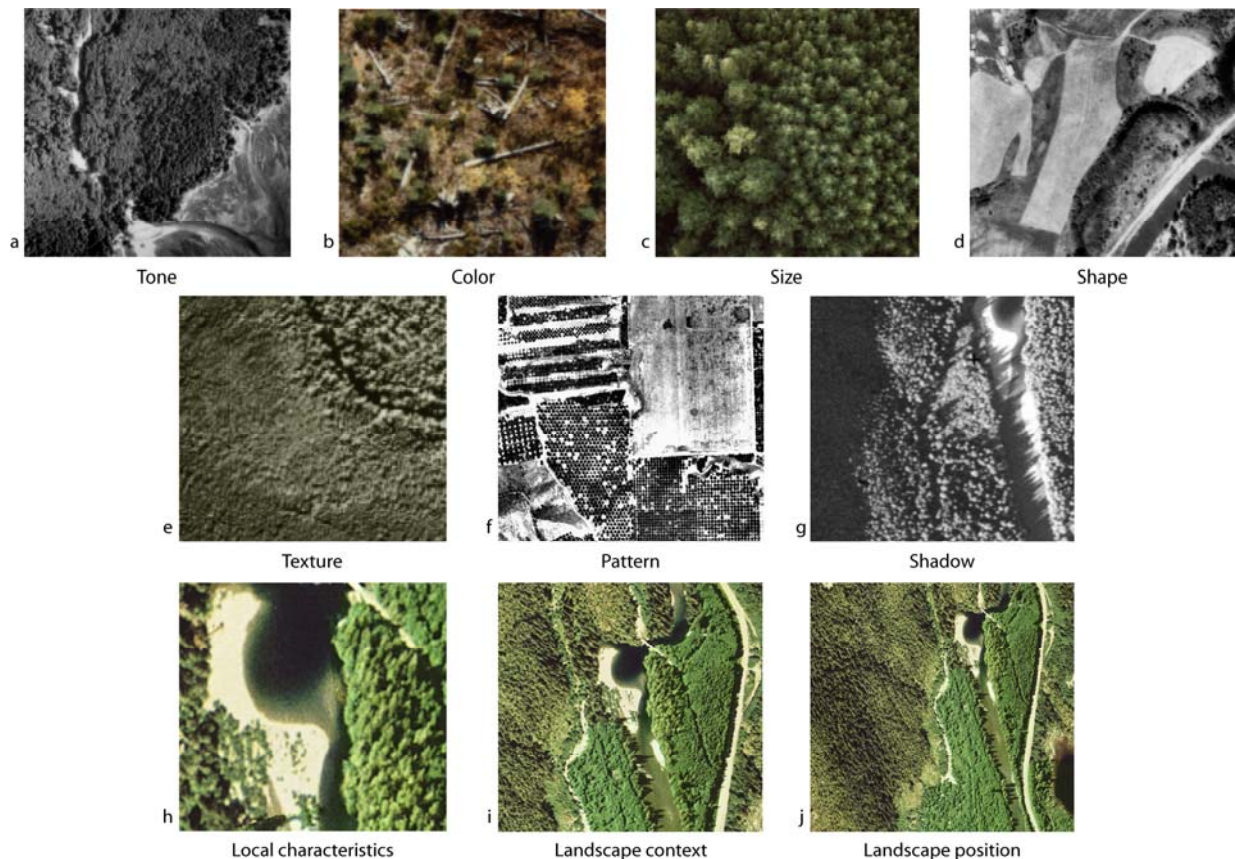


Table 2.4 The eight primary aerial photograph characteristics used in manual interpretation, related ecological features, and examples of corresponding digital methods which may also be useful for analysis of these attributes.

Characteristic	Related Ecological Features	Automated Technique	Description
Tone/Color The relative brightness or hue of pixels	Natural and anthropogenic feature identification (vegetation, soils, urban, etc.)	Contrast Manipulation	Modifies the manner in which pixel brightness values are displayed by splitting values (thresholding), grouping values together (density/level slicing), or adjusting their range of sensitivity (contrast stretching). See (Cohen et al. 1996).
Size The number of pixels that aggregate to form a group of pixels with similar characteristics	Vegetation age, structure Habitat suitability Urban features/land use	Variogram Analysis	Variograms measure spatial autocorrelation by plotting the variance between pixels as a function of distance. Related to correlograms. See (Johnson et al. 2003).
Shape The manner in which related groups of pixels are arranged; the complexity of a feature/patch border	Natural feature identification (irregular shape) Anthropogenic feature identification (geometric shape)	Spatial Feature Manipulation	Highlights specific areas of tonal variation by emphasizing large areas of brightness change (low pass spatial filters), local detail (high pass spatial filters), abrupt changes in brightness values (edge enhancement) or components of spatial frequency (Fourier analysis). See (Karniele et al. 1996, Rowe and Grewe 2001)
Texture The frequency of change in tone among pixels; smoothness or roughness	Vegetation identification Biodiversity estimates Surface properties (natural and anthropogenic features)	GLCM Texture	Based on the Grey-Level Co-occurrence Matrix (GLCM), which summarizes the frequency distribution of various combinations of pixel brightness values. Texture images are created by applying algorithms to each pixel within an image. See (Franklin et al. 2000, Jauhiainen et al. 2007).
Pattern The spatial arrangement and repetition of features (groups of pixels) across an area	Land use Natural/anthropogenic disturbance Habitat suitability Landscape structure	Wavelets	Mathematical function that divides imagery into frequency components at multiple scales. See (Strand et al. 2006).

Characteristic	Related Ecological Features	Automated Technique	Description
Shadow The combination of dark or 'shadow' pixels adjacent to brighter pixels	Natural/anthropogenic feature identification Orientation (landscape, feature, etc.)	Digital terrain correction	Digital terrain/elevation information is used to standardize imagery for brightness variation caused by topography. See (Sheperd and Dymond 2003).
Local Characteristics Conditions at the feature/patch level	Microclimate Local species identification Habitat suitability	Elevation Models	Elevation information, particularly at high spatial resolutions, can be highly useful for classification of local features (as well as land cover over broader scales). See (Dorner et al. 2002, Leckie et al. 2003).
Landscape Context Conditions adjacent to or surrounding a feature/patch	Land use Habitat suitability	Object-based Analysis	Quantitative contextual rules can be used to classify objects/patches based on surrounding conditions, and conditions measured over multiple spatial scales. Also measures characteristics related to tone, size, shape, and texture. See (Hay et al. 2003, Definiens 2007).
Landscape Position Feature/patch location within the landscape, often in relation to topography	Topographic location Vegetation patterns Natural/anthropogenic disturbance patterns	Spatial GIS Datasets	Ancillary datasets can provide a wide range of additional data, useful for image analysis. See (Florinsky 1998, Hoersch et al. 2002).

2.6.1 Tone/Color

Variation and relative differences in tone and color on photographs (radiometric properties) are the primary characteristics enabling feature identification. For example, foliage of deciduous tree species often reflects more light and appears brighter than coniferous species, which are darker because they reflect less light (Figure 2.1). Tone/color can also be used to make inferences related to the state or the condition of certain features. Surficial deposits with dark tones may suggest poor drainage (water absorbs/transmits energy) and high organic matter content, in comparison to lightly-colored deposits which are reflective and usually indicate well-drained materials such as sand or gravel (Keser 1979). Technically, tone and color both relate to the intensity of light reflected by an object/feature; with tone used to describe grayscale variation on black and white (panchromatic) photographs and color referring to the hue characteristics of color photographs (Avery and Berlin 1992). A result of complex interactions between the sun's radiation and the Earth's surface, tone and color are greatly influenced by conditions during photograph acquisition and digitization (Avery and Berlin 1992). Therefore, it is important to compare photographic tone/color and land cover relationships between adjacent photographs or among all photographs used in a project.

2.6.2 Size

The relative and absolute size of objects/features is important not only for identifying both cultural and natural features, but can also be used to make ecological inferences about the features being identified. Size is particularly significant due to its direct connection to spatial scale, a fundamental component of understanding ecological patterns and processes. In ecological applications, scale is often used to describe the size, or spatial unit, of a focal entity/phenomenon. Analyses can focus on multiple spatial scales, such as at the scale of individual tree crowns, where the sizes of individual trees differ according to age class (Figure

2.1); or at broader scales, where the relative sizes of habitat patches can provide indicators of suitability for different species (Turner et al. 1989). The absolute size of various features may also have important ecological implications. Riparian vegetation width is an illustration of this point, because riparian size is important for quantifying local protection afforded to a stream, such as in highly modified watersheds (Roth et al. 1996). Furthermore, spatial characteristics such as the distribution of canopy gaps and other forest structural properties can be identified from high spatial resolution aerial photographs, which are important parameters relevant for many wildlife species (Fox et al. 2000).

2.6.3 Shape

Shape is particularly useful for identifying cultural features, which usually have a specific geometry and obvious edges, as well as many natural features with distinctive forms (Avery and Berlin 1992). In particular, shape can be used to identify various geomorphic features such as fluvial landforms (e.g. fans or oxbow lakes), glacial landforms (e.g. drumlins or cirques) or organic landforms (e.g. swamps or fens) and disturbances such as landslides (Keser 1979). A relevant characteristic over a wide range of spatial scales, shape results from the contrast between the border of a specific feature or patch, and the surrounding environment. At fine scales, aerial photograph interpreters look for recognizable shapes to classify features, such as crown shape to identify tree species, or geometry to identify anthropogenic features, such as the long, linear characteristics of roads (Figure 2.1). At broader scales, patch shape can be used to distinguish between anthropogenic land use (logged stands or agriculture) and natural disturbances (fire or insect damage), and can provide indicators of landscape complexity. Interestingly, patch edges influence many important ecosystem and landscape processes such as habitat quality (Ries et al. 2004); thereby edge characteristics such as shape, play an important role in understanding the interaction between landscape structure and ecological processes.

2.6.4 Texture

Image texture is particularly useful for landform and land cover classification, and is related to variation in biophysical parameters, landscape heterogeneity, forest structural characteristics (Wulder 1998), and can be helpful for prediction of species distribution and biodiversity patterns (St-Louis et al. 2006, Fischer et al. 2008). Aerial photograph interpreters describe texture in terms of smoothness and roughness, and the relative variation of this attribute can be used to distinguish between various features (Avery and Berlin 1992). For example, the textures of different forested stands provide visual indicators of stand complexity, age, and crown closure (Figure 2.1). Texture is commonly used to help differentiate between tree species (Trichon 2001), and other features that may otherwise have similar reflectance and dimensional characteristics (Avery and Berlin 1992, Lillesand et al. 2004). Texture is also useful for identifying soil types, rangeland vegetation, various hydrologic characteristics, and agricultural crops (Lillesand et al. 2004). Texture generally focuses on fine-scale variation (the pixel level), in particular by emphasizing the spatial arrangement and frequency of variation in image tone (Paine and Kiser 2003, Lillesand et al. 2004). However, texture is directly related to spatial scale, meaning textural characteristics will change as the scale of the photograph changes (Avery and Berlin 1992), although textures generally appear smoother as scale increases, or as the altitude of the aircraft increases.

2.6.5 Pattern

In contrast to texture, which focuses on tonal variation at a fine-scale (the pixel level), pattern is concerned with the spatial arrangement of features or patches over coarser scales (Paine and Kiser 2003). Spatial pattern can be random or systematic (Jensen 2000) and is often very distinctive for many anthropogenic and natural features (Avery and Berlin 1992). For instance, trees in an orchard have a systematic pattern (Figure 2.1); whereas the distribution of gaps in old

growth forests may have a more random pattern. In this regard, spatial patterns of features in a photograph can provide important clues for identification of land use, forest structural characteristics, and disturbance types; all important to understand in terms of ecosystem management. In addition, patterns of different habitat or land cover patches can influence movement of organisms and materials across the landscape (Gergel and Turner 2002). The comprehensive approach of aerial photograph interpretation can also be particularly useful for gaining an understanding of the connections and interactions between spatial patterns of natural features and landscape structure. One such case used aerial photograph interpretation aided by information collected in the field to describe the connection between the spatial patterns of ribbon forests and the structure, lithology, and topography of the landscape in Glacier National Park, MT (Butler et al. 2003).

2.6.6 Shadow

Shadows may either help feature identification by providing information about an object/feature's height, shape, and orientation, or hinder classification by obscuring parts of the landscape. Shadows provide profiles or silhouettes of certain objects (Tsai 2006) and are particularly useful for small feature identification, topographic enhancement, or features otherwise lacking tonal contrast (Avery and Berlin 1992, Aronoff 2005). The shadows cast by the crowns of different trees on a contrasting background can be helpful for species identification (Figure 2.1); however excessive shadows can obscure features (Jensen 2000) and distort tone/color, and shape (Tsai 2006). Modern aerial data are typically collected within two hours of solar noon (Jensen 2000), thus limiting the extent of shadows; however shadows are often problematic on historic aerial photographs.

2.6.7 Site and Context

Site and context (sometimes termed association and/or location) are used in manual interpretation; yet, are often defined using overlapping and closely related concepts (Avery and Berlin 1992, Wolf and Dewitt 2000, Paine and Kiser 2003). Despite the confusion surrounding these characteristics, they relate quite well to three very distinct, yet fundamental, ecological concepts: patch characteristics versus landscape context (Pearson 1993), and landscape position (Swanson et al. 1988). Because these concepts are widely recognized as important in ecological planning and management, we propose refining the ideas around site, context, and association, to these three ecologically relevant and well-defined concepts. Local characteristics (at the feature or patch level) are important because they reflect fine-scale, microclimatic conditions (Chen et al. 1999). In contrast, landscape context (conditions surrounding the feature or patch) is essential because the properties of neighboring patches can impact a wide range of ecological phenomena, such as prediction of species for conservation planning (Mazerolle and Villard 1999). In the specific case of identifying high quality bird habitat, characteristics of the landscape surrounding a patch can even have more influence on patch occupancy than any characteristic within the patch itself (Pearson 1993). Finally, landscape position (the location of the feature or patch in relation to topography) is critical because characteristics such as slope, aspect, and moisture gradients affect processes such as vegetation patterns and natural disturbance events (Swanson et al. 1988, Dorner et al. 2002).

Local characteristics, landscape context, and landscape position are often used in tandem by an interpreter to identify various features. Identification of riparian forests, for instance, could be aided by several features: the presence of deciduous vegetation (patch characteristic); its adjacency to a river (landscape context), or by the fact that riparian forests occur in areas of lower relative elevation than upland forests (landscape position) (Figure 2.1). Classification of

bog types in higher latitudes, can also be aided by using local traits such as vegetation type and vegetation presence/absence, contextual attributes such as collapse scars and water pools, and positional traits including relative height (indicating permafrost thickness) and hummocks (Vitt et al. 1994).

2.7 New Approaches for Aerial Photograph Analysis

Recently developed automated methods of image enhancement and classification (typically applied to satellite imagery), are potentially quite useful for aerial photographs, and may help address some of the problems with traditional photo-interpretation (Table 2.3 and 2.5).

Automated analysis of digital imagery has evolved over time into two main approaches (Table 2.5). Conventional automated image analysis has been conducted on a per-pixel basis, whereby enhancement and classification algorithms are applied to individual pixels. While ‘pixel-based’ approaches are relatively easy to implement, the representation of landscape elements with pixels may be less applicable for some features. A contrasting approach is that of object-based analysis (Hay et al. 2003, Definiens 2007). The basic premise of the most common object-based approaches is that neighboring pixels of similar properties are merged to form objects (using a process termed segmentation) prior to analysis (Blaschke 2004). The resulting objects can then be classified using quantitative characteristics such as tone/color, size, shape, texture, and contextual relationships (Hay et al. 2003, Definiens 2007), similar to the approach used by manual interpreters. This method is particularly promising because it can create objects over multiple target scales/sizes to represent the hierarchical nature of ecosystems.

One of the advantages of automated, digital techniques is the ability to explicitly and separately analyze individual characteristics of photographs. Digital edge enhancement is one technique which can help identify shape characteristics by emphasizing abrupt changes in brightness values

Table 2.5 Comparative advantages and disadvantages of manual aerial photograph interpretation, conventional pixel-based analysis, and object-based classification methods.

	Advantages	Disadvantages
Manual Interpretation	<ul style="list-style-type: none"> • Can be fairly accurate • Limited image preparation required • Commonly used to make resource management maps • Comprehensive, uses human knowledge to make logical decisions • Well developed discipline (in some regions) 	<ul style="list-style-type: none"> • Subjective • Time consuming • Inconsistent among interpreters • Expensive • Dependent upon interpreters experience • Shortage of well trained and experienced interpreters • Accuracy standards vary widely
Pixel-based Classifiers	<ul style="list-style-type: none"> • Systematic • Consistent • Repeatable • Many well-developed and affordable software packages available • Pixel-based accuracy assessment techniques are well developed 	<ul style="list-style-type: none"> • Arbitrary analysis unit (pixel) • Tend to utilize only spectral information • Less suited to analysis of high spatial resolution imagery • Can produce speckled ‘salt and pepper’ results • No necessary relation between pixel-based classification and classes on the ground
Object-based Classifiers	<ul style="list-style-type: none"> • Systematic • Consistent • Repeatable • Ability to incorporate multiple scales • Better mimics human perception of objects • Integrates attributes important to landscape analysis (tone, shape, size, texture, context) 	<ul style="list-style-type: none"> • Object creation is difficult and can produce unexpected results • Less availability and affordability of software • Better suited to high spatial resolution imagery • Object-based accuracy assessment procedures less developed

between pixels to identify edges (Table 2.4). Edge detection techniques have been useful for identifying fine-scale features from aerial photographs with distinctive shapes such as roads (Rowe and Grewe 2001) and linear geologic features such as faults, joints, and folds (Karniele et al. 1996). The use of edge detection techniques was able to extract geologic features with results comparable to that of manual interpretation, and improved upon manual interpretation for identification of larger linear features (Karniele et al. 1996). Similarly, texture information is often incorporated by calculating separate texture layers (such as homogeneity or variance) based on the grey level co-occurrence matrix (Table 2.4) and has been helpful for improving the

accuracy of vegetation classifications (Franklin et al. 2000, Jauhiainen et al. 2007). Textural derivatives of this nature can extract various components of image texture (beyond the smooth/rough scale used by manual interpreters) and were useful for exploring drainage-driven vegetation dynamics in various mire sites using recent and historic aerial photography (Jauhiainen et al. 2007). Variogram analysis, which identifies autocorrelation over space (Table 2.4), is another useful tool, and can help identify spatial ranges (sizes) of ecological features or processes, such as disease influence in potato crops (Johnson et al. 2003).

Often, photograph or image analysis approaches incorporate multiple automated techniques, or use techniques which target multiple characteristics of features, to improve classification capacity or accuracy. Mapping individual tree locations is one goal which can be aided by the use of both thresholds (Table 2.4) to target specific tone/color characteristics, and window-based operators to target specific sized objects related to tree crowns; however aerial photographs of high spatial resolutions are required (Utterer et al. 1998). Similarly, wavelets utilize tone, size, and shape characteristics to identify patterns over multiple spatial and/or temporal scales (Table 2.4), and can be used to identify vegetation distribution characteristics such as woody plant encroachment over time (Strand et al. 2006). Object-based classification is another multi-scale approach particularly promising for vegetation and landscape analysis (Blaschke 2004) and was useful for investigating shrub encroachment dynamics (Laliberte et al. 2004). Shrubs $>2\text{m}^2$ in size were delineated from digitized aerial photographs using specific sizes (segmentation scales), and then classified using tone and contextual relationships among neighbors and over multiple spatial scales (Table 2.4) with accuracies of 87% (Laliberte et al. 2004). Since this approach mimics manual interpretation to a certain extent, and is better suited for high spatial resolution imagery (Table 2.5), this tool is particularly promising for aerial photograph analysis.

The integration of digital terrain information with aerial photographs and other remotely sensed imagery can expand mapping capabilities (Florinsky 1998). Local characteristics, such as micro relief can be obtained from highly detailed terrain information (Table 2.4), and is useful for fine-scale applications such as individual tree identification (Leckie et al. 2003). For example, incorporation of lidar with high spatial resolution aerial photographs greatly improves the identification of individual trees and other forest parameters, useful for forest inventory purposes (Leckie et al. 2003). Similarly, broad-scale landscape positional information (such as slope, aspect, and moisture indices) (Table 2.4), can be particularly useful when paired with digital imagery for classifying vegetation distributions in heterogeneous environments (e.g. (Hoersch et al. 2002)). Overall, there is much potential for automated approaches and ancillary datasets to aid analysis and classification of digital or digitized aerial photographs.

2.8 Accuracy Assessment

The value of any analysis or classification is highly dependent upon its accuracy. Thematic maps derived from the classification of remotely sensed imagery are routinely used for mapping land cover and monitoring land cover change. However, ‘poor’ quality or inaccurate land cover maps can render such maps unsuitable for operational purposes (Foody 2002), and inaccuracies can lead to ineffective, costly, or even detrimental ecosystem management decisions (Gergel et al. 2007, Thompson et al. 2007). Establishing the accuracy of a classified product is one of the biggest challenges associated with classification or map production, largely due to the uncertainties regarding the measurement of accuracy, and a lack of strict assessment guidelines suited to this purpose (Foody 2002). As a result, establishing the accuracy of maps derived from either manual interpretation or automated analysis can be problematic.

Accuracy is often estimated by comparison between the classified photograph/image, and reference data derived from field data or alternative thematic datasets (Foody 2002). Collecting field reference data can be problematic for remote or difficult to access locations, and can be expensive over large areas. Furthermore, some attributes identified on photographs may not be measurable from the field (e.g. spatial distributions of patches), and field measurements may be even less accurate than photographic mapping (e.g. canopy gaps) (Fox et al. 2000). As a result, reference data collected from the field is often limited. More common is the use of previous interpretations or other thematic datasets to assess the accuracy of new classifications. However, the accuracy of such original interpretations is rarely verified beyond limited ground checking, and many forest inventory maps are irregularly updated (Thompson et al. 2007). Furthermore, the misclassification rate of such inventories can reach as high as 60% (Thompson et al. 2007). Establishing the accuracy of historic aerial photograph classification has additional challenges, because historic reference data are often inexistent, and subsequent land cover changes frequently render field data collection impossible. Current stump survey data or historic land survey data such as the Public Land Survey (PLS) may provide supplemental reference point data (Manies and Mladenoff 2000). However, in many cases the accuracy of analyses from historical aerial photographs cannot be rigorously quantified. Therefore, any accuracy assessment requires careful consideration of the availability and quality of reference data. Further, data requirements may differ depending on whether pixel- or object-based classification was employed.

In general, two broad types of accuracy should be considered: positional and classification accuracy. Positional accuracy relates to the location of features and their borders, and is important because even small errors in positional accuracy can have important implications on analyses, such as the measurement of river channel movement through time (Hughes et al. 2006).

Positional accuracy of manual interpretation also has important implications, yet polygon position can be highly variable, and is often dependent upon interpreter style. ‘Lumpers’ are interpreters who tend to delineate larger polygons, thereby ‘lumping’ areas of somewhat similar character together. In contrast ‘splitters’ delineate smaller polygons recognizing areas with subtle differences. Point/dot grids and line transect methods may be less problematic and subjective than manual interpretation in terms of positional accuracy; however, these approaches are often time consuming and are primarily used for spatial estimates of cover (Paine and Kiser 2003). While it is arguable that the imposition of abrupt boundaries on natural ecosystems composed of gradients is inherently inaccurate, this type of generalization is a necessary simplification for classification. Methods which do assess border accuracy generally involve rigorous field data collection (Hughes et al. 2006) and therefore, positional accuracy is rarely addressed.

Classification accuracy is related to the labeling of classes, and can vary greatly among different classes. For instance, older stands and those of pure species composition, can generally be identified using photograph interpretation with higher accuracy than mixed species or second-growth stands (Thompson et al. 2007). Additionally, the accuracies of individual species identified using manual interpretation can range from complete misclassification, to near perfect (Thompson et al. 2007). While many methods of class accuracy assessment exist, the most common form of class accuracy representation is through the use of a confusion, or error matrix (Stehman 1997). This provides a cross-tabulation of the relationships between the reference data (‘truth’) and the classification data on a per-class basis for a sample of locations over the entire extent (Foody 2002). Recent work has explored the utility of alternative digital approaches for accuracy assessment including pixel and polygon based approaches for high spatial resolution imagery (Thompson and Gergel 2008), as well as accuracy assessments conducted across multiple spatial scales (Gergel et al. 2007). Although a full discussion is beyond the scope of this

paper, accuracy assessment should suit the data type, classification technique, and classification scheme used, and must work to ensure accuracy is represented as truthfully and completely as possible (Stehman 1997, Foody 2002).

2.9 Conclusions

Routinely used for decades by resource managers (Cohen et al. 1996, Johnston and Lowell 2000), aerial photographs provide a spectrum of useful information to managers and researchers, unique to other types of ecological inventory information. While ecosystem management dilemmas require a differing knowledge base and skill set related to aerial photograph usage, the potential for aerial photographs to help answer many current and pressing ecological questions is considerable. Reconstruction of historic ecosystem conditions from archive aerial photography can be important for characterizing the historic range of variability within ecosystems, useful for development of strategies aimed at managing for ecological integrity (Landres et al. 1999). Historic information from aerial photographs can also be useful for monitoring landscape and ecosystem change (Swetnam et al. 1999), such as tracking decline in foundation species (Trichon 2001, Ellison et al. 2005). Furthermore, archival aerial photographs provide a source of spatially continuous historic information, unlike several other historical reconstruction techniques which lack precise and/or continuous spatial coverage (e.g., dendrochronology or pollen samples) (Macdonald et al. 1991, Foster et al. 1992).

While aerial photographs are certainly useful for a variety of purposes, it is important to emphasize that they have a distinct place within remote sensing and ecology. As discussed throughout this review, there are numerous challenges associated with aerial photograph interpretation and analysis, as found with any other types of remotely sensed data. However, it is

crucial for researchers and managers to identify the strengths and weaknesses of different remotely sensed datasets, and use this knowledge to make informed decisions regarding spatial dataset selection. While aerial photographs are not suited for every mapping purpose, particularly over broader spatial scales (Nichol et al. 2006), they do offer a wealth of ecological information which may be used to answer a wide range of critical ecological questions. Our objective for this paper was to highlight specific uses of aerial photographs for ecosystem research and management, and outline some possible future directions for integration of their unique benefits into ecosystem management applications involving remote sensing.

With the demands for spatially explicit data by resource managers and scientists continuing to grow (Cohen et al. 1996), the use of digitized/digital aerial photographs and the development of automatic analysis techniques can improve the accuracy, consistency, and efficiency of results (Harvey and Hill 2001). Given the unique and important information available from aerial photographs, and the challenges inherent with their interpretation, further research and training with emerging image analysis techniques will be essential to fully avail ourselves of the potential of aerial photographs to assist in ecological management. Promise in combining optical imagery such as aerial photography, with detailed terrain data and other ancillary datasets, may also be of particular importance to explore for a variety of ecosystem applications. Overall, the advances in the field of remote sensing will only further our ability to utilize aerial photographs for ecological means.

2.10 References

- Aronoff S. 2005. Remote Sensing for GIS Managers. Redlands: ESRI Press.
- Avery TA, Berlin GL. 1992. Fundamentals of Remote Sensing and Air Photo Interpretation. Upper Saddle River: Prentice Hall.
- Blaschke T. 2004. Object-based contextual image classification built on image segmentation. IEEE TRANSACTIONS ON GEOSCIENCE AND REMOTE SENSING: 113-119.
- Butler DR, Malanson GP, Bekker MF, Resler LM. 2003. Lithologic, structural, and geomorphic controls on ribbon forest patterns in a glaciated mountain environment. Geomorphology 55: 203-217.
- Chen J, Saunders SC, Crow TR, Naiman RJ, Brosofske KD, Mroz GD, Brookshire BL, Franklin JF. 1999. Microclimate in Forest Ecosystem and Landscape Ecology? Variations in local climate can be used to monitor and compare the effects of different management regimes. BioScience 49: 288-297.
- Cohen WB, Kushla JD, Ripple WJ, Garman SL. 1996. An introduction to digital methods in remote sensing of forested ecosystems: Focus on the Pacific Northwest, USA. Environmental Management 20: 1432-1009.
- Definiens. 2007. Definiens Developer 7 User Guide. Munchen, Germany. Report no.
- Dorner B, Lertzman K, Fall J. 2002. Landscape pattern in topographically complex landscapes: issues and techniques for analysis. Landscape Ecology 17: 729-743.
- Ellison AM, et al. 2005. Loss of foundation species: consequences for the structure and dynamics of forested ecosystems. Frontiers in Ecology and the Environment 3: 479-486.
- Fensham RJ, Fairfax RJ. 2002. Aerial photography for assessing vegetation change: a review of applications and the relevance of findings for Australian vegetation history. Australian Journal of Botany 50: 415-429.

- Fischer J, Lindenmayer DB, Montague-Drake R. 2008. The role of landscape texture in conservation biogeography: a case study on birds in south-eastern Australia. *Diversity and Distributions* 14: 38-46.
- Florinsky IV. 1998. Combined analysis of digital terrain models and remotely sensed data in landscape investigations. *Progress in Physical Geography* 22: 33-60.
- Foody GM. 2002. Status of land cover classification accuracy assessment. *Remote Sensing of Environment* 80: 185-201.
- Foster DR, Zebryk T, Schoonmaker P, Lezberg A. 1992. Post settlement History Of Human Land-Use And Vegetation Dynamics Of A *Tsuga-Canadensis* (Hemlock) Woodlot In Central New-England. *Journal of Ecology* 80: 773-786.
- Fox TJ, Knutson MG, Hines RK. 2000. Mapping Forest Canopy Gaps Using Air-Photo Interpretation and Ground Surveys. *Wildlife Society Bulletin* 28: 882-889.
- Franklin SE, Hall RJ, Moskal LM, Maudie AJ, Lavigne MB. 2000. Incorporating texture into classification of forest species composition from airborne multispectral images. *International Journal of Remote Sensing* 21: 61-79.
- Gergel SE, Turner MG. 2002. *Learning Landscape Ecology: A Practical Guide to Concepts and Techniques*. USA: Springer Science+Business Media, LLC.
- Gergel SE, Stange Y, Coops NC, Johansen K, Kirby KR. 2007. What is the Value of a Good Map? An Example Using High Spatial Resolution Imagery to Aid Riparian Restoration. *Ecosystems* 10: 688-702.
- Harvey KR, Hill GJE. 2001. Vegetation mapping of a tropical freshwater swamp in the Northern Territory, Australia: a comparison of aerial photography, Landsat TM and SPOT satellite imagery. *International Journal of Remote Sensing* 22: 2911-2925.

- Hay GJ, Blaschke T, Marceau DJ, Bouchard A. 2003. A comparison of three image-object methods for the multi-scale analysis of landscape structure. *ISPRS Journal of Photogrammetry & Remote Sensing* 57: 327-345.
- Hoersch B, Braun G, Schmidt U. 2002. Relation between landform and vegetation in alpine regions of Wallis, Switzerland. A multi-scale remote sensing and GIS approach. *Computers, Environment and Urban Systems* 26: 113-139.
- Hughes ML, McDowell PF, Marcus WA. 2006. Accuracy assessment of georectified aerial photographs: Implications for measuring lateral channel movement in a GIS. *Geomorphology* 74: 1-16.
- Jauhainen S, Holopainen M, Rasinmaki A. 2007. Monitoring peat land vegetation by means of digitized aerial photographs. *Scandinavian Journal of Forest Research* 22: 168-177.
- Jensen JR. 2000. *Remote Sensing of the Environment: An Earth Resource Perspective*. Upper Saddle River: Prentice-Hall, Inc.
- Johnson DA, Alldredge JR, Hamm PB, Frazier BE. 2003. Aerial Photography Used for Spatial Pattern Analysis of Late Blight Infection in Irrigated Potato Circles. *Phytopathology* 93: 805-812.
- Johnston D, Lowell K. 2000. Forest Volume Relative to Cartographic Boundaries and Samples Spacing, Unit Size and Type. *Geographic & Environmental Modeling* 4: 105-120.
- Karniele A, Meisels A, Fisher L, Arkin Y. 1996. Automatic Extraction and Evaluation of Geologic Linear Features from Digital Remote Sensing Data Using a Hough Transform. *Photogrammetric Engineering & Remote Sensing* 62: 525-531.
- Keser N. 1979. *Interpretation of Landforms from Aerial Photographs*: Ministry of Forests, Province of British Columbia.

- Laliberte AS, Rango A, Havstad KM, Paris JF, Beck RF, McNeely R, Gonzalez AL. 2004. Object-oriented image analysis for mapping shrub encroachment from 1937 to 2003 in southern New Mexico. *Remote Sensing of Environment* 93: 198-210.
- Landres PB, Morgan P, Swanson FJ. 1999. Overview of the use of natural variability concepts in managing ecological systems. *Ecological Applications* 9: 1179-1188.
- Leckie D, Gougeon F, Hill D, Quinn R, Armstrong L, Shreenan R. 2003. Combined high-density lidar and multispectral imagery for individual tree crown analysis. *Canadian Journal of Remote Sensing* 29: 633-649.
- Lillesand TM, Kiefer RW, Chipman JW. 2004. *Remote Sensing and Image Interpretation*. USA: John Wiley & Sons, Inc.
- Macdonald GM, Larsen CPS, Szeicz JM, Moser KA. 1991. The Reconstruction Of Boreal Forest-Fire History From Lake-Sediments - A Comparison Of Charcoal, Pollen, Sedimentological, And Geochemical Indexes. *Quaternary Science Reviews* 10: 53-71.
- Manies KL, Mladenoff DJ. 2000. Testing methods to produce landscape-scale pre-settlement vegetation maps from the U.S. public land survey records. *Landscape Ecology* 15: 741-754.
- Mazerolle MJ, Villard MA. 1999. Patch characteristics and landscape context as predictors of species presence and abundance: A review. *Ecoscience* 6: 117-124.
- Nichol JE, Shaker A, Wong M-S. 2006. Application of high-resolution stereo satellite images to detailed landslide hazard assessment. *Geomorphology* 76: 68-75.
- Paine DP, Kiser JD. 2003. *Aerial Photography and Image Interpretation*, 2nd Edn. Hoboken, New Jersey: John Wiley & Sons, Inc.
- Pearson SM. 1993. The Spatial Extent and Relative Influences of Landscape-Level Factors on Wintering Bird Populations. *Landscape Ecology* 8: 3-18.

- Ries L, Fletcher RJ, Battin J, Sisk TD. 2004. Ecological Responses to Habitat Edges: Mechanisms, Models, and Variability Explained *Annual Review of Ecology, Evolution and Systematics* 35: 491-522.
- Roth NE, Allan JD, Erickson DL. 1996. Landscape influences on stream biotic integrity assessed at multiple spatial scales. *Landscape Ecology* 11: 141-156.
- Rowe NC, Grewe LL. 2001. Change detection for linear features in aerial photographs using edge-finding. *IEEE TRANSACTIONS ON GEOSCIENCE AND REMOTE SENSING* 39: 1608-1612.
- Sader SA, Vermillion S. 2000. Remote Sensing Education: An Updated Survey. *Journal of Forestry* 98: 31-37.
- Sheperd JD, Dymond JR. 2003. Correcting satellite imagery for the variance of reflectance and illumination with topography. *International Journal of Remote Sensing* 24: 3503-3514.
- St-Louis V, Pidgeon AM, Radeloff VC, Hawbaker TJ, Clayton MK. 2006. High-resolution image texture as a predictor of bird species richness. *Remote Sensing of Environment* 105: 299-312.
- Stehman SV. 1997. Selecting and interpreting measures of thematic classification accuracy. *Remote Sensing of Environment* 62: 77-89.
- Strand EK, Smith AMS, Bunting SC, Vierling LA, Hann BD, Gessler PE. 2006. Wavelet estimation of plant spatial patterns in multi-temporal aerial photography. *International Journal of Remote Sensing* 27: 2049-2054.
- Swanson FJ, Kratz TK, Caine N, Woodmansee RG. 1988. Landform effects on ecosystem patterns and processes. *Bioscience* 38: 92-98.
- Swetnam TW, Allen CD, Betancourt JL. 1999. Applied Historical Ecology: Using the Past to Manage for the Future. *Ecological Applications* 9: 1189-1206.

- Thompson ID, Maher SC, Rouillard DP, Fryxell JM, Baker JA. 2007. Accuracy of forest inventory mapping: Some implications for boreal forest management. *Forest Ecology and Management* 252.
- Thompson SD, Gergel SE. 2008. Conservation implications of mapping rare ecosystems using high spatial resolution imagery: recommendations for heterogeneous and fragmented landscapes. *Landscape Ecology* 23: 1023-1037.
- Trichon V. 2001. Crown typology and the identification of rain forest trees on large-scale aerial photographs. *Plant Ecology* 153: 301-312.
- Tsai VJD. 2006. A Comparative Study on Shadow Compensation of Color Aerial Images in Invariant Color Models. *IEEE TRANSACTIONS ON GEOSCIENCE AND REMOTE SENSING* 44: 1661-1671.
- Tuominen S, Pekkarinen A. 2004. Local radiometric correction of digital aerial photographs for multi source forest inventory. *Remote Sensing of Environment* 89: 72-82.
- Tuominen S, Pekkarinen A. 2005. Performance of different spectral and textural aerial photograph features in multi-source forest inventory. *Remote Sensing of Environment* 94: 256-268.
- Turner MG, O'Neil RV, Gardner RH, Milne BT. 1989. Effects of changing spatial scale on the analysis of landscape pattern. *Landscape Ecology* 3: 153-162.
- Uuttera J, Haara A, Tokola T, Maltamo M. 1998. Determination of the spatial distribution of trees from digital aerial photographs. *Forest Ecology and Management* 110: 275-282.
- Vitt DH, Halsey LA, Zoltai SC. 1994. The Bog Landforms of Continental Western Canada in Relation to Climate and Permafrost Patterns. *Arctic and Alpine Research* 26: 1-13.
- Warner W, Graham R, Read R. 1996. *Small Format Aerial Photography*. Bethesda, Maryland: American Society for Photogrammetry and Remote Sensing.

Wolf PR, Dewitt BA. 2000. Elements of Photogrammetry with Applications in GIS. USA:
McGraw-Hill.

Wulder M. 1998. Optical Remote Sensing Techniques for the Assessment of Forest Inventory
and Biophysical Parameters. *Progress in Physical Geography* 22: 449-476.

3 A COMPARISON OF MANUAL AND AUTOMATED APPROACHES FOR CLASSIFICATION OF DIGITAL AERIAL PHOTOGRAPHS²

3.1 Introduction

Interpretation of aerial photographs is one of the most commonly used methods for production of ecosystem classification and inventory maps, which are subsequently used to make many decisions related to resource management (Cohen et al. 1996, Hall 2003, Thompson et al. 2007).

While aerial photograph interpretation is one of the most accurate approaches for air photo classification (Wulder 1998), there are many issues inherent to this approach. Manual interpretation is the result of an individual's perception, meaning results are often inconsistent, subjective, and difficult to replicate (Fookes et al. 1991, Wulder et al. 2008). Furthermore, there is a severe lack of interpreters being trained to replace the large number of experienced interpreters nearing retirement. Along with these practical and methodological issues, manual interpretation is associated with high financial costs, as well as extensive time and labor requirements (Green 2000), which results in infrequent updates to interpretations.

Given the value of aerial photographs, and the current problems associated with traditional interpretation, there is a heightened need for development of new, automated methods for air photo analysis (Morgan et al. In Press). Fortunately, extensive advances have been made in the field of digital image analysis. Object-based analysis is one such approach which has shown considerable promise for a variety of mapping purposes, such as forest inventories (Chubey et al. 2006, Wulder et al. 2008), agricultural land use (Lucas et al. 2007, Watts et al. 2009), and changes in land cover over time (Laliberte et al. 2004, Pringle et al. 2009). While numerous

² A version of this paper is in the final stages of preparation for submission. Morgan, J.L. Gergel S.E. Comparison of Manual and Automated Approaches for Digital Aerial Photograph Analysis. *Canadian Journal of Remote Sensing*.

algorithms for object-based analysis have been developed (Hay et al. 2003, Shankar 2007), region-merging algorithms (which group neighboring pixels into regions of minimum within-object heterogeneity) are the most common, in part due to the commercial availability of software using this approach (Definiens 2007). This method is also used because it offers several advantages to pixel-based image analysis methods, such as the ability to represent landscape information over multiple spatial scales and the integration of contextual information (Benz et al. 2004, Blaschke 2004).

Another analysis method with potential for automated classification are Classification And Regression Tree (CART) models, which use measured variables to predict both categorical and continuous response variables (Bittencourt and Clarke 2003). CART analysis has proven useful for land cover mapping over various spatial scales (Hansen et al. 2000, Sugumaran et al. 2003). Recently, the integration of object-based segmentation and CART modeling approaches for digital imagery analysis has been explored with success (Chubey et al. 2006, Laliberte et al. 2007, Mallinis et al. 2008, Thomas et al. 2003). While this integrative approach has yielded promising results and is well suited to the high resolution of aerial photographs, few studies have compared the results achieved by automated approaches to manual interpretation. Exceptions focus on border accuracy, and include both qualitative (Leckie et al. 2003, Wulder et al. 2008) and quantitative comparisons (Radoux and Defourny 2007).

Our objective is to explore the use of object-based analysis and classification tree modeling as a tool for supplementing manual interpretation and addressing some of the issues inherent to interpretation. As traditional interpretation consists of two primary steps; 1) polygon delineation; and 2) polygon classification (Avery and Berlin 1992, Paine and Kiser 2003), we use 1) object-based segmentation; and 2) decision tree modeling, to mimic these steps. To determine the

ability of the automated approach to replicate manual interpretation, we quantitatively compare the results of this twofold approach over local, polygon and landscape scales. We use a set of historic aerial photographs within an un-harvested watershed for the comparison, and include texture and terrain data for the automated analyses. Historic aerial photographs are used because of the inherent value of historic landscape information for conservation and restoration (Swetnam et al. 1999). We believe our comprehensive and quantitative comparison of the manual interpretation process to a fully automated approach is novel, and provides the groundwork for further exploration of alternative methods to address the numerous challenges inherent to manual air photo interpretation.

3.2 Methods

3.2.1 Study Area and Spatial Data

The research was conducted within the Kennedy Lake watershed in Clayoquot Sound, BC, Canada (Figure 3.1). Located on the west coast of Vancouver Island, the watershed has a drainage area of approximately 55,013 ha and is dominated by temperate rainforest. Average precipitation for this area is 400-700cm, with mean temperatures ranging from 5-15°C.

Dominant tree species include western hemlock (*Tsuga heterophylla*), western redcedar (*Thuja plicata*), amabilis fir (*Abies amabilis*), yellow cedar (*Chamaecyparis nootkatensis*), sitka spruce (*Picea sitchensis*), and red alder (*Alnus rubra*). There are over 57 different vegetated ecosystems currently represented within the watershed according to provincial classification schema (TPC 2006). Much of the floodplain within the Kennedy Lake watershed has been harvested, and there is ongoing restoration occurring throughout this area.

Figure 3.1 The Kennedy Lake watershed is located on the west coast of Vancouver Island, British Columbia, Canada.



Panchromatic, vertical aerial photographs taken in 1937-38 were used for this analysis. Since riparian corridors and floodplain ecosystems are exceptionally diverse in this area, and have been highly modified as a result of extensive timber harvest, our sampled photographs were chosen to represent the historic diversity within these sites. Digital scans of the photographs were obtained from the National Air Photo Library in Ottawa, Canada. The original contact prints were scanned with a resolution of 1200dpi and radiometric corrections were applied to each photograph to balance grey levels across the images. Eight stereo-pairs (two adjacent photographs possessing spatial overlap from the same flight line) were selected spanning a range of watershed orders

(Appendix A). Further photographs were not included due to cost limitations associated with manual interpretation.

3.2.2 Manual Interpretation

The interpretation process used a digital approach, in which polygons were digitized and then classified from scanned stereo-pairs (APS 2008). This approach required the transformation of stereo-pairs into stereo-models, which are 3-dimensional digital models representing the area of overlap between photographs with accurate distances, angles, and areas. First, tie points (identical locations on both photographs) were created to link the stereo-pair and identify the area of overlap between the two photos. Next, spatial coordinates were assigned to the photographs using 1:20,000 Terrain Resource Information Management (TRIM) maps generated by the province of British Columbia (GeoBC 1996). A Triangulated Irregular Network (TIN), (the required format for digital topographic files within APS) was created from the TRIM data. Using this TIN, ten to twelve control points were collected from identical locations (x, y, and z) on the two photographs and the TRIM data. Residual errors were less than 1m for all eight sites.

Once the stereo-models were created, all eight landscapes were manually classified. Photograph interpretation was performed by a certified air photo interpreter in coastal British Columbia, and consisted of two primary steps. First, polygons representing areas of uniform land cover characteristics were digitized on the stereo-models. The second step involved assignment of classification attributes to the created polygons. Manual interpretation is executed using a ‘convergence of evidence’ approach, in which traits over numerous spatial scales including tone, shape, size, texture, pattern, shadow, site (local topography) and context (neighboring characteristics) are considered in combination.

Categories identified were based upon the Vegetation Resources Inventory standards of British Columbia (Province of British Columbia 2002) and included historic values for leading species, vertical complexity, overall productivity, site position, and surface expression (Table 3.1).

Leading species is the tree species of highest proportion within a polygon. Vertical complexity is an important indicator of potential wildlife habitat, and represents canopy complexity based on stand age, species composition, and disturbances (Province of British Columbia 2002). Higher values indicate more complexity, and therefore greater variability of tree height and age within the stand. Site productivity is a relative measure of the potential for tree growth based on site-specific conditions (such as soil moisture or exposure to sunlight). Site position is related to the dominant soil moisture regime, and refers to the polygon location in terms of slope position within a catchment. Surface expression is the dominant form of the surficial material, and is useful for deduction of soil parent material (Province of British Columbia 2002).

3.2.3 Automated Object Creation

Classification of forest parameters in previous research has been aided by both image texture (Franklin et al. 2000; Wulder et al. 2004), and terrain information (Swanson et al. 1988, Treitz and Howarth 2000). Thus, textural and topographic derivatives were generated for all eight landscapes to better capture variability within these areas. Correlation, entropy, and homogeneity (which represent tonal characteristics) were calculated using the co-occurrence matrix of each photograph and a processing window of 3 x 3 pixels (ENVI 2007). These texture layers were selected based on their low inter-layer correlations ($\text{abs}(r) < 0.65$). A Digital Elevation Model (DEM) was created by converting TRIM mass points into a raster DEM (ESRI 2006), and then resampling the data to match the spatial resolution of the photographs which was 0.5m. (The data were resampled because matching spatial resolutions are required for data input into the object-based software. While data resampling is artificially increases information content, subsequent

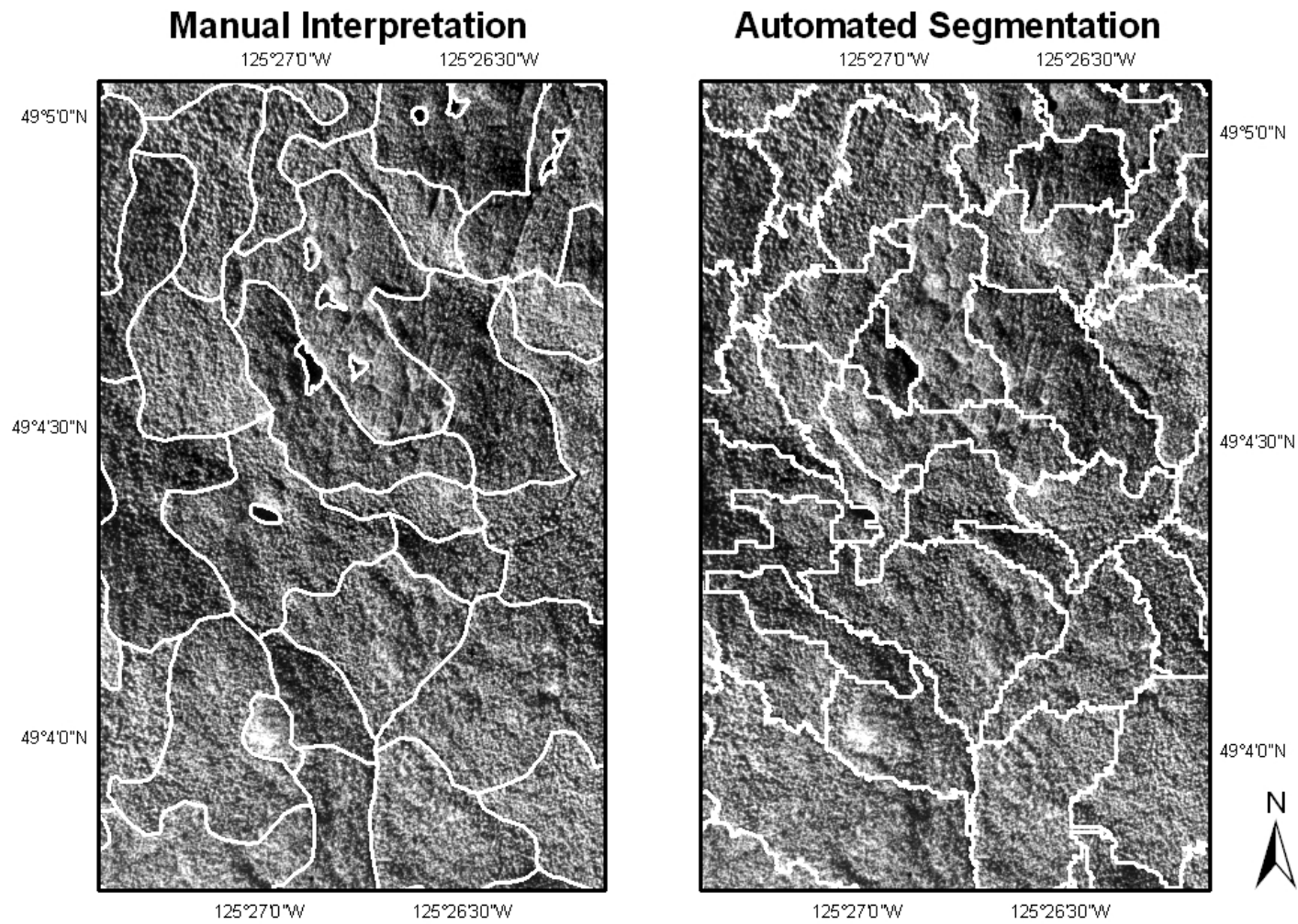
Table 3.1 Five classification schemes as used within the Vegetation Resources Inventory in British Columbia (Province of British Columbia 2002). Note: For polygons marked none, the absence of forest cover, shadows or other interfering factors impeded classification.

Classification Scheme	Class Label	Definition	Percentage of polygons (N=541) assigned to each class by the interpreter
Leading Species	Cw	Cedar, Western Red	44.5
	Hw	Hemlock , Western	21.2
	Ss	Spruce, Sitka	1.1
	Yc	Cedar, Yellow	2.6
	Hm	Hemlock, mountain	3.9
	Fd	Fir, Douglas	0.4
	Ba	Fir, Amabilis	10.7
	Dr	Alder, Red	15.2
	None	No classification	0.4
Vertical Complexity	None	No classification	15.2
	1	Very Uniform	36.2
	2	Uniform	34.6
	3	Moderately Uniform	6.8
	4	Non-uniform	5.9
	5	Very non-uniform	1.3
Site Productivity	VP	Very Poor	27.7
	PR	Poor	38.8
	MD	Moderate	15.0
	GD	Good	7.4
	VG	Very Good	9.6
	None	No classification	1.5
Site Position	Cr	Crest	3.7
	Up	Upper Slope	1.8
	Mid	Middle Slope	24.4
	Low	Lower Slope	11.5
	Toe	Toe	16.5
	Fl	Flat	19.9
	Dep	Depression	10.0
	Wet	Wetland	10.4
	None	No Classification	1.8
Surface Expression	C	Cone	20.1
	D	Depression	1.7
	F	Fan	0.7
	H	Hummock	25.3
	M	Rolling	23.7
	N	No dominant expression	0.7
	P	Plain	10.0
	R	Ridge	7.4
	T	Terrace	6.1
	U	Undulating	0.2
None	No Classification	4.1	

segmentation groups this data into objects larger in size than the resolution of the original TRIM data). In addition to the elevation data, an aspect layer (ESRI 2006) and a topographic wetness index (Gessler et al. 1995) were generated to represent different attributes of terrain. The aspect layer was rescaled with a cosine transformation to represent data from 180° (north) to -180° (south). Values for the topographic wetness index ranged from -1.5 to 25 and represented potential moisture.

The segmentation process within the object-based classifier (Definiens 2007) was used to generate objects for comparison to the manually delineated polygons (Figure 3.2). Segmentation creates objects by grouping neighboring pixels of similar characteristics, and is controlled by three user-defined factors: a set of input layers, a scale parameter, and the homogeneity criterion (Definiens 2007). The settings for most factors were determined iteratively. First, segmentations in which the reflectance values of the photographs (weight =3) were weighted to have equal influence to the terrain data (weight =1 for DEM, aspect, and TWI) yielded objects that were qualitatively the most similar to manual polygons. The textural derivatives were not used for object creation. Scale parameters (which indirectly influence how large the objects will be) ranged from 1200-1650 and were selected to produce approximately the same number of objects as compared to manual polygons. Finally, a homogeneity criterion (which primarily dictates the shape of the resulting object) with a weighting of 0.7 to favor object tone (versus shape) and 0.7 in favor of compactness (versus smoothness) produced objects most similar in appearance to manually digitized polygons.

Figure 3.2 An illustrative example of manually-delineated polygons and segmented objects (shown in white) for a subset of an example landscape.

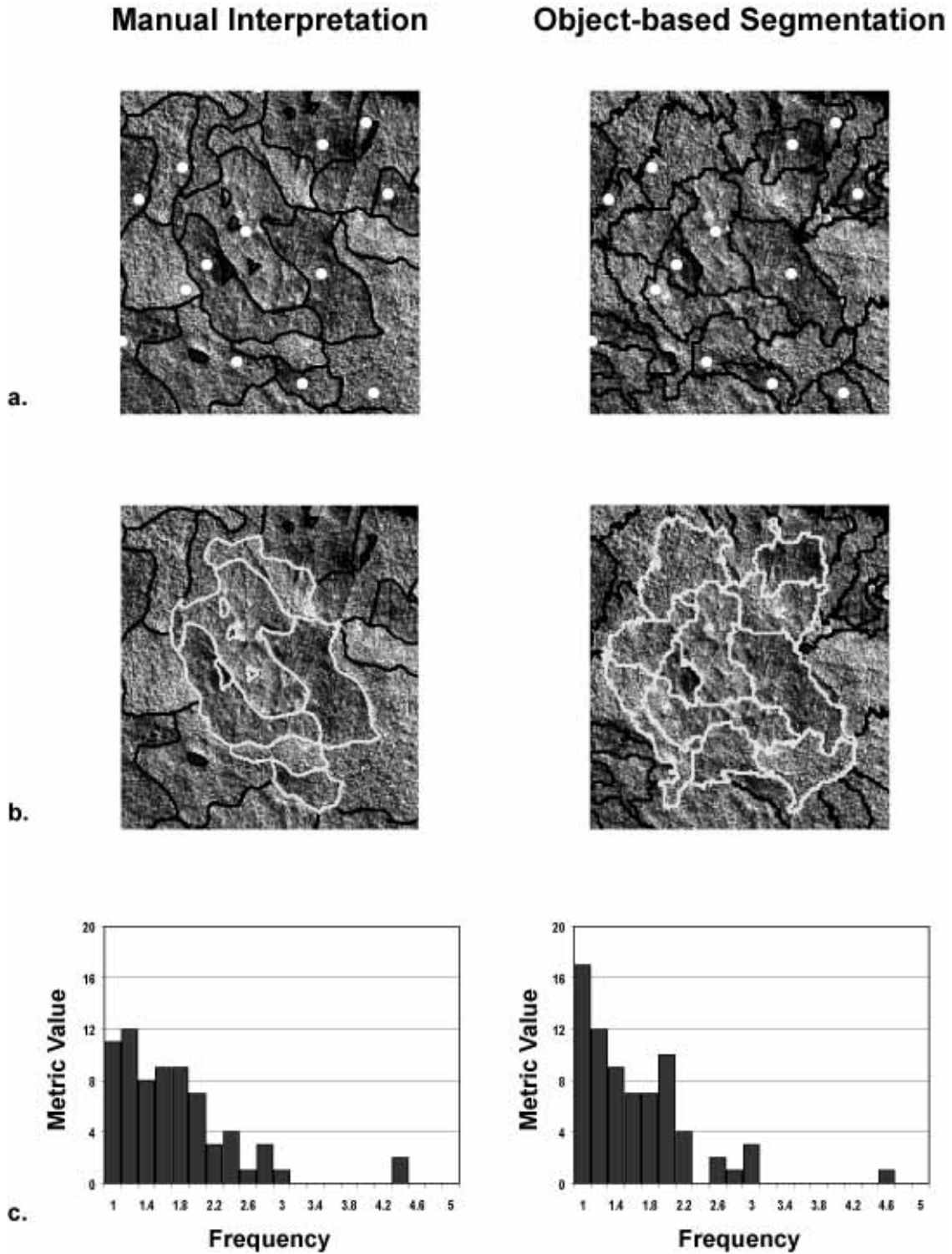


3.2.4 Comparison of Manually-delineated Polygons and Segmented Objects

The two approaches were evaluated by comparing quantitative metrics describing characteristics of individual objects and polygons. Thirty object-based metrics related to object size, shape, tone, texture, topography, and context were first calculated for all segmented objects within the eight landscapes (listed in results). In order to calculate the same object-based metrics for the manually-delineated polygons, a shape file of the manual polygons was used to define the objects for a second segmentation at each landscape. Essentially, rather than a segmentation based on input layers, scale parameters, and a homogeneity criterion, the second segmentation was based upon the manual polygons. Once the same 30 metrics were calculated for the automated segmentations and the manual interpretations at each landscape, all metrics were exported as text files. Polygons or objects adjacent to borders of the photograph were excluded from this comparison in order to avoid the influence of edges on the statistics and to avoid using ‘incomplete’ polygons. (Approximately 50% of the polygons were excluded as a result.)

Three non-parametric statistical tests were used to compare results over local, polygon, and landscape scales for each of the eight landscapes (Figure 3.3). First, the two approaches were evaluated at a localized level, by comparing mean values of object characteristics across paired locations using paired t-tests (SAS 2003). A random sample of 15 paired locations for each landscape (representing approximately 1/3rd of the manual polygons and delineated objects) was selected such that no polygon or object was sampled twice. Second, the ranked means of the 30 metrics were compared at the polygon level, using the Wilcoxon rank-sum test (SAS 2003). Lastly, the distributions of the 30 metrics for all polygons within the entire landscape were compared with the Kolmogorov-Smornoff test (SAS 2003). If the means or distributions were not statistically different, this indicated statistical similarities between the manual polygons and the segmented objects. All tests used a significance value of 0.05. Non-parametric methods were

Figure 3.3 The three spatial levels of statistical comparison between the manually-delineated polygons and segmented objects (shown in black) including a) a subset of one image showing paired locations (white dots); b) a subset of one image showing non-border polygons (shown in gray); and c) an example of two frequency distributions of the objects and polygons as shown in b.



used because most metrics failed tests of normality. Results were summarized according to the number of landscapes in which a test was not significantly different. Therefore, the higher the number of landscapes for which a metric was not statistically different, the greater likelihood the segmented objects were similar to the manually delineated polygons.

3.2.5 Automated Object Classification

A Classification and Regression Tree (CART) approach was used to classify the segmented objects. The end product of CART analysis is a logical model, which classifies objects using a series of predictor variables (Sherrod 2008). The predictor variables were the 30 object-based used for comparison of the manual delineation and automated segmentation results (listed in results), and the target classes were the five historic classification schemes used for the manual interpretation (Table 3.1). Classification trees were built using the Gini splitting (tree fitting) algorithm, which defines classes based on a process of binary recursive partitioning (Bittencourt and Clarke 2003, Sherrod 2008). A series of binary splits are used to iteratively divide all entities into homogenous groups, using predictor variables best able to differentiate the data into the target classes. CART models were built using the five classification schemes two ways. First, models were built for individual landscapes to account for tonal (and textural) variability among the eight photographs for a total of 40 models. Second, combined datasets were used to assess the practicality of implementing CART analysis over photographs from various flight lines by using a dataset combining all landscapes for a total of 5 models.

Classification tree sizes and accuracies were determined using minimum cost complexity within a 10 V-fold cross validation method (Sherrod 2008). This process works by building ten test trees using a subset of the data. Each tree is built using 90% of the total data; however, different portions of the data are used to create each tree. As a result, each 10% increment of data not used

to build the models is completely unique, and therefore suitable for independent validation (Sherrod 2008). To determine tree size, classification error rates were calculated for each step (or split) of the model and weighted according to the size of the model (or number of splits). Minimum weighted classification error (or cost) was used to determine tree size. Comparative classification accuracy was assessed using the reserved validation data and represented with confusion matrices and misclassification values. Acceptable overlap accuracies for producer's and user's statistics were also calculated for classification schemes with ranked classes (such as vertical complexity which ranges from uniform to very complex). Essentially, if a class was incorrectly classified as its neighboring class (for example, a polygon with low slope position was incorrectly labeled as having either a toe or middle slope position), this still represented an acceptable classification. For each classification scheme, this information was summarized across all landscapes, and used to quantify model and individual class accuracy. Classification trees built using the combined data for all landscapes, were used to provide models for the five schemes, and determine the metrics best able to predict classes within each scheme.

3.3 Results

3.3.1 Comparison of Object and Polygon Characteristics

Over 70% of the metrics compared between the two approaches were statistically similar across local, polygon, and landscape scales (Table 3.2). Locally, only the shape index and the standard deviation of the aspect layer were significantly different using paired comparisons. These were the only metrics that differed significantly in all three statistical tests. Along with these two metrics, object compactness and border length were also statistically different when comparing the rank scores of object characteristics at the polygon level. In contrast, almost one-third of the distributions of object characteristics were statistically different at the landscape level. Metrics for which distributions were significantly different included size, most shape based measures,

Table 3.2 Comparison of 30 characteristics for objects derived from an automated segmentation and manual interpretation over three spatial scales. The number of landscapes (N = 8) in which the segmented objects were statistically similar to the manually-delineated polygons are shown. Numbers shown in bold indicate polygon characteristics not well mimicked by the automated approach.

Object/Polygon characteristic (object-based metric)	Local – Mean paired samples	Polygon – Mean rank scores	Landscape – Empirical distribution	Abbreviation
Area	8	8	1	Area
Length	7	8	0	Length
Width	8	8	1	Width
Length/width	8	8	6	Length_wid
Compactness	7	2	1	Compact
Shape index	1	0	0	Shape_ind
Border length	6	1	0	Border
Distance to image border	8	8	8	Distanceto
Radius of largest enclosed ellipse	7	7	3	Radius
Mean aspect	8	7	7	MeanAspect
Mean correlation	8	6	7	MeanCorrel
Mean DEM	8	8	8	MeanDEM
Mean entropy	6	7	8	MeanEntrop
Mean homogeneity	6	7	8	MeanHomog
Mean photo	8	7	7	MeanPhoto
Mean TWI	8	7	8	MeanTWI
Standard deviation aspect	0	0	0	SD_asp
Standard deviation correlation	8	7	8	SD_corr
Standard deviation DEM	7	8	5	SD_DEM
Standard deviation entropy	6	6	8	SD_ent
Standard deviation homogeneity	7	8	8	SD_hom
Standard deviation photo	6	7	7	SD_pho
Standard deviation TWI	7	8	8	SD_TWI
Mean difference to neighbors (aspect)	8	8	3	MD_asp
Mean difference to neighbors (correlation)	8	7	6	MD_corr
Mean difference to neighbors (DEM)	8	6	8	MD_DEM
Mean difference to neighbors (entropy)	7	8	5	MD_ent
Mean difference to neighbors (homogeneity)	7	7	5	MD_hom
Mean difference to neighbors (photo)	7	7	8	MD_pho
Mean difference to neighbors (TWI)	8	7	8	MD_TWI

and metrics related to aspect. Mean values of border length, the shape index, and compactness were higher for the automated objects than the manually delineated polygons, whereas the standard deviation of aspect was lower. Mean difference to neighbors of the aspect layer exhibited greater variance among the segmented objects than the manual polygons; however variability of mean object area and other size metrics were greater for the manual polygons.

3.3.2 Comparative Accuracy of the Five Classification Schemes

Comparative accuracies for the five historic classification schemes ranged from 53.9 - 64.4% when totaled across the eight landscapes (Table 3.3-3.7), and decreased to 50.7 - 53.5% when using the dataset combining all landscapes (Table 3.8). All accuracies as reported in this analysis are comparative accuracies between the manual interpretation and the classification tree model, and are therefore not reflective of actual ground accuracy. The Leading Species classification model had the highest overall accuracy of the five schemes (Table 3.3), and was highly dependent upon textural information for class separation (Table 3.8). The Leading Species model built using the combined dataset accounted for only three tree species and polygons with no classification (Figure 3.4), yet these classes made up 92% of the total data. The Vertical Complexity scheme had relatively low accuracies (Table 3.4), being highly dependent upon tonal information for model development (Table 3.8). The third classification scheme, Site Productivity, had low accuracies for all models (Table 3.5 and 3.8), and identified only half of the classes when using the combined dataset. The Site Position classification scheme generally produced poor models (Table 3.6 and 3.8) yet identified the highest proportion of classes (6/9 describing 93% of the data), out of the five classification schemes. Topographic data contributed to the relatively higher classification accuracies for the Surface Expression classification scheme (Table 3.7 and 3.8, Figure 3.5).

Table 3.3 Totalled accuracy assessment results summarized over all eight landscapes for the Leading Species classification scheme (defined in Table 3.1).

		Predicted Category									
		Class (N)	Ba	Cw	Dr	Fd	Hm	Hw	None	Ss	Yc
Actual Category	Ba	22	26	0	0	2	7	1	0	0	58
	Cw	9	190	0	0	3	31	5	0	4	242
	Dr	0	1	0	0	0	1	0	0	0	2
	Fd	0	0	0	0	0	2	0	0	0	2
	Hm	2	8	0	0	6	3	2	0	0	21
	Hw	5	46	0	0	5	49	10	0	0	115
	None	3	13	0	0	1	6	58	0	1	82
	Ss	0	1	0	0	0	4	0	0	0	5
	Yc	2	8	0	0	1	0	2	0	1	14
	Total	43	293	0	0	18	103	78	0	6	541
Producer's Accuracy (%)		51.2	64.8	0	0	33.3	47.6	74.4	0	16.7	
User's Accuracy (%)		37.9	78.5	0	0	28.6	42.6	70.7	0	7.1	
Overall Accuracy (%)		25.5	76.1	0	0	23.3	33.5	44.8	0	3.6	64.4

Table 3.4 Totalled accuracy assessment results summarized over all eight landscapes for the Vertical Complexity classification scheme (defined in Table 3.1). Acceptable overlap accuracies for producer's and user's accuracies are shown in brackets.

		Predicted Category						
		Class (N)	None	1	2	3	4	5
Actual Category	None	52	15	13	0	2	0	82
	1	4	122	65	2	3	0	196
	2	7	59	110	1	10	0	187
	3	0	11	21	1	4	0	37
	4	0	5	16	0	11	0	32
	5	0	2	4	0	1	0	7
Total	63	214	229	4	31	0	541	
Producer's Accuracy (%)		82.5	57.0	48.0	25.0	35.5	0	
		(n/a)	(84.6)	(85.6)	(50.0)	(51.6)	(0)	
User's Accuracy (%)		63.4	62.2	58.8	2.7	34.4	0	
		(n/a)	(95.4)	(90.9)	(70.3)	(34.4)	(14.3)	
Overall Accuracy (%)		34.8	51.7	59.7	1.2	20.1	0	53.9

Table 3.5 Totalled accuracy assessment results summarized over all eight landscapes for the Site Productivity classification scheme (defined in Table 3.1). Acceptable overlap accuracies for producer's and user's accuracies are shown in brackets.

		Predicted Category						Total (N)
		Class (N)	None	VP	PR	MD	GD	
Actual Category	None	59	0	2	13	5	2	81
	VP	1	0	0	6	0	1	8
	PR	0	0	6	31	3	0	40
	MD	6	0	2	153	39	10	210
	GD	4	0	2	63	68	13	150
	VG	1	0	0	18	17	16	52
	Total	71	0	12	284	132	42	541
	Producer's Accuracy (%)	83.1 (n/a)	0 (0)	50.0 (66.7)	53.9 (87.0)	51.5 (93.9)	37.1 (69.0)	
User's Accuracy (%)	72.8 (n/a)	0 (0)	15.0 (92.5)	72.6 (92.4)	45.3 (96.0)	30.8 (63.5)		
Overall Accuracy (%)		47.6	0	15.2	64.4	44.3	31.2	53.9

Table 3.6 Totalled accuracy assessment results summarized over all eight landscapes for the Site Position classification scheme (defined in Table 3.1). Acceptable overlap accuracies for producer's and user's accuracies are shown in brackets.

		Predicted Category									Total (N)
		Class (N)	Cr	Up	Mid	Low	Toe	Flat	Depr	Wet	
Actual Category	Cr	1	13	2	0	5	1	0	0	0	22
	Up	2	34	14	1	4	2	0	0	0	57
	Mid	2	13	48	6	10	5	0	0	1	85
	Low	0	3	18	12	24	5	0	0	0	62
	Toe	1	3	13	7	70	13	0	1	0	108
	Flat	0	0	2	2	15	112	0	0	1	132
	Depr	0	0	3	1	2	4	0	0	0	10
	Wet	0	0	1	3	2	2	0	1	1	10
	None	1	2	3	1	3	4	0	2	39	55
	Total	7	68	104	33	135	148	0	4	42	541
Producer's Accuracy (%)	14.3 (42.9)	50.0 (88.2)	46.2 (76.9)	36.4 (75.8)	51.9 (80.7)	75.7 (87.2)	0 (0)	25.0 (25.0)	92.9 (n/a)		
User's Accuracy (%)	4.5 (63.6)	59.6 (87.7)	56.5 (78.8)	19.4 (87.1)	64.8 (83.3)	84.8 (96.2)	0 (40.0)	10.0 (10.0)	70.9 (n/a)		
Overall Accuracy (%)		2.8	33.0	43.7	18.0	45.3	0	67.8	5.0	49.9	58.5

Table 3.7 Totalled accuracy assessment results summarized over all eight landscapes for the Surface Expression classification scheme (defined in Table 3.1).

		Predicted Category											Total (N)
		Class (N)	C	D	F	H	M	N	None	P	R	T	
Actual Category	C	80	0	0	17	10	0	0	0	1	0	0	108
	D	1	0	0	1	4	0	0	3	0	0	0	9
	F	1	0	0	1	1	0	1	0	0	0	0	4
	H	33	0	0	85	14	0	1	2	1	0	0	136
	M	11	0	1	11	86	0	3	13	4	0	1	130
	N	0	0	0	0	3	0	0	0	1	0	0	4
	None	0	0	0	3	9	0	36	5	1	0	0	54
	P	0	0	0	1	13	0	0	25	0	0	1	40
	R	1	0	0	9	4	0	0	0	19	0	0	33
	T	0	0	0	0	0	0	0	1	0	0	0	1
	U	0	0	0	1	6	0	0	9	3	0	3	22
	Total	127	0	1	129	150	0	41	58	30	0	5	541
	Producer's Accuracy (%)		62.9	0	0	65.9	57.3	0	87.8	43.1	63.3	0	60.0
User's Accuracy (%)		73.4	0	0	62.5	66.2	0	66.7	62.5	57.6	0	13.6	
Overall Accuracy (%)		49.9	0	0	38.9	49.7	0	39.2	49.7	20.7	0	11.1	61.9

Table 3.8 Variables of importance for class differentiation within the five classification schemes (as defined by models built using a combined dataset), and the overall accuracy of each model.

Classification scheme	Variables of importance for classification tree model	Overall accuracy of combined dataset (%)
Leading Species	Standard deviation homogeneity Mean difference to neighbors (correlation) Standard deviation correlation Mean DEM Standard deviation DEM Mean TWI	53.5
Vertical Complexity	Standard deviation homogeneity Standard deviation photo Mean photo Mean correlation Mean homogeneity	52.7
Site Productivity	Standard deviation photo Mean DEM Mean difference to neighbors (entropy)	51.1
Site Position	Mean DEM Mean correlation Mean difference to neighbors (entropy) Standard deviation DEM Standard deviation TWI Mean TWI	50.7
Surface Expression	Mean TWI Standard deviation correlation Standard deviation DEM Mean correlation Mean entropy Mean photo Standard deviation photo	52.4

Figure 3.4 Pruned classification tree (Sherrod 2008) developed to model leading species (defined in Table 3.1) based on the combined dataset. Metric abbreviations are shown in Table 3.2. Target classes (terminal nodes) are shown in grey, along with the number of polygons correctly classified out of the total polygons identified by that split.

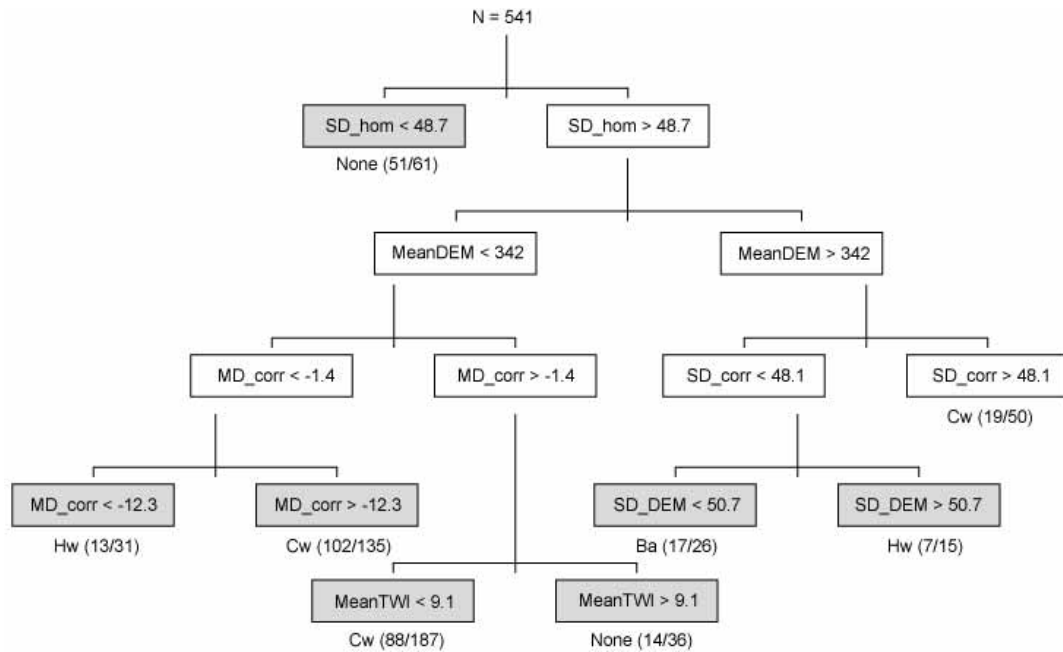
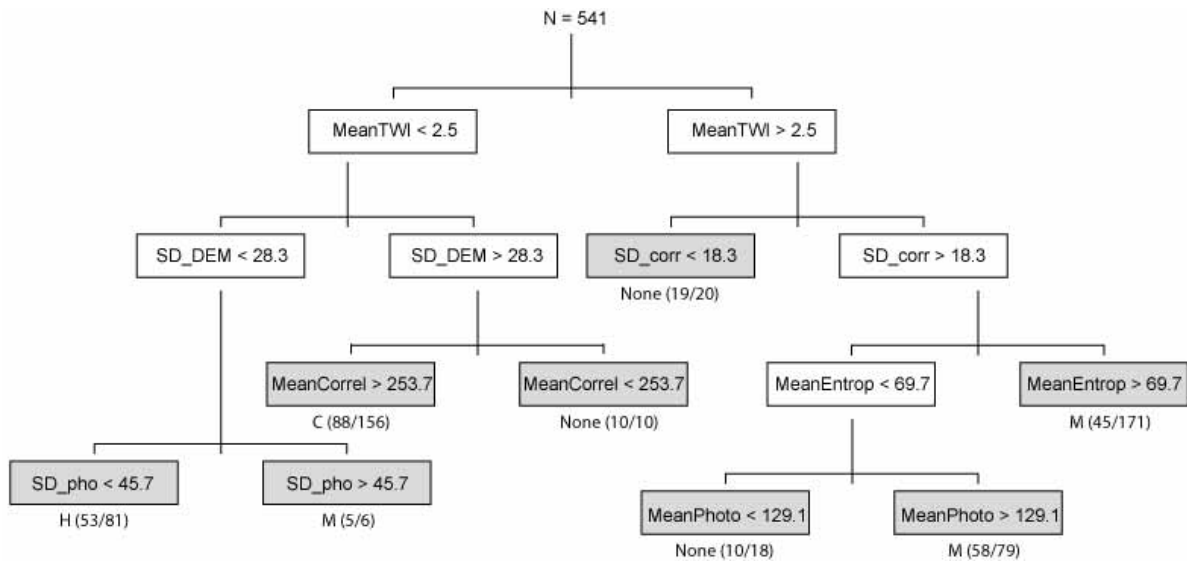


Figure 3.5 Pruned classification tree (Sherrod 2008) developed to model surface expression (defined in Table 3.1) based on the combined dataset. Metric abbreviations are shown in Table 3.2. Target classes (terminal nodes) are shown in grey, along with the number of polygons correctly classified out of the total polygons identified by that split.



Individual class accuracies of the 41 target classes were highly variable among the five classification schemes (Table 3.3-3.7). Both user's and producer's accuracies were higher on average than overall class accuracies. Only western red cedar (Cw), uniform vertical complexity (2), moderate site productivity (MD) and flat site topography (F1) had mean class accuracies $\geq 60\%$. In contrast, more than a quarter of all classes had user's and producer's accuracies $\geq 60\%$. In general, the more objects assigned to an individual class, the higher the accuracy of that class. For instance, classes present in $\geq 20\%$ of the total objects segmented from all eight landscapes, often had user's and producer's accuracies approaching or exceeding 60%. (An exception was objects classified as having very poor productivity, which had 0% accuracy.) Rare classes (defined as those present in $\leq 10\%$ of all segmented objects) had average user's and producer's accuracies of 25% and 20%, respectively. Over half of all the classes met this definition of rare (Table 3.1).

Overlap accuracies were often higher than class-to-class comparative accuracies for most classes within the Vertical Complexity, Site Productivity, and Site Position classification schemes (Table 3.4, 3.5, and 3.6). Individual class overlap accuracies increased 27.3% on average (ranging from 0 – 77.5% increase) as compared to the original class-to-class comparisons. Over 66% of all classes within the Vertical Complexity, Site Productivity, and Site Position classification schemes had producer's and user's overlap accuracies $\geq 60\%$. Of the individual classes with poor overlap accuracies, all were defined as rare with the exception of the very poor Site Productivity class (Table 3.5). Of the three classification schemes for which overlap accuracies could be calculated, the Site Productivity scheme observed the highest average increase in individual class accuracy when using the overlap statistics as compared to the original class-to-class comparisons.

3.4 Discussion

3.4.1 Object Creation

A variety of object-based approaches have been explored in previous research for delineation of forest stands (Chubey et al. 2006, Hay et al. 2005, Leckie et al. 2003, Pascual et al. 2008, Wulder et al. 2008). While results have suggested the potential for automating (or semi-automating) the object delineation process, quantitative validation of this potential has been rare. Our study was unique in that it quantitatively showed that at local, polygon, and landscape levels, many characteristics of the objects created using the segmentation process were statistically similar to characteristics of the manually delineated polygons. We found that mean, standard deviation, and contextual measures for the input layers (photographs, texture, and terrain), were similar across all scales compared (with the exception of aspect). At local and polygon levels, object size and most shape characteristics were also the same. Overall, it appears that the segmented objects were most similar to the manual interpretation when compared at local levels, and least similar when compared across the entire landscape.

Statistical discrepancies in several shape and aspect-related characteristics found over all three scales may demonstrate inherent differences between the two approaches. Shapes of the manually derived polygons were less complex and more compact, indicating the manual interpreter digitized smoother, non-complex lines. In contrast, the automated segmentation approach produced more complex object borders sometimes following variations between individual pixels. As a result, there were inconsistencies between the shape characteristics of the segmented objects and the manual polygons across all three scales of comparison, such as the higher average polygon perimeters produced by the automated segmentation, also observed in (Wulder et al. 2008). Aspect characteristics may have been different between methods, because the aspect layer was weighted to account for ~15% of the information used to create every object

within the segmentation process. The degree to which aspect was utilized by the interpreter is unknown and unquantifiable, and may have varied greatly, even across the same landscape.

Likewise, the inability of the automated approach to replicate the empirical distributions of manual polygons may be related to the ability of the manual interpreter to produce polygons with a wider range of object characteristics within the same landscape. For example, a greater range in sizes of manually-delineated polygons as compared to automated object-based approaches has also been found in previous research (Wulder et al. 2008). Criticisms of the region merging algorithm used in this study have highlighted the disconnect between the scale parameter and object size as problematic for ecological analysis (Hay et al. 2003, Hay et al. 2005). However, the ease of implementation, strength of results achieved using this approach, and the lack of other commercial segmentation software, may outweigh some of these issues for some applications.

3.4.2 Object Classification

The Leading Species and Surface Expression schemes had the highest overall class-to-class comparative accuracies when totaled across the eight landscapes (Table 3.3 and 3.7), and were among the highest accuracies achieved using the combined dataset (Table 3.8). It was expected that identification of historic Leading Species would be challenging due to the narrow spectral range of panchromatic, historic aerial photographs. However, accuracy results were likely highly influenced by the dominance of the western red cedar class, which was present in nearly 45% of all manually classified polygons (Table 3.1). The Leading Species scheme experienced the greatest decrease in accuracy for the model built using the combined dataset when compared to model accuracies totaled across the eight landscapes (Table 3.3 and 3.8). This decrease in accuracy was likely caused by the dominance of texture for class separation (Table 3.8 and

Figure 3.4), and the tonal (and textural) variability among the photographs. The Surface Expression scheme also had slightly higher accuracies, likely because classes were more evenly represented across the eight landscapes, and possessed more distinct terrain characteristics, reflected in the dominance of topographic variables for classification tree development (Table 3.8 and Figure 3.5).

Accuracy standards for manual interpretations often consider a class to be correct provided it is assigned to a value within +/-1 unit value (or within a bordering class) of the true class (Resources Information Standards Committee, 2009). The calculation of overlap accuracy statistics greatly improved the results for the Vertical Complexity, Site Productivity, and Site Position schemes (Table 3.4, 3.5, and 3.6) and may better represent the potential of classification tree analysis. For the three schemes with stepwise or 'ranked' classes (e.g. Vertical Complexity classes ranging from very uniform to very non-uniform; and Site Position classes ranging from toe to crest slope position), errors often occurred between bordering or adjacent classes. However, when considering class accuracy within these commonly used overlap guidelines, individual class accuracies were often well within the range of acceptable requirements for provincial VRI mapping standards (Resources Information Standards Committee, 2009).

Overall, variability in the comparative accuracies within these classification schemes may be explained by several factors. First, low class-to-class comparative accuracies may be the result of using complex classification categories which are better suited to human cognition. For instance, analysis of Site Productivity requires consideration of local conditions, as well as contextual circumstances. As this type of classification is complex and arguably subjective, automated classification will likely be difficult no matter what classification approach is used. Second, while the scale used in the segmentation process may be suitable for creating objects close in size

to manual polygons, this single scale is likely not optimal for certain classes. For example, an important cue used to classify Vertical Complexity is size variation among individual trees within a stand. Relevant information over different spatial scales is therefore obscured when analysis occurs solely at the stand level. Third, classification accuracies may be limited by the limited number of samples for certain classes. Finally, the lower accuracies produced with the combined datasets may be caused by tonal (and textural) variability among the historic photographs, and the limited spectral information available from panchromatic photographs.

The wide range of class accuracies reported in previous research and this study is likely due to the dependence of classification tree accuracy on sample size, with rare classes generally having lower class-to-class comparative accuracies and overlap accuracies (Chubey et al. 2006, Yu et al. 2006). Despite variability among individual class accuracies, CART analysis has been more effective for classification of segmented imagery than alternative methods. For example, CART analysis was more accurate when classifying forest vegetation on a segmented image than a nearest neighbor algorithmic approach (Mallinis et al. 2008). Another advantage of CART analysis is the ability to identify the metrics or variables best able to differentiate amongst classes (Laliberte et al. 2007, Yu et al. 2006), making this approach highly suitable for handling the large amount of metrics produced by object-based analysis (Chubey et al. 2006). While CART analysis may not be suitable for all classification schemes, this technique is highly suited to integration with object-based segmentation.

3.5 Future Work and Conclusions

Several components of this research should be addressed in future work. First, the accuracy of the object borders created using object-based segmentation should be examined (as per Radoux and Defourny 2007) to assess the ability of the segmentation process to replicate positional

accuracy. Second, reference data from the field should be used to establish the true classification accuracies of both the manual interpretation and object-based segmentation approaches. Third, further development of CART models should be undertaken to investigate the potential of using this approach for additional classifications schemes, including continuous variables such as tree height and crown closure. The use of additional object-based metrics and the modification of binary rules as defined by CART should also be explored within an object-based environment. For example, the incorporation of data over several spatial scales may increase the accuracy of the classifications, as may the inclusion of more object-based metrics for training within CART analysis. Furthermore, by implementing and modifying the CART classification rules within the object-based environment, classification accuracy may be improved.

The goal of this study was to test the ability of an object-based segmentation and CART classification approach to mimic the historic delineation and classification results achieved by manual interpretation, which has potential use as a restoration tool. In this regard, our results reflect similarities and comparative accuracies between approaches. Due to problems of subjectivity and inconsistency among manual interpreters, the use of manual interpretation as reference data may be perceived as problematic (Wulder et al. 2008). However, the development of automated techniques for replicating or assisting manual interpretation is arguably unwise without direct comparison. Therefore, the results of this study highlight the potential for combined object-based analysis and CART analysis to replicate certain aspects of manual interpretation.

3.6 References

- APS. 2008. Alta Photogrammetry Suite Version 7.1. Quebec City, QC, Canada: Groupe Alta.
- Avery TA, Berlin GL. 1992. Fundamentals of Remote Sensing and Air Photo Interpretation. Upper Saddle River: Prentice Hall.
- Benz UC, Hofmann P, Willhauck G, Lingenfelder I, Heynen M. 2004. Multi-resolution, object-oriented fuzzy analysis of remote sensing data for GIS-ready information. *ISPRS Journal of Photogrammetry & Remote Sensing* 58: 239-258.
- Bittencourt HR, Clarke RT. 2003. Use of classification and regression trees (CART) to classify remotely-sensed digital images. Pages 3751-3753. *Geoscience and Remote Sensing Symposium Proceedings: 2003 IEEE International*.
- Blaschke T. 2004. Object-based contextual image classification built on image segmentation. *IEEE TRANSACTIONS ON GEOSCIENCE AND REMOTE SENSING*: 113-119.
- Chubey MS, Franklin SE, Wulder MA. 2006. Object-based Analysis of Ikonos-2 Imagery for Extraction of Forest Inventory Parameters. *Photogrammetric Engineering & Remote Sensing* 72: 383-394.
- Cohen WB, Kushla JD, Ripple WJ, Garman SL. 1996. An introduction to digital methods in remote sensing of forested ecosystems: Focus on the Pacific Northwest, USA. *Environmental Management* 20: 1432-1009.
- Definiens. 2007. Definiens Developer 7 User Guide. Munchen, Germany. Report no.
- ENVI. 2007. ENVI Version 4.4. Boulder, CO, USA: ITT Visual Information Solutions.
- ESRI. 2006. ArcDoc Version 9.3. Redlands, CA, USA: Environmental Systems Research Institute.
- Fookes PG, Dale SG, Land JM. 1991. Some observations on a comparative aerial photography interpretation of a land slipped area. *Quarterly Journal of Engineering Geology* 24: 249-265.

- GeoBC. 1996. Terrain Resource Information Management (TRIM) Maps. Crown Registry and Geographic Base Map Data. Victoria, BC: Province of British Columbia.
- Gessler PE, Moore ID, McKenzie NJ, Ryan PJ. 1995. Soil-landscape modeling and spatial prediction of soil attributes. *International Journal of Geographical Information Systems* 9: 421-432.
- Green K. 2000. Selecting and Interpreting High-Resolution Images. *Journal of Forestry* 37-39.
- Hall RJ. 2003. The roles of aerial photographs in forestry remote sensing image analysis. Pages 47-75 in Wulder M, Franklin SE, eds. *Remote Sensing of Forest Environments: Concepts and Case Studies*. Boston: Kluwer.
- Hansen MC, Defries RS, Townshend JRG, Sohlberg R. 2000. Global land cover classification at 1 km spatial resolution using a classification tree approach. *International Journal of Remote Sensing* 21: 1331-1364.
- Hay GJ, Blaschke T, Marceau DJ, Bouchard A. 2003. A comparison of three image-object methods for the multi-scale analysis of landscape structure. *ISPRS Journal of Photogrammetry & Remote Sensing* 57: 327-345.
- Hay GJ, Castilla G, Wulder M, Ruiz JR. 2005. An automated object-based approach for the multi-scale image segmentation of forest scenes. *International Journal of Applied Earth Observation and Geoinformation* 7: 339-359.
- Laliberte AS, Frederiksen EL, Rango A. 2007. Combining Decision Trees with Hierarchical Object-oriented Image Analysis for Mapping Arid Rangelands. *Photogrammetric Engineering & Remote Sensing* 73: 197-207.
- Laliberte AS, Rango A, Havstad KM, Paris JF, Beck RF, McNeely R, Gonzalez AL. 2004. Object-oriented image analysis for mapping shrub encroachment from 1937 to 2003 in southern New Mexico. *Remote Sensing of Environment* 93: 198-210.

- Leckie D, Gougeon F, Walsworth N, Paradine D. 2003. Stand delineation and composition estimation using semi-automated individual tree crown analysis. *Remote Sensing of Environment* 85: 355-369.
- Lucas R, Rowlands A, Brown A, Keyworth S, Bunting P. 2007. Rule-based classification of multi-temporal satellite imagery for habitat and agricultural land cover mapping. *ISPRS Journal of Photogrammetry & Remote Sensing* 62: 165-185.
- Mallinis G, Koutsias N, Tsakiri-Strati M, Karteris M. 2008. Object-based classification using Quickbird imagery for delineating forest vegetation polygons in a Mediterranean test site. *ISPRS Journal of Photogrammetry & Remote Sensing* 63: 237-250.
- Morgan JL, Gergel SE, Coops NC. In Press. *Aerial Photography: A Rapidly Evolving Tool for Ecological Management*. BioScience.
- Paine DP, Kiser JD. 2003. *Aerial Photography and Image Interpretation*, 2nd Edn. Hoboken, New Jersey: John Wiley & Sons, Inc.
- Pascual C, Garcia-Abril A, Garcia-Montero LG, Martin-Fernandez S, Cohen WB. 2008. Object-based semi-automatic approach for forest structure characterization using lidar data in heterogeneous *Pinus sylvestris* stands. *Forest Ecology and Management* 255: 3677-3685.
- Pringle RM, Syfert M, Webb JK, Shine R. 2009. Quantifying historical changes in habitat availability for endangered species: use of pixel- and object-based remote sensing. *Journal of Applied Ecology* 46: 544-553.
- Province of British Columbia. 2002. *Vegetation Resources Inventory: Photo Interpretation Process in Terrestrial Information Branch MoSRM*. Resources Inventory Committee.
- Radoux J, Defourny P. 2007. A quantitative assessment of boundaries in automated forest stand delineation using very high resolution imagery. *Remote Sensing of Environment* 110: 468-475.

- Resources Information Standards Committee. 2009. Photo Interpretation Quality Assurance Procedures and Standards, Version 3.2. Forest Analysis and Inventory Branch. Ministry of Forests and Range.
- SAS. 2003. SAS 9.1. Cary, NC: SAS Institute Inc.
- Shankar BU. 2007. Novel Classification and Segmentation Techniques with Application to Remotely Sensed Images. Pages 295-380. Transaction on Rough Sets VII, vol. 4400/2007. Berlin / Heidelberg: Springer.
- Sherrod PH. 2008. DTREG Predictive Modeling Software. Users Manual: www.dtreg.com/DTREG.pdf.
- Sugumaran R, Pavuluri MK, Zerr D. 2003. The Use of High-Resolution Imagery for Identification of Urban Climax Forest Species Using Traditional and Rule-based Classification Approach. IEEE TRANSACTIONS ON GEOSCIENCE AND REMOTE SENSING 41: 1933-1939.
- Swanson FJ, Kratz TK, Caine N, Woodmansee RG. 1988. Landform effects on ecosystem patterns and processes. Bioscience 38: 92-98.
- Swetnam TW, Allen CD, Betancourt JL. 1999. Applied Historical Ecology: Using the Past to Manage for the Future. Ecological Applications 9: 1189-1206.
- Thomas N, Hendrix C, Congalton RG. 2003. A Comparison of Urban Mapping Methods Using High-Resolution Digital Imagery. Photogrammetric Engineering & Remote Sensing 69: 963-972.
- Thompson ID, Maher SC, Rouillard DP, Fryxell JM, Baker JA. 2007. Accuracy of forest inventory mapping: Some implications for boreal forest management. Forest Ecology and Management 252.

- TPC CSTPC. 2006. Kennedy Lake Watershed Plan. Ucluelet, BC: Ministry of Forests, Ministry of Environment, Integrated Land Management Bureau, Ministry of Agriculture and Lands and Central Region Chiefs Administration. Report no.
- Treitz P, Howarth P. 2000. Integrating Spectral, Spatial, and Terrain Variables for Forest Ecosystem Classification. *Photogrammetric Engineering & Remote Sensing* 66: 305-317.
- Watts JD, Lawrence RL, Miller PR, Montagne C. 2009. Monitoring of cropland practices for carbon sequestration purposes in north central Montana by Landsat remote sensing. *Remote Sensing of Environment* 113: 1846-1852.
- Wulder M. 1998. Optical Remote Sensing Techniques for the Assessment of Forest Inventory and Biophysical Parameters. *Progress in Physical Geography* 22: 449-476.
- Wulder M, White JC, Hay GJ, Castilla G. 2008. Towards automated segmentation of forest inventory polygons on high spatial resolution satellite imagery. *The Forestry Chronicle* 84: 221-230.
- Yu Q, Gong P, Clinton N, Biging G, Kelly M, Schirokauer D. 2006. Object-based Detailed Vegetation Classification with Airborne High Spatial Resolution Remote Sensing Imagery. *Photogrammetric Engineering & Remote Sensing* 72: 799-811.

4 QUANTIFYING LANDSCAPE HETEROGENEITY FROM HISTORIC AERIAL PHOTOGRAPHS USING OBJECT-BASED ANALYSIS³

4.1 Introduction

One of the most important concepts of landscape ecology, and a theme central to ecosystems, is that of heterogeneity. Heterogeneity can be broadly defined as the degree of spatial variability of some property within a system (Li and Reynolds 1995), and is dependent upon both the spatial and temporal scales over which it is measured (Wiens 1989). Heterogeneity influences important ecological processes (Turner 1989), and can impact species diversity, resilience, and ecosystem function (Huston 1999) making heterogeneity relevant to management concerns such as ecosystem restoration (Sklenicka and Lhota 2002) and sustainable forest management (Lindenmayer et al. 2006). Additionally, since natural levels of spatial heterogeneity and complexity are linked to certain ecosystem functions, changes in heterogeneity over time and space caused by resource extraction can be used to gauge the ecological consequences of such activities (Turner et al. 2003).

Ecosystem baselines offer a basis upon which changes in natural heterogeneity and variability can be measured. Acting as pre-disturbance benchmarks for conditions prior to major anthropogenic modification, ecological baselines can be used to monitor ecosystem change and can enhance our understanding of ecological processes (Arcese and Sinclair 1997). Analysis of the natural range of variability in an ecosystem can also provide a basis for evaluation of proposed management actions and goals (Landres et al. 1999; Swetnam et al. 1999). One of the oldest sources of fine-scale, spatially continuous baseline information is aerial photography

³ A version of this chapter has been submitted for publication and is undergoing review. Morgan, J.L., Gergel, S.E. Quantifying Landscape Heterogeneity from Historic Aerial Photographs using Object-based Analysis. *Landscape Ecology*.

(Morgan et al. In Press). Collected since the early 1930's, historic aerial photographs provide unique ecological information over long time periods (Paine and Kiser 2003). As a result, aerial photographs have traditionally played an important role in ecosystem management, and have long been used for purposes such as forest inventories, disturbance mapping, and wildlife management (Avery and Berlin 1992). Historic aerial photographs therefore have enormous potential for providing baseline data necessary for quantitative mapping and monitoring of landscape heterogeneity over time.

Many techniques have been developed to describe spatial heterogeneity and vary widely among disciplines. For example, landscape ecology most often conceptualizes heterogeneity from the perspective of the patch mosaic paradigm. This approach relates patch-based indices calculated from categorical data to represent landscape structure (Gustafson 1998; Cushman et al. 2008). This method can be problematic because (despite the continuous nature of most ecological variables), the categorical (discrete) representation of heterogeneity may simplify the landscape to the point of unacceptable loss of ecological information (McGarigal et al. 2009). In contrast, there are methods which depict spatial variability using continuous gradients. Geostatistics can represent spatial gradients through interpolation and analysis of point data (spatial autocovariance) (Curran and Atkinson 1998). Surface heterogeneity is often characterized in remote sensing using digital terrain modeling to represent topography (Pike 2000) and spectral measures such as image texture (Nagendra 2001; St-Louis et al. 2006). While the concept of landscape heterogeneity as a gradient may be theoretically ideal, such execution is challenging, and only recently have continuous surface gradients been used in landscape ecology to quantify landscape structure (McGarigal et al. 2009).

Here we use object-based analysis as a new approach to quantify landscape heterogeneity. This technique merges neighboring pixels with similar characteristics into somewhat homogeneous objects or patches (Blaschke 2003; Benz et al. 2004) and has recently shown much potential in image analysis (Laliberte et al. 2004; Pringle et al. 2009). One of the benefits of this approach is the ability to represent the hierarchical nature of landscapes by creating objects over multiple spatial scales (Hay et al. 2003). Quantitative metrics can then be generated for each individual object, and used to describe various elements of landscape variability through characteristics such as tone, shape, size, texture, as well as contextual relationships among neighboring objects. Another compelling aspect of this approach is that object-based metrics can quantify continuous variability within objects (e.g. variation of tone within an object), in addition to representing the continuous variability over the landscape (e.g. topography). Thus, this method can account for the within-object heterogeneity ignored in the patch mosaic perspective.

Our primary goal is to explore the utility of object-based analysis as a tool for historic landscape assessment. Our objectives are to: (1) Quantify historic landscape heterogeneity using an object-based approach; and (2) Compare historic heterogeneity between two distinct landscape types (riparian and upland). To do this, we combine historical aerial photographs, image texture information, and terrain data for an un-harvested watershed into an object-based analysis to represent various sources of heterogeneity. By using an object-based approach to quantify heterogeneity, we investigate an alternative approach with unique capabilities for defining landscape heterogeneity, and improve our ability to quantitatively map baseline conditions.

4.2 Methods

4.2.1 Study Area

The study area encompasses the Kennedy Lake Watershed within Clayoquot Sound, on the west coast of Vancouver Island, BC, Canada (Figure 4.1). Kennedy Lake watershed has a drainage area of 55,013 ha. A significant portion of the watershed is occupied by Kennedy Flats, a low-lying area of low gradient streams covering 12,900 ha. Climate of the area is temperate and wet, with mean temperatures ranging from 5 – 15°C and precipitation averaging 400-700cm depending on elevation. The watershed falls predominantly within the coastal western hemlock zone in British Columbia (Meidinger and Pojar 1999), which is the dominant zone on Vancouver Island. While the area encompasses diverse sites of varying moisture and nutrient gradients, we distinguished two broad landscape types for comparison: riparian and upland. Riparian sites (adjacent to streams and rivers) are dominated by fluvial disturbances, and tend to be highly productive, occurring at lower elevations and in local depressions (Montgomery 1999). In contrast, upland sites occur in higher elevations, often on slopes of higher gradient and in general, lack some of the complexity and diversity seen in riparian sites due to decreased productivity caused by fewer moisture and nutrient resources (Swanson et al. 1988).

4.2.2 Spatial Data

Historic aerial photographs captured in 1937-1938 were obtained for the Kennedy Lake watershed from the National Air Photo Library (NAPL) in Ottawa, Canada. Photographs are panchromatic with a spatial extent of approximately 12km², and were captured at a vertical angle using Fairchild 3.9 or 3.10 cameras (R.C.A.F. 1937-1938). The photographs were scanned at a resolution of 1200dpi and were auto-dodged by the vendor (an image enhancement technique which equalizes dark and light areas across an image for a monochromatically balanced product) (NAPL). Four photographs of each landscape type (riparian and upland), were randomly selected

from the suitable photographs (Appendix B). Photographs of poor quality or with extensive water coverage or cloud cover were discarded prior to selection.

Figure 4.1 The study area encompasses the entire Kennedy Lake watershed, from which eight photographs were selected to represent contrasting riparian and upland landscapes.



The selected aerial photographs were orthorectified using Alta Photogrammetry Suite (APS 2008), a process which adds spatial coordinates to an image for accurate representation of distance, area, and angles. Orthorectification was necessary for the accuracy of the object-based analysis because this step ensured precise spatial alignment with the input terrain layers (British Columbia's 1:20,000 Terrain Resource Information Management (TRIM) maps) (GeoBC 1996). Eight to ten ground control points (GCPs) were collected from identical locations on the TRIM

data and each photograph to provide x and y coordinates to the imagery. Residual errors ranged from 0.5 – 1.6m. Each photograph was also warped to a vector terrain model automatically generated from the TRIM mass points (a grid of evenly spaced points containing x, y, and z information) within APS, to provide elevation (z coordinate) data. Once corrected, the images were then re-sampled to a spatial resolution of 0.5m using bicubic convolution (APS 2008) based on the scale of the original photographs (~1:20,000) and the scanning resolution (Jensen 2000).

Image texture was quantified to account for tonal heterogeneity because texture has been linked to important ecological parameters such as vegetation structure and species identification (Franklin et al. 2000; Wulder et al. 2004). Several texture layers were calculated using the co-occurrence matrix for all photographs, each with a processing window of 3 x 3 pixels in size (ENVI 2007). Highly redundant layers were eliminated based on the results of a correlation analysis of the original photographs and the derived texture layers. Texture layers representing tonal variation, including entropy (a measure of randomness), variance, homogeneity, and correlation were retained (Table 4.1), all with correlations less than 43% ($abs(r) < 0.65$). All texture layers were rescaled to the same range of values as the original photograph to ensure equal influence in subsequent analyses.

In order to incorporate surface complexity into our description of landscape heterogeneity, a Digital Elevation Model (DEM), and derivative terrain layers were generated from the same TRIM data used to orthorectify the photographs (Table 4.1). TRIM contour lines were converted into a raster DEM with a resolution of 15m using ArcGIS (ESRI 2006; Hengl 2006). The DEM was then resampled to a resolution of 0.5m to match the spatial resolution of the aerial photographs. (An identical spatial resolution for all input layers is important for analysis with an object-based classifier. Despite the coarse resolution of the original raster DEM, elevation data

Table 4.1 Input layers used in the segmentation process to create objects and define landscape heterogeneity.

Data	Layer	Weight	Total Weight	Methods used to generate layer
Tone	Photograph	12	12	Scanned from original prints at a resolution of 1200dpi with radiometric adjustment and orthorectification. Processed in (APS 2008).
	Variance	3	12	Generated based on the co-occurrence matrices of the original photographs, using texture filters in ENVI (ENVI 2007).
Texture	Correlation	3		
	Homogeneity	3		
	Entropy	3		
Topography	Elevation	4	12	Mass points converted to raster DEM (ESRI 2006), where each pixel represents an elevation value. Elevation range for the study area is 0 – 1,633m.
	Aspect	4		Aspect as calculated within ArcGIS is expressed in degrees from 0 to 359.9° (ESRI 2006), measured clockwise from north. A cosine transformation was used to rescale the data to represent aspect from 180° (north) to -180° (south).
	Topographic Wetness Index (TWI)	4		$(TWI) = \ln(A_s/\tan\beta)$ Where A_s is the specific catchment area (upslope area (m ²) per unit contour length) and β is the slope (Gessler et al. 1995). Values range from -1.5 to 25 and represent potential moisture.

and topographic derivatives were critical to this study, therefore despite its recognized limitations, we used TRIM data because it was the only freely available elevation data for this area.) Once the DEM was created, various terrain layers were derived using raster surface algorithms within ArcGIS (ESRI 2006). A topographic wetness index layer was also generated (Table 4.1). The original DEM, aspect, and topographic wetness were selected to represent terrain because of their low between-layer correlations ($abs(r) < 0.65$) and their ecological relevance. For example, both elevation and aspect influence solar energy and water regimes, which are closely related to vegetation patterns (Swanson et al. 1988). Similarly, topographic indices are used to describe patterns of soil moisture (Burt and Butcher 1985), and are linked to

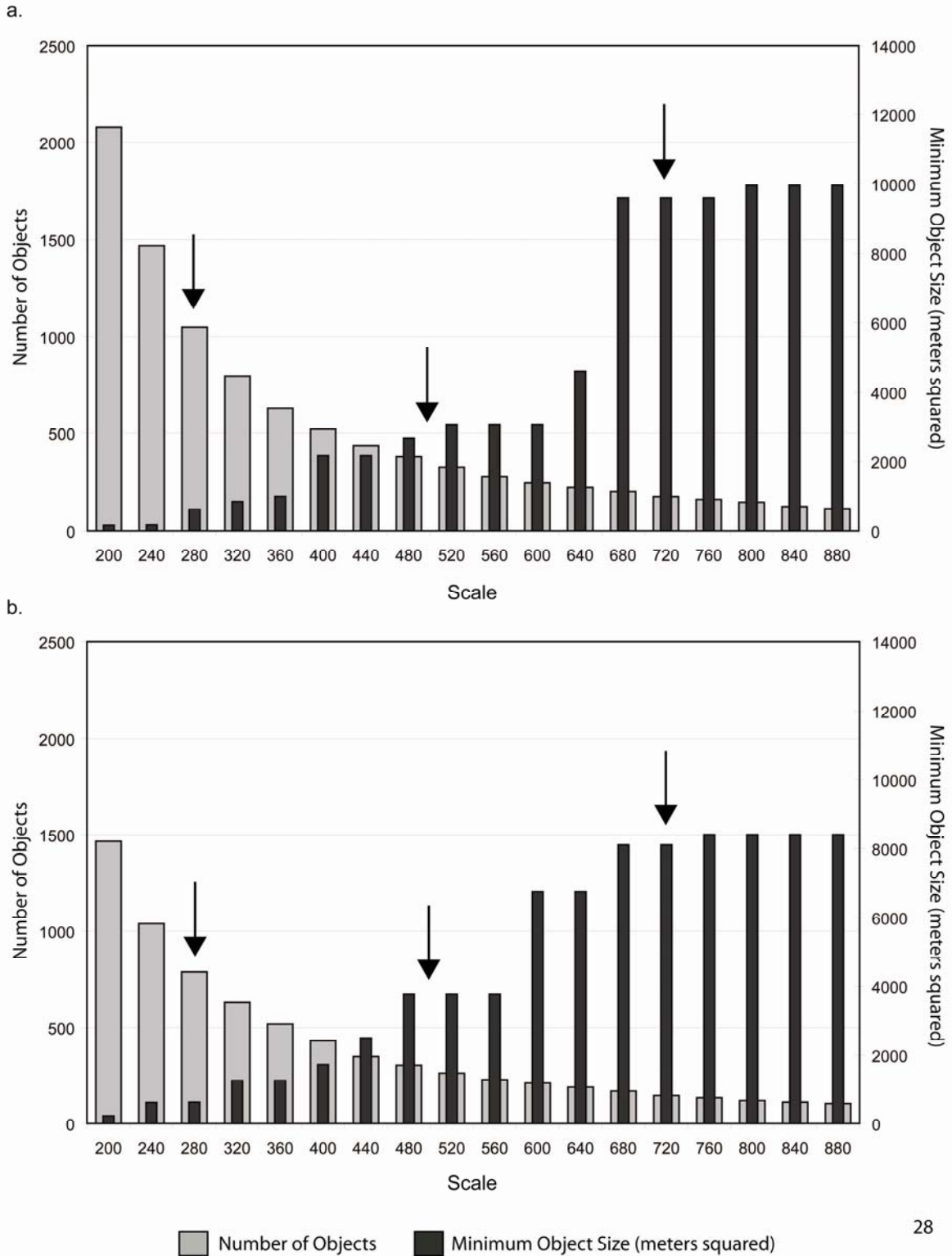
variation of vegetation patterns (Zinko et al. 2005). All three terrain layers were clipped to the spatial extent of the selected photographs.

4.2.3 Object-based Analysis

We used the segmentation process within the object-based classifier (Definiens 2007) to define objects based on eight input layers (Table 4.1). Segmentation is the creation of objects with minimum within-object heterogeneity and uses a bottom up, pixel merging approach. Objects were defined according to three primary factors: a set of input layers, a homogeneity criterion, and a scale parameter (Definiens 2007). The eight input layers were weighted to ensure the three primary data types (tone, texture, and topography) had equal influence (33% each) on the segmentation process and thus, the resulting definition of heterogeneity (Table 4.1). The homogeneity criterion within Definiens consists of tone and shape, which are the two main characteristics used to create objects. Tone and shape parameters allow the user to control the degree of influence that photographic tone and object shape have on the segmentation output. Tone and shape were both weighted equally (0.5) to ensure equivalent representation of these characteristics. Shape is further broken down into compactness and smoothness. In order to avoid favoring a specific shape type, these categories were also assigned equal weightings (0.5).

The third factor related to object definition is the scale parameter, which influences the size of the objects to be created. Scale selection is often problematic because no optimal scale(s) exist for any landscape (Li and Wu 2004). Therefore, we used scale breaks evident in two object metrics (number of objects and minimum object size) measured over a range of spatial scales (segmentations) to define relevant scales (Figure 4.2). The first metric, minimum object size, revealed an obvious pattern of plateaus as the scale parameter increased, suggesting a series of underlying thresholds related to object size and homogeneity. The second metric (number of

Figure 4.2 Changes in the number of objects and the minimum object size for segmentations using different scale parameters. Panel a. Representative riparian landscape (as shown in Figure 4.3a); Panel b. Representative upland landscape (as shown in Figure 4.3b). The plateaus were used to guide selection of scale parameters suited to all eight landscapes. The resulting scale parameters selected were 280, 500 and 720 (shown with arrows).

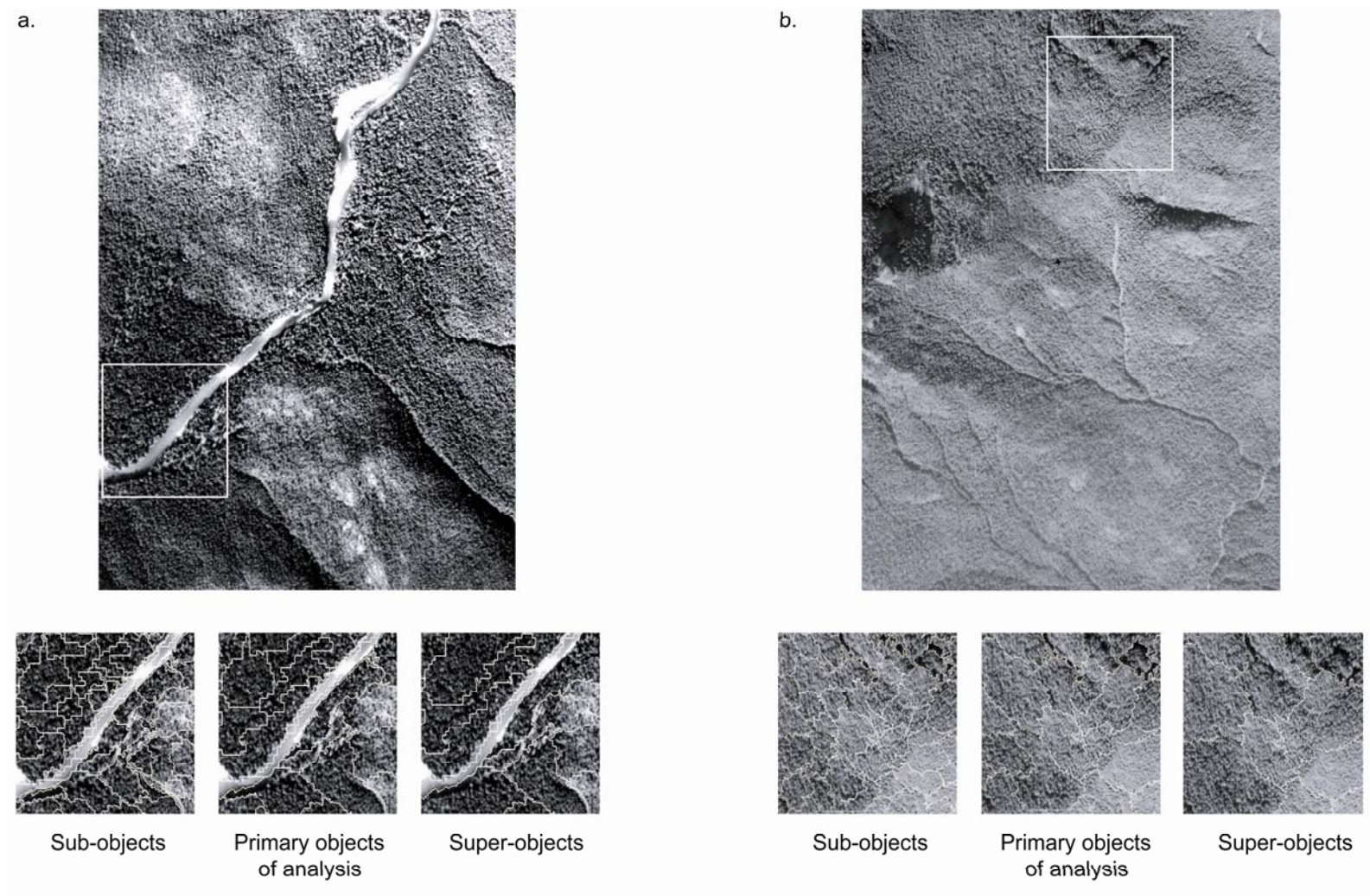


objects) decreased exponentially and leveled out around 150 objects, indicating further segmentations would yield minimal information gain. The finest scale (composed of sub-objects contained within objects at higher scales) was selected within the mid-range of the first noticeable plateau in minimum object size (Table 4.2 and Figure 4.3). These sub-objects represent small groups of trees and small stream units. The largest scale (called super-objects because they encompass objects at lower scales) was selected near the start of the plateau at which the number of objects began to level out (~150 objects). This scale represented larger tree stands and lakes. The middle scale, which is the primary layer of analysis, was selected from within the plateau between these high and low scales and represented medium-sized groups of trees and stream reaches. Thus, three scale parameters (280, 500 and 720) were selected for all eight landscapes (Table 4.2 and Figure 4.3).

Table 4.2 The scale hierarchy selected for all eight landscapes based on the trends in minimum object size and number of objects (shown in Figure 4.3). Associated size statistics (averaged over all eight landscapes) and the biophysical features they are meant to represent are described. Examples of images segmented using this scale hierarchy are shown in Figure 4.2.

Object type	Scale	Minimum object size (m²)	Number of objects	Average object size (m²)	Biophysical features represented
Sub-objects	280	665	960	10,219	Small clumps of trees (10-50 visible crowns), small stream units and small bogs.
Primary objects of analysis	500	2,752	311	32,107	Medium sized clumps of trees (50-150 visible crowns), and stream reaches.
Super-object	720	6,428	165	59,849	Larger stands of trees (150-300 visible crowns), and small lakes.

Figure 4.3 An example photograph (landscape) and segmentation results shown on a subsection of each photograph for a. a representative riparian landscape, and b. a representative upland landscape. The scale hierarchy is nested, and object outlines are shown in white on the photographs and are described further in Table 4.2.



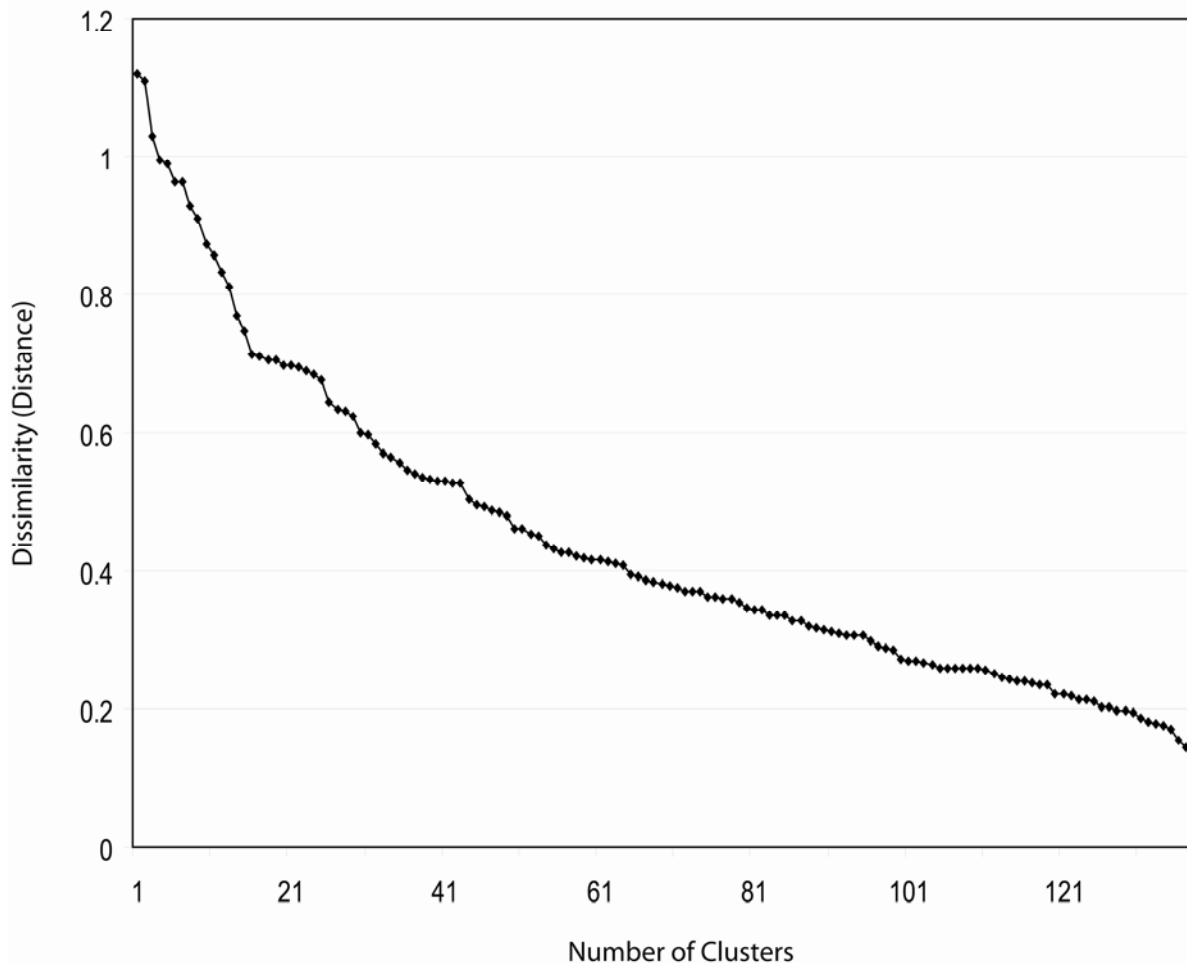
4.2.4 Statistical Analysis

Factor analysis was used to reduce the redundancy within a set of object-based metrics calculated from the segmentation results for each photograph. Two-hundred metrics were initially calculated for all objects within each landscape (Appendix C), with the exception of border objects which were masked out of the analysis. These object-based metrics were related to object size, shape, values of the input layers, relationships between neighbors, and relationships between sub- and super-objects. Pair-wise Pearson's correlation coefficients were calculated for all 200 metrics, and used to identify metrics that were highly correlated. When metrics were highly correlated (>65%), the simpler and/or more ecologically meaningful metric was retained and the others were discarded, resulting in 62 metrics being retained for all landscapes (Appendix C). These 62 remaining metrics, were used in a factor analysis with varimax rotation (to create simple factor structure and maximize interpretability) to identify orthogonal axes describing different 'dimensions' of the data (SAS 2003; Manley 2005). The latent root criterion was used to identify significant factors, meaning all factors with an eigenvalue greater than one were retained for each landscape.

Agglomerative hierarchical cluster analysis was used to group the factors retained from all eight landscapes into clusters representing specific elements of landscape heterogeneity (SAS 2003; Cushman et al. 2008). The average linkage method was used to cluster factors together based on their factor pattern, which is the correlation between all input metrics and the factor itself (Appendix D). The metrics with high loadings (correlations) for a given factor pattern represent the information summarized by that particular factor. Therefore, clusters were labeled based on the properties of the object-based metrics with the highest consistent loadings within each group of factors. As cluster analysis requires pair-wise measures of dissimilarity among input entities (in this case among extracted factors), a distance matrix was calculated (where distance is 1-

$\text{abs}(r)$, and r is the correlation of the factor patterns) for all of the retained factors from all eight landscapes ($N = 138$) as per (Cushman et al. 2008; McGarigal et al. 2009). Within the distance matrix, a value of 0 represents perfect correlation, whereas a value of 1 represents complete independence. A plot of fusion distances, which represents the degree of dissimilarity among clusters as they are subsequently fused together, was used to determine the final cluster solution (Figure 4.4) (Cushman et al. 2008; McGarigal et al. 2009). In short, factor analysis was used to identify independent axes of landscape pattern over various landscapes, and cluster analysis was used to group related factors together into elements of heterogeneity (Appendix D).

Figure 4.4 Plot of hierarchical clustering results, displaying the distances at which factors (and clusters) are grouped/fused together. Fusion distances represent dissimilarity, and are based on the correlations between factors.



We represented the overall importance of the elements (clustered factors) based on three measures: (1) Universality, which is a percentage representation of how often the element was identified over all landscapes, (2) Strength, or the average eigenvalue and percent variance explained by each element, and (3) Consistency, which used the average pair-wise Pearson's correlation ($abs(r)$) among each cluster to measure how stable/uniform the meaning of a particular element was over different landscapes, similar to (Cushman et al. 2008). We calculated these measures over all landscapes, and also separately for riparian and upland landscapes.

4.3 Results

An average of 17 factors (range 15 – 19) were retained for each landscape using the latent root criterion, which cumulatively explained 74.29 – 77.81% of the variance within all 62 object-based metrics. Riparian landscapes retained one additional factor on average (18), as compared to the upland landscapes (which retained 17 factors on average). However, the average amount of variance explained by riparian (75.7%) and upland (76.3%) landscape types was very similar (within 0.6%). When the factors retained across all landscapes were clustered based on their factor structures, sixteen unique clusters were identified over all eight landscapes (Table 4.3), based on the inflection point of the fusion distance plot (Figure 4.4). This sixteen cluster solution explained 76.5% of the variance within all 138 original factors, and ten of these clusters were universal across all landscape types (Table 4.4). The average variance explained by a cluster was 4.5% (range 7.03 – 2.51%), which indicates that the strength of the extracted clusters was fairly low, and that there was low redundancy within the original object-based metrics. Consistency of the clustered factors was highly variable, ranging from 0.91 – 0.23. However, average cluster consistency was 0.63 indicating significant correlation within the clusters, especially when compared to an average correlation of 0.13 amongst all 138 factors.

Table 4.3 The sixteen elements (clusters) identified as important for describing baseline landscape heterogeneity. The object-based metrics with the highest loadings for factors within each element and the potential ecological relevance of each element is included.

Label	Definition (and Object-based metrics with high loadings)	Possible Ecological Relevance
Sub-object variability	Overall variability/heterogeneity of sub-objects/pixels. (Sub-object density/area/texture/tone)	Represents within object heterogeneity, or local variability, and may be related to biodiversity.
Tone	Average spectral reflectance. (Mean tone)	Reflectance is related to biophysical characteristics.
Proximity to edge	Continuous measure of distance to the super-object border. (Distance to super-object center)	Habitat conditions vary at forest stand edges as compared to interior forest.
Texture variability	The degree of texture variation within the object: smooth versus coarse. (Standard deviation of correlation/variance)	Related to variation in crown size, tree species type, canopy closure, and stand structure.
Aspect	Object aspect: north/south/east/west. (Mean aspect)	Relates to local solar energy and water regimes.
Compactness	Object shape complexity. (Compactness, length/width)	Feature recognition, such as geomorphic landforms.
Landscape position	Topographic position of the object within the landscape. (Ratio to super-object DEM/TWI)	Topographic position influences patterns of moisture, natural disturbances and thus, vegetation.
Position within super-object	Categorical measure of whether the object is interior or border. (Is end/center of super object)	Habitat conditions vary at forest stand edges as compared to interior forest.
Object orientation	Object direction derived from object's location within the landscape. (Main direction)	May be related to geomorphic landforms, such as crest and swale patterns, or river channels.
Slope orientation	The aspect of the object in relation to the landscape. (Ratio to super-object aspect)	Relates to solar energy and water regimes over coarse scales.
Texture context	The texture of neighboring/surrounding objects. (Mean difference to neighbors homogeneity/entropy)	Useful for differentiating stand age or species composition of contrasting, neighboring tree stands.
Landscape context	Relates to whether an object is higher/lower in elevation than its neighbors. (Mean difference to neighbors DEM/TWI)	Neighboring topography related to moisture potential, natural disturbances and thus, vegetation.
Dissimilarity to super-object	Measure of how different an object's tone/texture is to the tree stand it's located within. (Standard deviation ratio to super-object entropy/correlation/tone)	Identifies anomalous habitat features within a stand, and may be indicative of specialized or rare habitat types.
Curvature	Relates to the sum of changes in direction of the main line of the object, or sinuosity. (Curvature/ length, border length)	Indicative of specific geomorphic features, such as water channels or mountain ridges.
Size	Object size. (Area)	Forest patch size can be linked to habitat quality.
Site	Local topography of the object, or micro-topography. (Mean DEM/TWI)	Reflects microclimatic and local moisture conditions, and therefore, local species.

Table 4.4 The sixteen elements (clusters) identified over all landscapes, along with their universality (percentage the element is present over all landscapes), strength (average eigenvalue and % variance explained), and consistency (average Pearson’s absolute pairwise correlation).

	Label	Universality (%)	Average eigenvalue	Average variance (%)	Average correlation
1	Sub-object variability	100	5.43	7.03	0.91
2	Tone	100	4.90	6.44	0.68
3	Proximity to edge	100	3.92	5.67	0.74
4	Texture variability	100	3.35	4.97	0.51
5	Aspect	100	2.61	4.53	0.58
6	Compactness	100	2.45	4.44	0.72
7	Landscape position	100	2.10	3.92	0.71
8	Position within super-object	100	1.63	3.32	0.88
9	Object orientation	100	1.39	2.95	0.75
10	Slope orientation	100	1.36	2.89	0.51
11	Texture context	87.5	2.08	3.65	0.26
12	Landscape context	87.5	1.86	3.81	0.49
13	Dissimilarity to super-object	75	2.89	4.66	0.61
14	Curvature	75	1.22	2.51	0.23
15	Size	62.5	3.76	5.25	0.73
16	Site	50	5.14	6.63	0.66

When dividing the results into the two landscape types, the number of universal clusters identified increased to twelve for both riparian and upland landscapes (Table 4.5). The twelve universal clusters identified in the upland landscapes, explained an additional 5% of the total variance within the factors (56%), as compared to the variance explained by the twelve universal clusters identified in the riparian landscapes (51%). However, the consistency of the clusters identified in riparian landscapes (0.67) was higher on average than upland landscapes (0.60). In both landscape types, sub-object variability and tone were the two factors that explained the most amount of variance in the data. The sub-object variability cluster explained the most variance within riparian landscapes. However, the clusters ranked second and third in upland landscapes (sub-object variability and proximity, respectively) explained a much higher amount of overall variance when compared to similarly ranked clusters in riparian landscapes.

Table 4.5 Universal elements (clusters) identified for riparian and upland landscapes, listed in order of average % variance explained. Also shown is the consistency (average Pearson’s absolute pair-wise correlation) of the elements within each landscape type.

		Riparian		Upland		
	Factor	Average Variance	Average correlation	Factor	Average Variance	Average correlation
1	Sub-object variability	7.26	0.93	Tone	7.05	0.58
2	Tone	5.67	0.84	Sub-object variability	6.81	0.91
3	Texture variability	4.68	0.46	Proximity to edge	6.68	0.78
4	Dissimilarity to super-object	4.66	0.66	Aspect	4.77	0.57
5	Proximity to edge	4.65	0.67	Texture variability	4.51	0.64
6	Compactness	4.55	0.84	Compactness	4.35	0.65
7	Aspect	4.22	0.60	Landscape position	4.12	0.81
8	Landscape position	3.71	0.64	Texture context	4.08	0.22
9	Position within super-object	3.38	0.88	Landscape context	3.79	0.52
10	Slope orientation	2.94	0.58	Position within super-object	3.27	0.87
11	Object orientation	2.91	0.76	Object orientation	2.99	0.75
12	Curvature	2.54	0.22	Slope orientation	2.85	0.43

4.4 Discussion

4.4.1 Quantitative description of spatial landscape heterogeneity

Our object-based approach provides a highly unique and novel description of landscape variability (Table 4.3). The extraction of sixteen landscape elements (clusters) from 62 largely unrelated object-based metrics explained over half of the total variance within the original data (metrics). Ten of these elements were identified over all of the landscapes, despite being calculated from two very different landscape types. However, several of the factors which were not universally identified (such as object size and site) explained a significant amount of the variance when present (Table 4.4). Thus, defining landscape heterogeneity based solely on the ten universal factors could mean that a large amount of variability within certain landscapes could be unaccounted for. Therefore, a generalized, quantitative description of landscape heterogeneity based on our object-based approach should likely include all sixteen of the elements identified.

Potentially problematic was the low consistency of several landscape elements (Table 4.4). However, this may be explained by the highly variable nature of the elements. For instance, the textural elements identified (texture context and texture variability) are composed of four separate texture layers, meaning that clusters representing these attributes are likely related to different properties of the input texture layers. Similarly, the elements related to contextual relationships (texture context and landscape context) would also be expected to be highly variable and likely related to different properties of the relevant input layers. Therefore, while the factors contained within several of the clusters may be statistically unrelated, these elements may still possess similar theoretical meaning.

A major finding of our study was the extraction of new elements that may describe different characteristics of landscape heterogeneity, not previously identified using conventional patch mosaic-based approaches. For instance, within-object heterogeneity (sub-object variability), and homogeneity over broad spatial areas (dissimilarity to super-object), account for variability over multiple spatial scales (Table 4.3). Likewise, landscape position, landscape context, and slope orientation describe positional variability over various spatial scales and topographic surfaces. While characteristics such as context and topographic position have long been conceptually important to ecology (Swanson et al. 1988; Montgomery 1999; Dorner et al. 2002), our object-based approach identifies these terrain-based elements in a quantitatively unique manner, making them useful for a wide range of ecological applications. Furthermore, terrain-driven elements explained close to half of the total variability explained by all sixteen clusters, underscoring the importance of including terrain information and surface complexity into ecosystem and landscape analyses (Dorner et al. 2002; Porter et al. 2002; McGarigal et al. 2009). Based on our results, we contend that there are several new axes of landscape heterogeneity and new ways of quantifying landscape elements important to heterogeneity that have previously been unexplored due to limitations with previous approaches.

Despite a fundamentally different approach, many of the elements identified using our object-based approach can be found in previously established definitions of heterogeneity. Patch compaction (compactness), perimeter/shape complexity (shape), patch size, texture, and edge contrast/neighborhood similarity (context) are all common themes between our results and the results of many patch mosaic-based approaches (Li and Reynolds 1995; Riitters et al. 1995; Cushman et al. 2008). There are also similarities between our results and the eight components (tone, size, shape, texture, pattern, shadow, site, and context) aerial photograph interpreters use to qualitatively characterize landscape variability from manually-drawn polygons (Avery and

Berlin 1992). Object tone, shape, size, texture, site (topography), and context are all elements of both manual interpretation and our results. Given the differences by which landscape ecology (categorical classification of patches), aerial photograph interpretation (qualitative description of polygons), and object-based analysis (quantitative variability within objects) define heterogeneity, it was somewhat surprising that there was such a high degree of similarity among the results of these techniques. However, the identification of similar landscape elements amongst very different approaches may emphasize how universal these characteristics are for describing heterogeneity.

4.4.2 Heterogeneity over landscapes with different structure

The similarity between, and relative importance of, clusters identified for both riparian and upland landscapes is surprising. This similarity suggests that overall landscape heterogeneity may be described using similar elements for both landscape types, despite their obvious ecological and biophysical differences. In fact, all of the universally identified clusters were ranked within one or two places of each other between landscape types, with the exception of aspect, which explained a higher amount of variance in upland landscapes (likely due to the relatively flat and low gradient topography in riparian areas, as opposed to the more extreme changes in aspect in mountainous regions) (Table 4.5). Furthermore, the number of factors originally retained for each landscape type and the total variance explained by those sets of factors was very similar. While the similarities in results among the two landscape types suggest that application of a universal definition of heterogeneity to every landscape may be feasible, there may still be instances where heterogeneity in these different landscape types might require different landscape elements to address specific questions related to structural complexity, vegetation composition, and disturbance dynamics.

Overall, it appears that finer-scale variation in local characteristics of objects may be slightly more important for describing riparian heterogeneity, whereas upland landscape heterogeneity may be related to processes occurring over coarser scales. Structurally, riparian corridors are highly diverse and possess unique ecological characteristics important to biodiversity (Muller 1997). Riparian areas also possess a lot of fine scale variability due to local diversity of vegetation (such as species or age class) and landforms (such as alluvial features or coarse woody debris). These traits may account for the high ranking of sub-object variability and texture variability within such landscapes, as these elements represent heterogeneity on a local level (Table 4.5). In contrast, upland areas often lack some of the structural and ecological diversity as compared to riparian sites because landscape changes tend to occur over broader, more subtle gradients. (For example, the transition between a river and adjacent riparian forest is quite abrupt, whereas changes in species range in higher elevations are more gradual.) This may account for the higher ranking of proximity to super-object edge and the inclusion of contextual elements (landscape context and texture context), which relate to processes occurring over broader scales. Further exploration is warranted to explore differences among landscape types.

4.4.3 Object-based analysis as a landscape analysis tool

Object-based analysis acts as a hybrid approach between landscape ecology and remote sensing by utilizing the rich information found in spatial datasets, within the framework of a patch-based perspective. As such, this approach addresses some problems with the use of categorical data as the basis for landscape analysis. Most existing metrics in landscape ecology which measure elements of spatial heterogeneity (such as Shannon's diversity or Simpson's diversity index) are based on categorical classifications, and are largely dependent on the proportion of habitat type or number of classes used in the classification scheme (Diaz-Varela et al. 2009). In contrast, all of the metrics used in this study were calculated based on trends in the continuous spatial data, so

problems associated with classification such as arbitrary classification schemes, inappropriate thematic resolution (number of classes), and classification errors, are avoided. Furthermore, the quantification of contextual data or object/patch border characteristics in the absence of class data is a new way of incorporating such relationships, and may be helpful in overcoming the categorical limitations of previous approaches used to define heterogeneity.

Potential may also exist in the use of object-based techniques to help address some of the scaling issues inherent to landscape analysis. A common criticism of the patch-mosaic paradigm approach, and other analyses of landscape structure and heterogeneity, is that arbitrary or inappropriate spatial and/or thematic resolutions (scale) are often used for analysis (Li and Wu 2004). Commonly, thematic maps used in such patch-based analyses are derived from manual aerial photograph interpretation, which is subjective and inconsistent, and often has only one focal scale related to the purposes of the original classification (often forest inventory) (Foody 2002; Thompson et al. 2007). In contrast, our approach is consistent (provided the same parameters are used), and relies on statistical variability within the data to generate an almost limitless range of scales from various sources of remotely sensed data (as opposed to the single scale present in most thematic maps). Furthermore, as information derived from an object-based classifier can be calculated and used simultaneously over numerous spatial scales, this broadens the potential scope of including ecological scales meaningful to multiple species, entities, or spatial processes.

Despite the intrinsic advantages of object-based analysis, this approach has several limitations. First, results achieved from the segmentation process can be confusing, and object definition can be 'black-box'. User parameterization within the object-based classifier may be difficult to grasp, such as the scale parameter, which is unitless and related to within-object variability. While the

use of size-based metrics to extract scale breaks (as done in this study) may be a useful approach for defining meaningful scales related to landscape pattern, linking such hierarchies to specific ecological processes remains problematic (Hay et al. 2003). Finally, as the ecological relevance of some object-based metrics may be less apparent, metric choice should be undertaken with care. In this regard, further exploration of object-based analysis for defining landscape heterogeneity is justified. However, we suggest that enormous potential may exist in the use of object-based approaches, particularly within landscape ecology.

4.5 Significance

Landscape change has been occurring globally over the past several centuries due to anthropogenic-driven disturbance (DeFries et al. 2004). One of the foremost challenges for degraded ecosystems is the development of restoration strategies which integrate knowledge of historical conditions, while accounting for widespread environmental transformation such as climate change (Harris et al. 2006). Often, development of ecosystem restoration approaches incorporate elements of landscape heterogeneity to set restoration targets. Indices of landscape heterogeneity are particularly useful because they act as surrogate measures of various ecological properties (Gustafson 1998), and can therefore be linked to the ecological integrity of a target area. However, the majority of studies which quantify landscape-level heterogeneity focus on current (and often highly disturbed) landscapes, and rarely quantify historic heterogeneity. Our assessment of baseline landscape heterogeneity may therefore provide a framework for quantifying much needed baseline information, relevant to landscape reconstruction and restoration.

This exploratory study has demonstrated the use of object-based analysis as a new approach for quantifying landscape heterogeneity. One of the biggest advantages of this approach was the ability to quantitatively represent specific and complex landscape elements; which we suggest could help form the basis of a new definition of landscape heterogeneity. We end with several recommendations. First, further development of methodologies for meaningful scale extraction should be emphasized, and priority should be placed on linking these scales to ecological processes. Secondly, the integration of thematic data into this approach should be used to explore the effects of combining continuous information and discrete thematic classes. In this regard, future definitions of landscape heterogeneity could not only be based off of the variability within the continuous data, but could also incorporate ecologically relevant thematic classifications. Third, we recommend that a similar approach should be applied to landscapes that have experienced significant changes due to anthropogenic disturbance, in order to explore how an object-based definition of heterogeneity changes as the landscape changes over time.

4.6 References

- APS. 2008. Alta Photogrammetry Suite Version 7.1. Quebec City, QC, Canada: Groupe Alta.
- Arcese P, Sinclair ARE. 1997. The Role of Protected Areas as Ecological Baselines. *The Journal of Wildlife Management* 61: 587-602.
- Avery TA, Berlin GL. 1992. *Fundamentals of Remote Sensing and Air Photo Interpretation*. Upper Saddle River: Prentice Hall.
- Benz UC, Hofmann P, Willhauck G, Lingenfelder I, Heynen M. 2004. Multi-resolution, object-oriented fuzzy analysis of remote sensing data for GIS-ready information. *ISPRS Journal of Photogrammetry & Remote Sensing* 58: 239-258.
- Blaschke T. 2003. Object-based contextual image classification built on Image Segmentation. *Advances in Techniques for Analysis of Remotely Sensed Data*: 113-119.
- Burt TP, Butcher DP. 1985. Topographic controls of soil-moisture distributions. *Journal of Soil Science* 36: 469-486.
- Curran PJ, Atkinson PM. 1998. Geostatistics and remote sensing. *Progress in Physical Geography* 22.
- Cushman SA, McGarigal K, Neel MC. 2008. Parsimony in landscape metrics: Strength, universality, and consistency. *Ecological Indicators* 8: 691-703.
- DeFries RS, Foley JA, Asner GP. 2004. Land-use choices: balancing human needs and ecosystem function. *Frontiers in Ecology and the Environment* 2: 249-257.
- Diaz-Varela ER, Marey-Perez MF, Rigueiro-Rodriguez A, Alvarez-Alvarez P. 2009. Landscape metrics for characterization of forest landscapes in a sustainable management framework: Potential application and prevention of misuse. *Annals of Forest Science* 66: 301.
- Dorner B, Lertzman K, Fall J. 2002. Landscape pattern in topographically complex landscapes: issues and techniques for analysis. *Landscape Ecology* 17: 729-743.
- ENVI. 2007. ENVI Version 4.4. Boulder, CO, USA: ITT Visual Information Solutions.

- ESRI. 2006. ArcDoc Version 9.3. Redlands, CA, USA: Environmental Systems Research Institute.
- Foody GM. 2002. Status of land cover classification accuracy assessment. *Remote Sensing of Environment* 80: 185-201.
- Franklin SE, Hall RJ, Moskal LM, Maudie AJ, Lavigne MB. 2000. Incorporating texture into classification of forest species composition from airborne multispectral images. *International Journal of Remote Sensing* 21: 61-79.
- GeoBC. 1996. Terrain Resource Information Management (TRIM) Maps. Crown Registry and Geographic Base Map Data. Victoria, BC: Province of British Columbia.
- Gessler PE, Moore ID, McKenzie NJ, Ryan PJ. 1995. Soil-landscape modeling and spatial prediction of soil attributes. *International Journal of Geographical Information Systems* 9: 421-432.
- Gustafson EJ. 1998. Quantifying Landscape Spatial Pattern: What Is the State of the Art? *Ecosystems* 1: 143-156.
- Harris JA, Hobbs RJ, Higgs E, Aronson J. 2006. Ecological Restoration and Global Climate Change. *Restoration Ecology* 14: 170-176.
- Hay GJ, Blaschke T, Marceau DJ, Bouchard A. 2003. A comparison of three image-object methods for the multi-scale analysis of landscape structure. *ISPRS Journal of Photogrammetry & Remote Sensing* 57: 327-345.
- Hengl T. 2006. Finding the right pixel size. *Computers & Geosciences* 32: 1283-1298.
- Huston MA. 1999. Local Processes and Regional Patterns: Appropriate Scales for Understanding Variation in the Diversity of Plants and Animals. *Oikos* 86: 393-401.
- Jensen JR. 2000. *Remote Sensing of the Environment: An Earth Resource Perspective*. Upper Saddle River: Prentice-Hall, Inc.

- Laliberte AS, Rango A, Havstad KM, Paris JF, Beck RF, McNeely R, Gonzalez AL. 2004. Object-oriented image analysis for mapping shrub encroachment from 1937 to 2003 in southern New Mexico. *Remote Sensing of Environment* 93: 198-210.
- Landres PB, Morgan P, Swanson FJ. 1999. Overview of the Use of Natural Variability Concepts in Managing Ecological Systems. *Ecological Applications* 9: 1179-1188.
- Li H, Reynolds JF. 1995. On Definition and Quantification of Heterogeneity. *Oikos* 73: 280-284.
- Li H, Wu J. 2004. Use and misuse of landscape indices. *Landscape Ecology* 19: 389-399.
- Lindenmayer DB, Franklin JF, Fischer J. 2006. General management principles and a checklist of strategies to guide forest biodiversity conservation. *Biological Conservation* 131: 433-445.
- Manley BFJ. 2005. *Multivariate Statistical Methods: A Primer*. Boca Raton: Chapman & Hall/CRC.
- McGarigal K, Tagil S, Cushman SA. 2009. Surface metrics: an alternative to patch metrics for the quantification of landscape structure. *Landscape Ecology* 24: 433-450.
- Meidinger D, Pojar J. 1999. *The Ecology of the Coastal Western Hemlock Zone*. Victoria, B.C.: Ministry of Forests Research Branch. Report no.
- Montgomery DR. 1999. Process domains and the River Continuum *Journal of the American Water Resources Association* 35: 397-410.
- Muller E. 1997. Mapping riparian vegetation along rivers: old concepts and new methods. *Aquatic Botany* 58: 411-437.
- Nagendra H. 2001. Using remote sensing to assess biodiversity. *International Journal of Remote Sensing* 22: 2377-2400.
- Paine DP, Kiser JD. 2003. *Aerial Photography and Image Interpretation, 2nd Edn*. Hoboken, New Jersey: John Wiley & Sons, Inc.

- Pike RJ. 2000. Geomorphometry - diversity in quantitative surface analysis. *Progress in Physical Geography* 24: 1-20.
- Porter WP, Sabo JL, Tracy CR, Reichman OJ, Ramankutty R. 2002. Physiology on a Landscape Scale: Plant-Animal Interactions. *Integrative and Comparative Biology* 42: 431-453.
- Pringle RM, Syfert M, Webb JK, Shine R. 2009. Quantifying historical changes in habitat availability for endangered species: use of pixel- and object-based remote sensing. *Journal of Applied Ecology* 46: 544-553.
- R.C.A.F. 1937-1938. Air Film Reports. Ottawa: Royal Canadian Air Force Photographic Section. Report no.
- Riitters KH, O'Neil RV, Hunsaker CT, Wickham JD, Yankee DH, Timmins SP, Jones KB, Jackson BL. 1995. A factor analysis of landscape pattern and structure metrics. *Landscape Ecology* 10: 23-39.
- SAS. 2003. SAS 9.1. Cary, NC: SAS Institute Inc.
- Sklenicka P, Lhota T. 2002. Landscape heterogeneity- a quantitative criterion for landscape reconstruction. *Landscape and Urban Planning* 58: 147-156.
- St-Louis V, Pidgeon AM, Radeloff VC, Hawbaker TJ, Clayton MK. 2006. High-resolution image texture as a predictor of bird species richness. *Remote Sensing of Environment* 105: 299-312.
- Swanson FJ, Kratz TK, Caine N, Woodmansee RG. 1988. Landform effects on ecosystem patterns and processes. *Bioscience* 38: 92-98.
- Swetnam TW, Allen CD, Betancourt JL. 1999. Applied Historical Ecology: Using the Past to Manage for the Future. *Ecological Applications* 9: 1189-1206.
- Thompson ID, Maher SC, Rouillard DP, Fryxell JM, Baker JA. 2007. Accuracy of forest inventory mapping: Some implications for boreal forest management. *Forest Ecology and Management* 252.

- TPC CSTPC. 2006. Kennedy Lake Watershed Plan. Ucluelet, BC: Ministry of Forests, Ministry of Environment, Integrated Land Management Bureau, Ministry of Agriculture and Lands and Central Region Chiefs Administration. Report no.
- Turner MG. 1989. Landscape Ecology: The Effect of Pattern on Process. *Annual Review of Ecology and Systematics* 20: 171-197.
- Turner MG, Collins SL, Lugo AE, Magnuson JJ, Rupp TS, Swanson FJ. 2003. Disturbance Dynamics and Ecological Response: The Contribution of Long-Term Ecological Research. *Bioscience* 53: 46-56.
- Wiens JA. 1989. Spatial Scaling in Ecology. *Functional Ecology* 3: 385-397.
- Wulder MA, Hall RJ, Coops NC, Franklin SE. 2004. High spatial resolution remotely sensed data for ecosystem characterization. *Bioscience* 54: 511-521.
- Zinko U, Seibert J, Dynesius M, Nilsson C. 2005. Plant Species Numbers Predicted by a Topography-based Groundwater Flow Index. *Ecosystems* 8: 430-441.

5 CONCLUSION

5.1 Research Summary and Implications

Decades of archival aerial photographs provide one of the only sources of spatially continuous data linking the past to the present. This historical data source is critical for understanding the dramatic changes that have occurred over past decades and centuries. Information on historic conditions is also useful for understanding the natural range of variability within ecosystems and improving restoration and conservation planning (Landres et al. 1999, Swetnam et al. 1999).

With growing evidence of the benefit of historic data for providing insights to complex ecosystem processes, managers and researchers across various disciplines are recognizing the importance of incorporating long-term information into ecological management and planning (Foster et al. 2003). Therefore, improved methods for extracting such historic information are crucial.

Recent advances in image analysis technology have enabled researchers and managers to derive an ever-broadening range of information from spatial imagery, yet are rarely applied to historical aerial photographs. Object-based analysis is one such technique which has provided an alternative methodological framework in which spatial data is summarized in a more meaningful way as compared to traditional pixel-based analyses (Hay et al. 2003). In order to demonstrate the value of aerial photography, my research applied object-based analysis to aerial photographs to explore several objectives. The overall goal of this thesis was to explore the practical and theoretical integration of aerial photography and object-based analysis within three disciplines; ecological management, remote sensing, and landscape ecology. My research made several valuable contributions, explored next.

As demonstrated in chapter two, there is enormous ecological value within historical aerial photographs, and significant promise in using object-based analysis to extract this valuable information. The potential of object-based analysis to analyze aerial photographs was explored in detail in chapter three, which evaluated the ability of automated analysis techniques to mimic the steps of traditional manual interpretation. This comparison was significant because manual interpretation is the most commonly used tool for production of forest inventories, and forms the basis for many management decisions (Hall 2003); however this traditional approach is problematic, being subjective, inefficient, and inconsistent among interpreters (Wulder et al. 2008). Results of this comparison found many similarities between manual interpretation and automated object-based procedures. This research can help provide a foundation for updating the methods used to analyze aerial photography.

Ecological indicators are commonly used to monitor landscape conditions over time (Dale and Beyeler 2001), yet historic values for many indicators can rarely be determined. In chapter 4 object-based analysis was applied to archival aerial photography to quantify historic landscape heterogeneity, an important indicator of diversity and critical to the discipline of landscape ecology. My results not only provided a new definition of heterogeneity, but also develop a possible framework for further development of historic landscape indicators based on aerial photographs.

5.2 Future Research

The ability of automated analysis techniques and aerial photographs to aid ecological management has been demonstrated throughout this thesis, and several important avenues of future research within the discipline of aerial photograph analysis are discussed next. First, there is a need to utilize the valuable information contained within historical aerial photograph

archives and incorporate this data into ecological research and management. Second, continued exploration of object-based analysis as a tool for mapping natural resources from aerial photographs is important because of the enormous potential demonstrated thus far. Finally, an emergent theme of this research is a lack of training related to aerial photograph analysis in both academic and management. Reinvigoration training of expert personnel is necessary for continued and optimal utilization of aerial photographs.

As many scientists identify the need for ecological research to occur over broader temporal scales (Foster et al. 2003), the unique information contained within historic aerial photography merits specific attention for future research. Research should focus on techniques capable of handling the unique challenges associated with historic aerial photographs, such as refinement of geometric and radiometric correction procedures. Such procedures could be particularly beneficial for handling large (and highly variable) sets of photographs and increase their availability to ecosystem managers (and other non-specialists). Integration with additional auxiliary datasets, such as highly detailed terrain data derived from lidar (light detection and ranging), should also be explored as terrain information can improve the quality of data extraction from historic photographs (St-Onge and Achaichia 2001, Vega and St-Onge 2008).

Object-based analysis is particularly promising for analysis of aerial photographs, and researchers have just begun to explore the practical use of this technique for ecological management (Chubey et al. 2006, Wulder et al. 2008). Development and refinement of object-based analysis should target expanded classification schemes, and further assess the ability of this approach to represent landscape structure. Focus should also be placed on assessment of border positional accuracy (Radoux and Defourny 2007) and classification accuracy with respect to manual interpretation and field reference data (Foody 2002, Thompson et al. 2007).

Taken together, this research underscores the lack of training in aerial photograph processing and analysis. Anticipated shortages of personnel with technical capabilities specific to aerial photographs is problematic for the future of natural resource management, which is heavily dependent upon this data source and relevant techniques. Along with the growing demand for spatial data by resource managers and scientists (Cohen et al. 1996), is the need for new data to integrate well with existing mapping procedures based primarily on manual interpretation. Therefore, techniques in which data are produced in an immediately useable format to resource managers and planners are necessary (such as object-based techniques), and could be particularly promising for decreasing the costs and labor requirements of mapping.

Despite the inherent value of aerial photographs, existing challenges associated with the preparation and analysis of this data source threatens their continued contribution to ecology- and resource-based dilemmas. By focusing on the application of object-based analysis to aerial photographs, this thesis has provided a glimpse into the possible future of aerial photography as a tool for ecological research and management.

5.3 References

- Chubey MS, Franklin SE, Wulder MA. 2006. Object-based Analysis of Ikonos-2 Imagery for Extraction of Forest Inventory Parameters. *Photogrammetric Engineering & Remote Sensing* 72: 383-394.
- Cohen WB, Kushla JD, Ripple WJ, Garman SL. 1996. An introduction to digital methods in remote sensing of forested ecosystems: Focus on the Pacific Northwest, USA. *Environmental Management* 20: 1432-1009.
- Dale VH, Beyeler SC. 2001. Challenges in the development and use of ecological indicators. *Ecological Indicators* 1: 3-10.
- Foody GM. 2002. Status of land cover classification accuracy assessment. *Remote Sensing of Environment* 80: 185-201.
- Foster D, Swanson F, Aber J, Burke I, Brokaw N, Tilman D, Knapp A. 2003. The Importance of Land-Use Legacies to Ecology and Conservation. *BioScience* 53: 77-88.
- Hall RJ. 2003. The roles of aerial photographs in forestry remote sensing image analysis. Pages 47-75 in Wulder M, Franklin SE, eds. *Remote Sensing of Forest Environments: Concepts and Case Studies*. Boston: Kluwer.
- Hay GJ, Blaschke T, Marceau DJ, Bouchard A. 2003. A comparison of three image-object methods for the multi-scale analysis of landscape structure. *ISPRS Journal of Photogrammetry & Remote Sensing* 57: 327-345.
- Landres PB, Morgan P, Swanson FJ. 1999. Overview of the use of natural variability concepts in managing ecological systems. *Ecological Applications* 9: 1179-1188.
- Radoux J, Defourny P. 2007. A quantitative assessment of boundaries in automated forest stand delineation using very high resolution imagery. *Remote Sensing of Environment* 110: 468-475.

- St-Onge BA, Achaichia N. 2001. Measuring forest canopy height using a combination of lidar and aerial photography data. *The International Archives of the Photogrammetry, Remote Sensing and Spatial Information Science XXXIV- 3/W4*: 131-137.
- Swetnam TW, Allen CD, Betancourt JL. 1999. Applied Historical Ecology: Using the Past to Manage for the Future. *Ecological Applications* 9: 1189-1206.
- Thompson ID, Maher SC, Rouillard DP, Fryxell JM, Baker JA. 2007. Accuracy of forest inventory mapping: Some implications for boreal forest management. *Forest Ecology and Management* 252.
- Vega C, St-Onge B. 2008. Height growth reconstruction of a boreal forest canopy over a period of 58 years using a combination of photogrammetric and lidar models. *Remote Sensing of Environment* 112: 1784-1794.
- Wulder M, White JC, Hay GJ, Castilla G. 2008. Towards automated segmentation of forest inventory polygons on high spatial resolution satellite imagery. *The Forestry Chronicle* 84: 221-230.

APPENDICES

Appendix A.

Locations and photo numbers for the 8 photographs analyzed within the Kennedy Lake watershed for Chapter 3. Locations representing a diversity of watershed orders were selected.



Federal Flight line Photo Numbers:

Site 1: A5646_047

Site 2: A5681_039

Site 3: A5776_066

Site 4: A5682_012

Site 5: A5776_035

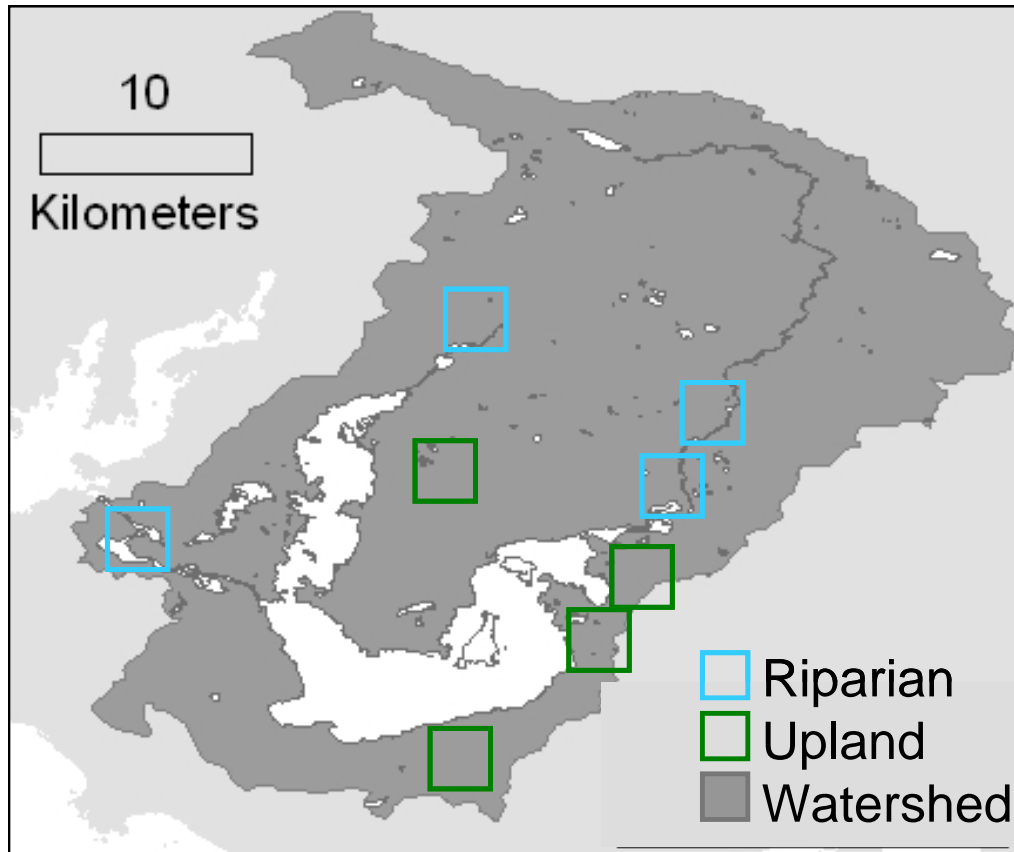
Site 6: A5682_005

Site 7: A5775_074

Site 8: A6275_086

Appendix B.

Approximate locations and photo numbers for the 8 photographs analyzed within the Kennedy Lake watershed for Chapter 4.



Federal Flight line Photo Numbers:

Riparian 1: A5776_066

Riparian 2: A5776_035

Riparian 3: A5744_040

Riparian 4: A5681_039

Upland 1: A5683_058

Upland 2: A6332_011

Upland 3: A5775_074

Upland 4: A6275_086

Appendix C.

The original 200 object-based metrics calculated from the object-based segmentation for defining landscape heterogeneity in Chapter 4. Reduced to a set of 62 metrics (shown in bold) with correlations less than 65%.

- 1 inner_x
- 2 inner_y
- 3 **Area**
- 4 **Area of sub-objects mean (1)**
- 5 **Area of sub-objects stddev (1)**
- 6 Asymmetry
- 7 **Asymmetry of sub-objects mean (1)**
- 8 **Asymmetry of sub-objects stddev (1)**
- 9 Average branch length
- 10 Average length of edges (polygon)
- 11 **Avrg. area represented by segments**
- 12 Avrg. mean diff to neighbors of sub-objects Aspect (1)
- 13 Avrg. mean diff to neighbors of sub-objects Correlation (1)
- 14 Avrg. mean diff to neighbors of sub-objects DEM (1)
- 15 Avrg. mean diff to neighbors of sub-objects Entropy (1)
- 16 Avrg. mean diff to neighbors of sub-objects Homogeneity (1)
- 17 Avrg. mean diff to neighbors of sub-objects Photo (1)
- 18 Avrg. mean diff to neighbors of sub-objects TWI (1)
- 19 Avrg. mean diff to neighbors of sub-objects Variance (1)
- 20 Border index
- 21 **Border length**
- 22 Brightness
- 23 **Compactness**
- 24 **Compactness (polygon)**
- 25 **Contrast to neighbor pixels Aspect (3)**
- 26 Contrast to neighbor pixels Correlation (3)
- 27 **Contrast to neighbor pixels DEM (3)**
- 28 Contrast to neighbor pixels Entropy (3)
- 29 **Contrast to neighbor pixels Homogeneity (3)**
- 30 **Contrast to neighbor pixels Photo (3)**
- 31 Contrast to neighbor pixels TWI (3)
- 32 Contrast to neighbor pixels Variance (3)
- 33 **Curvature/length (only main line)**
- 34 Degree of skeleton branching
- 35 Density
- 36 Density of sub-objects mean (1)
- 37 **Density of sub-objects stddev (1)**
- 38 **Direction of sub-objects mean (1)**
- 39 **Direction of sub-objects stddev (1)**
- 40 Distance to image border
- 41 **Distance to super-object center (1)**
- 42 Elliptic Fit
- 43 **Elliptic distance to super-object center (1)**
- 44 **Is center of super-object (1)**
- 45 **Is end of super object (1)**
- 46 Length
- 47 **Length of longest edge (polygon)**
- 48 Length of main line (no cycles)

- 49 Length of main line (regarding cycles)
- 50 **Length/Width**
- 51 Length/Width (only main line)
- 52 **Main direction**
- 53 Max. diff.
- 54 Max. pixel value Aspect
- 55 Max. pixel value Correlation
- 56 Max. pixel value DEM
- 57 Max. pixel value Entropy
- 58 Max. pixel value Homogeneity
- 59 Max. pixel value Photo
- 60 Max. pixel value TWI
- 61 Max. pixel value Variance
- 62 Maximum branch length
- 63 **Mean Aspect**
- 64 Mean Correlation
- 65 **Mean DEM**
- 66 Mean Diff. to neighbors Aspect (0)
- 67 Mean Diff. to neighbors Correlation (0)
- 68 **Mean Diff. to neighbors DEM (0)**
- 69 Mean Diff. to neighbors Entropy (0)
- 70 Mean Diff. to neighbors Homogeneity (0)
- 71 **Mean Diff. to neighbors Photo (0)**
- 72 Mean Diff. to neighbors TWI (0)
- 73 Mean Diff. to neighbors Variance (0)
- 74 Mean Entropy
- 75 Mean Homogeneity
- 76 **Mean Photo**
- 77 **Mean TWI**
- 78 Mean Variance
- 79 **Mean diff. to brighter neighbors Aspect**
- 80 Mean diff. to brighter neighbors Correlation
- 81 **Mean diff. to brighter neighbors DEM**
- 82 Mean diff. to brighter neighbors Entropy
- 83 **Mean diff. to brighter neighbors Homogeneity**
- 84 **Mean diff. to brighter neighbors Photo**
- 85 **Mean diff. to brighter neighbors TWI**
- 86 **Mean diff. to brighter neighbors Variance**
- 87 Mean diff. to darker neighbors Aspect
- 88 Mean diff. to darker neighbors Correlation
- 89 Mean diff. to darker neighbors DEM
- 90 Mean diff. to darker neighbors Entropy
- 91 Mean diff. to darker neighbors Homogeneity
- 92 Mean diff. to darker neighbors Photo
- 93 Mean diff. to darker neighbors TWI
- 94 Mean diff. to darker neighbors Variance
- 95 **Mean diff. to super-object Aspect (1)**
- 96 Mean diff. to super-object Correlation (1)
- 97 Mean diff. to super-object DEM (1)
- 98 Mean diff. to super-object Entropy (1)
- 99 Mean diff. to super-object Homogeneity (1)
- 100 **Mean diff. to super-object Photo (1)**
- 101 Mean diff. to super-object TWI (1)

102 Mean diff. to super-object Variance (1)
 103 Mean of inner border Aspect
 104 Mean of inner border Correlation
 105 Mean of inner border DEM
 106 Mean of inner border Entropy
 107 Mean of inner border Homogeneity
 108 Mean of inner border Photo
 109 Mean of inner border TWI
 110 Mean of inner border Variance
 111 Mean of outer border Aspect
 112 Mean of outer border Correlation
 113 Mean of outer border DEM
 114 Mean of outer border Entropy
 115 Mean of outer border Homogeneity
 116 Mean of outer border Photo
 117 Mean of outer border TWI
 118 Mean of outer border Variance
 119 Mean of sub-objects stddev Aspect (1)
 120 Mean of sub-objects stddev Correlation (1)
 121 Mean of sub-objects stddev DEM (1)
 122 Mean of sub-objects stddev Entropy (1)
 123 **Mean of sub-objects stddev Homogeneity (1)**
 124 **Mean of sub-objects stddev Photo (1)**
 125 **Mean of sub-objects stddev TWI (1)**
 126 Mean of sub-objects stddev Variance (1)
 127 Min. pixel value Aspect
 128 Min. pixel value Correlation
 129 Min. pixel value DEM
 130 Min. pixel value Entropy
 131 Min. pixel value Homogeneity
 132 Min. pixel value Photo
 133 Min. pixel value TWI
 134 Min. pixel value Variance
 135 Number of edges (polygon)
 136 Number of inner objects (polygon)
 137 Number of segments
 138 Perimeter (polygon)
 139 Polygon self-intersection (polygon)
 140 Radius of largest enclosed ellipse
 141 Radius of smallest enclosing ellipse
 142 Ratio Aspect
 143 Ratio Correlation
 144 Ratio DEM
 145 Ratio Entropy
 146 Ratio Homogeneity
 147 Ratio Photo
 148 Ratio TWI
 149 Ratio Variance
 150 **Ratio to super-object Aspect (1)**
 151 Ratio to super-object Correlation (1)
 152 **Ratio to super-object DEM (1)**
 153 Ratio to super-object Entropy (1)
 154 Ratio to super-object Homogeneity (1)

155 Ratio to super-object Photo (1)
 156 **Ratio to super-object TWI (1)**
 157 Ratio to super-object Variance (1)
 158 Rectangular Fit
 159 **Rel. area to super-object (1)**
 160 Rel. inner border to super-object (1)
 161 Rel. rad. position to super-object (1)
 162 Roundness
 163 Shape index
 164 **Standard deviation Aspect**
 165 Standard deviation Correlation
 166 **Standard deviation DEM**
 167 **Standard deviation Entropy**
 168 Standard deviation Homogeneity
 169 **Standard deviation Photo**
 170 **Standard deviation TWI**
 171 Standard deviation Variance
 172 **StdDev Ratio to super-object Aspect (1)**
 173 **StdDev Ratio to super-object Correlation (1)**
 174 **StdDev Ratio to super-object DEM (1)**
 175 **StdDev Ratio to super-object Entropy (1)**
 176 StdDev Ratio to super-object Homogeneity (1)
 177 **StdDev Ratio to super-object Photo (1)**
 178 **StdDev Ratio to super-object TWI (1)**
 179 StdDev Ratio to super-object Variance (1)
 180 StdDev diff. to super-object Aspect (1)
 181 StdDev diff. to super-object Correlation (1)
 182 StdDev diff. to super-object DEM (1)
 183 StdDev diff. to super-object Entropy (1)
 184 StdDev diff. to super-object Homogeneity (1)
 185 StdDev diff. to super-object Photo (1)
 186 StdDev diff. to super-object TWI (1)
 187 StdDev diff. to super-object Variance (1)
 188 **StdDev. to neighbor pixels Aspect (3)**
 189 **StdDev. to neighbor pixels Correlation (3)**
 190 StdDev. to neighbor pixels DEM (3)
 191 **StdDev. to neighbor pixels Entropy (3)**
 192 StdDev. to neighbor pixels Homogeneity (3)
 193 **StdDev. to neighbor pixels Photo (3)**
 194 StdDev. to neighbor pixels TWI (3)
 195 **StdDev. to neighbor pixels Variance (3)**
 196 **Stddev Curvature (only main line)**
 197 Stddev of area represented by segments
 198 Stddev of length of edges (polygon)
 199 Width
 200 Width (only main line)

Appendix D.

Factor patterns for the sixteen clusters identified as elements of landscape heterogeneity in Chapter 4.

Sub-object variability cluster Factor Rank	Riparian Landscapes				Upland Landscapes			
	1	1	2	2	3	5	4	1
Area	0.2	0.3	0.5	0.4	0.3	0.3	0.1	0.3
Area_of_sub_objects__mean	-0.7	-0.6	-0.4	-0.5	-0.6	-0.5	-0.7	-0.6
Area_of_sub_objects__stddev	0.4	0.6	0.6	0.5	0.5	0.3	0.3	0.5
Asymmetry_of_sub_mean	0.1	0.0	0.1	0.0	0.2	0.2	0.2	0.2
Asymmetry_of_sub_stddev	0.7	0.8	0.8	0.8	0.8	0.8	0.7	0.8
Avrg__area_segment	0.0	0.1	0.2	0.1	0.1	0.1	0.0	0.1
Border_length	0.4	0.5	0.5	0.5	0.4	0.4	0.3	0.4
Compactness	0.2	0.1	0.0	0.0	0.1	0.0	0.3	0.1
Compactness__polygon	-0.3	-0.4	-0.3	-0.3	-0.2	-0.2	-0.4	-0.2
Contrast_to_neig_pix_Asp	0.0	0.1	0.0	0.0	0.2	0.0	0.0	0.1
Contrast_to_neig_pix_DEM	0.1	-0.1	-0.1	0.0	0.0	-0.1	0.0	-0.1
Contrast_to_neig_pix_Hom	-0.1	0.1	0.0	-0.1	0.0	0.0	0.2	-0.1
Contrast_to_neig_pix_Photo	0.1	0.0	0.1	0.0	0.0	0.1	0.1	0.1
Curvature_length	0.0	0.0	-0.3	-0.2	-0.1	-0.2	-0.2	-0.1
Density_of_sub_stddev	0.8	0.8	0.8	0.8	0.8	0.8	0.7	0.8
Direction_of_sub_mean	0.0	0.0	0.1	0.0	0.1	-0.1	0.0	0.0
Direction_of_sub_stddev	0.7	0.8	0.7	0.7	0.6	0.6	0.6	0.5
Distance_to_super_obj	0.0	-0.1	-0.1	0.0	0.0	-0.1	0.0	0.0
Elliptic_distance_to_super	-0.1	-0.1	-0.2	0.0	-0.1	-0.2	-0.2	-0.2
Is_center_of_super_object	0.0	0.1	0.0	0.0	0.0	0.0	0.1	0.1
Is_end_of_super_object	-0.1	-0.1	0.0	0.0	-0.1	0.0	-0.1	0.0
Length_of_longest_edge	0.1	0.0	0.0	0.0	0.0	0.0	0.1	0.1
Length_Width	-0.1	-0.1	-0.1	0.0	-0.1	-0.1	0.0	0.0
Main_direction	0.0	0.0	0.0	0.0	-0.1	-0.1	0.1	0.0
Mean_Aspect	0.0	0.1	0.0	0.1	0.1	0.1	0.1	0.1
Mean_DEM	-0.1	-0.1	-0.1	0.0	0.0	-0.1	0.1	0.0
Mean_Diff__to_neig_DEM	0.0	0.1	0.0	0.0	0.0	0.0	0.0	-0.1
Mean_Diff__to_neig_Photo	0.0	0.0	0.0	0.0	-0.1	0.0	-0.1	0.0
Mean_Photo	0.1	0.0	-0.1	0.0	-0.1	0.0	-0.1	0.0
Mean_TWI	0.1	0.0	0.0	0.0	0.0	0.0	0.0	0.0
Mean_diff_to_bri_neigh_asp	0.0	0.0	0.0	-0.1	0.0	-0.2	0.0	0.0
Mean_diff_to_bri_neigh_DEM	0.1	0.0	0.0	0.1	0.2	0.1	0.0	0.2
Mean_diff_to_bri_neigh_hom	0.2	0.2	0.0	0.1	0.0	0.1	0.1	0.2
Mean_diff_to_bri_neigh_pho	0.0	0.0	0.1	0.0	0.0	0.0	0.1	0.1
Mean_diff_to_bri_neigh_TWI	0.1	0.1	0.1	0.0	0.1	0.2	-0.1	0.1
Mean_diff_to_bri_neigh_var	-0.1	0.0	-0.1	0.0	-0.1	-0.1	0.0	-0.1
Mean_diff__to_super_Asp	0.0	0.0	0.0	0.1	0.0	0.0	-0.1	0.0
Mean_diff__to_super_Photo	-0.1	-0.1	-0.1	0.0	0.0	0.1	0.1	0.0
Mean_of_sub_stddev_Hom	0.8	0.7	0.7	0.6	0.6	0.6	0.8	0.8
Mean_of_sub_stddev_Photo	0.8	0.7	0.8	0.7	0.7	0.8	0.8	0.8
Mean_of_sub_stddev_TWI	0.3	0.3	0.4	0.3	0.6	0.4	0.3	0.4
Ratio_to_super_Aspect	0.0	-0.1	-0.1	0.0	0.0	0.1	0.0	-0.1
Ratio_to_super_DEM	0.0	-0.1	0.1	-0.1	0.1	-0.2	-0.1	0.1
Ratio_to_super_WI	0.0	-0.1	-0.1	0.0	0.0	0.0	0.0	0.0
Rel__area_to_super_object	0.0	0.2	0.4	0.0	0.1	0.2	0.1	0.1
Standard_deviation_Aspect	0.2	0.2	0.1	0.0	0.1	0.1	0.2	0.1
Standard_deviation_DEM	0.1	0.1	0.0	0.2	0.2	0.2	0.2	0.2

Standard_deviation_Entropy	0.2	0.2	0.1	0.2	0.1	0.2	0.1	0.2
Standard_deviation_Photo	0.3	0.2	0.3	0.1	0.2	0.3	0.2	0.3
Standard_deviation_TWI	0.0	0.1	0.0	0.1	0.1	0.1	0.0	0.0
StdDev_Ratio_to_super_Asp	0.1	0.2	0.2	0.1	0.1	0.3	0.0	0.1
StdDev_Ratio_to_super_Cor	0.0	0.0	-0.1	-0.1	0.1	0.0	0.1	0.0
StdDev_Ratio_to_super_DEM	0.2	0.2	0.3	0.2	0.1	0.2	0.1	0.1
StdDev_Ratio_to_super_Ent	0.1	0.1	0.1	0.1	0.2	0.1	0.2	0.2
StdDev_Ratio_to_super_Photo	0.1	0.0	0.1	0.1	0.2	0.2	0.2	0.2
StdDev_Ratio_to_super_TWI	0.0	0.1	0.0	0.0	0.1	-0.1	0.0	0.0
StdDev__to_neighbor_Aspec	0.0	0.1	0.1	-0.1	0.0	0.1	0.1	0.0
StdDev__to_neighbor_Corre	0.0	0.1	-0.1	-0.1	0.1	0.0	-0.1	0.0
StdDev__to_neighbor_Entro	0.1	0.0	-0.1	0.1	0.0	0.0	-0.1	0.1
StdDev__to_neighbor_Photo	0.2	0.1	0.1	0.1	0.1	0.2	0.1	0.1
StdDev__to_neighbor_Varia	0.2	0.2	0.1	0.0	0.1	0.1	0.1	0.0
Stddev_Curvature_main	0.0	0.0	0.1	0.0	0.0	0.1	0.1	-0.1

Tone cluster Factor Rank	Riparian Landscapes				Upland Landscapes				
	4	6	6	1	5	10	1	1	6
Area	0.0	0.0	-0.1	-0.1	0.2	0.0	0.2	0.1	0.0
Area_of_sub_objects__mean	0.0	0.0	0.0	-0.1	0.1	0.0	0.3	0.2	0.0
Area_of_sub_objects__stddev	0.1	0.0	-0.1	0.0	0.1	0.0	0.1	0.0	0.0
Asymmetry_of_sub_mean	0.1	0.0	-0.1	0.0	0.0	0.0	-0.2	0.0	-0.1
Asymmetry_of_sub_stddev	-0.1	0.0	0.0	-0.1	0.0	0.0	0.1	0.1	0.0
Avrg__area_segment	0.0	0.0	0.0	0.0	0.1	0.0	0.3	0.1	0.0
Border_length	0.0	-0.1	0.0	0.0	0.2	0.0	0.2	0.2	0.0
Compactness	-0.1	-0.1	0.0	0.1	-0.1	-0.1	-0.5	-0.2	-0.1
Compactness__polygon	0.0	0.1	0.0	-0.1	-0.1	0.0	0.1	-0.1	0.1
Contrast_to_neig_pix_Asp	-0.1	-0.1	0.0	0.0	-0.1	0.1	0.1	0.0	0.2
Contrast_to_neig_pix_DEM	0.2	0.0	0.1	0.1	0.0	0.0	-0.1	0.1	0.0
Contrast_to_neig_pix_Hom	-0.4	-0.1	0.2	-0.5	-0.1	0.0	-0.8	-0.7	0.0
Contrast_to_neig_pix_Photo	0.7	0.6	0.7	0.9	0.9	0.0	0.7	0.7	0.5
Curvature_length	0.0	0.1	0.0	0.0	-0.1	-0.1	-0.3	-0.2	0.0
Density_of_sub_stddev	0.0	0.0	0.0	-0.1	-0.1	0.0	0.1	0.1	0.0
Direction_of_sub_mean	-0.1	0.1	0.0	0.0	0.0	0.0	0.1	0.0	0.0
Direction_of_sub_stddev	0.0	-0.1	0.0	0.0	0.0	0.0	0.1	0.1	0.2
Distance_to_super_obj	0.0	0.0	0.0	0.0	0.0	0.0	0.0	0.0	0.1
Elliptic_distance_to_super	-0.1	0.0	0.0	0.0	0.1	0.0	0.1	-0.1	0.0
Is_center_of_super_object	0.0	0.1	0.0	0.0	0.0	0.0	0.0	0.0	0.0
Is_end_of_super_object	0.0	0.0	0.0	-0.1	0.0	0.0	0.0	0.0	0.0
Length_of_longest_edge	-0.1	-0.1	-0.1	0.0	0.0	0.1	0.1	0.1	-0.1
Length_Width	0.0	0.0	0.0	0.0	-0.1	0.0	0.0	-0.2	-0.1
Main_direction	0.0	0.0	-0.1	0.0	-0.1	0.0	0.0	-0.1	0.0
Mean_Aspect	-0.1	-0.2	-0.1	0.0	-0.2	0.0	-0.3	-0.1	-0.2
Mean_DEM	0.0	-0.1	0.1	0.1	-0.1	0.0	0.0	-0.1	-0.1
Mean_Diff__to_neig_DEM	0.2	0.0	0.2	0.1	0.1	0.0	0.0	0.1	0.1
Mean_Diff__to_neig_Photo	0.9	0.9	0.9	0.9	0.8	0.4	0.9	0.8	0.9
Mean_Photo	0.7	0.6	0.6	0.8	0.5	0.2	0.7	0.7	0.7
Mean_TWI	-0.1	0.0	0.1	-0.2	-0.6	0.0	-0.1	-0.3	0.1
Mean_diff_to_bri_neigh_asp	0.0	0.0	0.0	0.1	0.0	0.0	0.2	0.1	0.1
Mean_diff_to_bri_neigh_DEM	-0.1	0.0	-0.1	0.1	0.1	0.0	0.1	0.1	-0.1
Mean_diff_to_bri_neigh_hom	0.1	0.0	-0.1	0.4	0.0	-0.1	0.3	0.2	0.0
Mean_diff_to_bri_neigh_phot	-0.8	-0.8	-0.8	-0.8	-0.7	-0.2	-0.8	-0.8	-0.7
Mean_diff_to_bri_neigh_TWI	0.0	-0.1	-0.1	0.1	0.1	0.0	0.0	0.0	-0.1

Mean_diff_to_bri_neigh_var	-0.5	-0.3	0.1	-0.2	-0.2	0.0	-0.8	-0.8	-0.1
Mean_diff_to_super_Asp	0.0	0.1	0.0	0.0	0.1	-0.3	-0.2	0.0	0.0
Mean_diff_to_super_Ph	0.7	0.6	0.6	0.3	0.3	0.8	0.8	0.6	0.5
Mean_of_sub_stddev_Hom	0.1	0.1	0.0	0.2	-0.1	0.0	0.0	-0.1	0.0
Mean_of_sub_stddev_Ph	0.2	0.1	0.0	0.2	0.0	0.0	0.1	0.1	0.0
Mean_of_sub_stddev_TWI	0.0	0.0	0.0	0.2	-0.1	0.0	0.1	-0.1	0.1
Ratio_to_super_Aspect	0.0	0.0	-0.1	0.0	0.0	0.0	0.0	0.0	0.1
Ratio_to_super_DEM	0.0	0.1	0.1	0.0	-0.1	0.2	0.1	0.0	0.1
Ratio_to_super_WI	-0.1	0.0	-0.1	0.1	0.0	-0.7	-0.1	-0.3	0.1
Rel_area_to_super_object	0.0	-0.1	0.1	-0.1	-0.1	0.0	0.0	0.0	-0.1
Standard_deviation_Aspect	0.0	0.1	0.0	0.1	-0.4	0.1	0.0	-0.1	-0.1
Standard_deviation_DEM	-0.1	0.0	-0.1	0.1	0.0	-0.1	0.1	0.1	0.0
Standard_deviation_Entropy	0.0	0.3	-0.1	0.1	-0.2	0.0	-0.2	-0.4	0.0
Standard_deviation_Ph	0.3	0.2	-0.1	0.6	0.1	0.0	0.8	0.6	0.0
Standard_deviation_TWI	0.0	-0.1	0.0	0.0	-0.6	0.1	-0.1	-0.2	0.1
StdDev_Ratio_to_super_Asp	-0.1	0.1	-0.1	-0.1	-0.1	0.1	0.1	0.0	0.0
StdDev_Ratio_to_super_Cor	0.2	0.1	0.3	0.0	0.0	0.7	-0.2	0.8	0.1
StdDev_Ratio_to_super_DEM	-0.1	0.0	0.0	0.0	-0.1	0.0	0.1	0.1	0.1
StdDev_Ratio_to_super_Ent	0.0	0.1	-0.1	0.1	0.0	-0.2	-0.2	-0.2	-0.1
StdDev_Ratio_to_super_Ph	0.1	0.0	0.1	0.0	-0.1	0.2	0.7	0.8	0.0
StdDev_Ratio_to_super_TWI	-0.1	-0.1	0.0	0.0	0.0	-0.2	0.0	-0.1	-0.1
StdDev_to_neighbor_Aspec	-0.1	0.0	-0.1	-0.1	-0.1	0.1	0.1	0.0	-0.2
StdDev_to_neighbor_Corre	0.1	0.0	0.1	0.2	0.0	0.0	0.0	0.1	0.2
StdDev_to_neighbor_Entro	-0.1	-0.2	-0.1	-0.1	0.0	0.1	0.0	-0.1	0.1
StdDev_to_neighbor_Ph	-0.1	-0.2	-0.1	-0.2	-0.1	0.1	0.0	-0.2	0.0
StdDev_to_neighbor_Varia	-0.1	-0.1	0.0	0.1	-0.1	0.0	-0.1	-0.1	-0.1
Stddev_Curvature_main	-0.1	0.0	0.1	-0.1	0.0	0.0	-0.1	0.0	0.1

Proximity to border cluster Factor Rank	Riparian Landscapes					Upland Landscapes		
	6	4	11	3	12	6	3	15
Area	0.0	-0.1	0.0	0.1	0.1	-0.1	-0.2	0.0
Area_of_sub_objects__mean	0.2	-0.1	0.1	0.1	0.1	-0.1	-0.2	0.0
Area_of_sub_objects__stddev	0.0	-0.1	0.0	0.1	0.0	0.0	-0.1	0.0
Asymmetry_of_sub_mean	-0.1	0.0	0.0	0.0	0.0	0.1	0.1	0.0
Asymmetry_of_sub_stddev	0.1	0.1	0.1	0.0	0.0	0.0	-0.1	-0.1
Avg__area_segment	0.0	0.0	0.0	0.0	0.1	-0.1	-0.1	0.0
Border_length	0.1	-0.2	0.0	0.2	0.1	-0.1	-0.3	0.0
Compactness	0.0	-0.2	-0.1	0.2	0.0	0.1	-0.2	-0.1
Compactness__polygon	0.0	0.1	0.0	-0.2	0.0	0.0	0.0	0.0
Contrast_to_neig_pix_Asp	0.0	0.1	0.1	0.0	0.0	0.2	0.1	0.0
Contrast_to_neig_pix_DEM	-0.2	-0.1	0.0	0.0	0.0	0.0	-0.1	0.0
Contrast_to_neig_pix_Hom	-0.7	0.9	-0.2	-0.8	-0.3	0.9	0.9	-0.1
Contrast_to_neig_pix_Ph	0.4	-0.5	-0.1	0.2	0.0	-0.3	-0.5	-0.1
Curvature_length	0.0	-0.2	0.0	0.3	0.1	0.2	-0.1	-0.3
Density_of_sub_stddev	0.1	0.0	0.0	-0.1	0.0	0.0	-0.1	-0.1
Direction_of_sub_mean	0.0	0.0	0.0	0.0	0.0	0.0	0.0	0.0
Direction_of_sub_stddev	0.0	0.0	0.0	0.1	0.0	-0.1	-0.1	-0.1
Distance_to_super_obj	0.0	0.0	-0.1	0.0	0.1	-0.1	-0.1	0.0
Elliptic_distance_to_super	0.0	0.0	0.0	0.1	0.0	-0.1	0.1	-0.2
Is_center_of_super_object	0.0	0.0	0.0	0.1	-0.1	0.0	0.0	0.0
Is_end_of_super_object	0.0	0.0	0.1	0.0	0.0	0.1	0.0	0.0
Length_of_longest_edge	0.0	0.0	-0.1	0.0	0.0	-0.1	0.0	-0.1

Length_Width	-0.1	0.1	0.0	-0.1	-0.1	0.0	0.1	-0.1
Main_direction	0.0	0.1	0.0	0.0	-0.1	0.0	0.0	0.0
Mean_Aspect	0.0	0.0	0.0	0.1	0.0	0.0	0.0	0.0
Mean_DEM	0.0	0.1	0.1	0.0	-0.1	0.1	0.1	0.0
Mean_Diff__to_neig_DEM	0.0	-0.1	0.1	0.0	0.0	0.0	-0.1	0.0
Mean_Diff__to_neig_Photo	0.2	-0.2	0.1	0.0	-0.1	0.1	0.0	0.2
Mean_Photo	0.0	-0.2	0.0	-0.1	-0.1	0.0	0.0	0.1
Mean_TWI	-0.1	0.0	-0.1	-0.3	-0.1	0.0	0.2	0.0
Mean_diff_to_bri_neigh_asp	0.0	0.0	0.0	-0.1	0.0	0.0	0.0	0.1
Mean_diff_to_bri_neigh_DEM	0.1	0.1	0.0	0.1	0.0	0.1	0.0	0.0
Mean_diff_to_bri_neigh_hom	0.5	-0.7	0.2	0.5	0.1	-0.5	-0.4	0.1
Mean_diff_to_bri_neigh_pho	0.0	0.1	0.0	0.2	0.0	-0.1	0.0	-0.1
Mean_diff_to_bri_neigh_TWI	0.0	-0.1	0.0	0.2	0.1	-0.1	-0.1	0.0
Mean_diff_to_bri_neigh_var	-0.5	0.8	-0.1	-0.6	-0.2	0.7	0.8	-0.1
Mean_diff__to_super_Asp	0.0	0.0	-0.2	-0.2	-0.1	0.1	0.0	-0.2
Mean_diff__to_super_Pho	0.2	0.1	0.5	0.3	-0.1	0.0	0.0	0.7
Mean_of_sub_stddev_Hom	0.1	-0.1	0.0	-0.1	0.0	0.0	0.0	0.1
Mean_of_sub_stddev_Phot	0.2	-0.2	0.1	0.1	0.0	-0.1	-0.2	0.2
Mean_of_sub_stddev_TWI	0.0	0.0	0.0	0.1	0.0	0.1	0.0	0.0
Ratio_to_super_Aspect	0.0	0.1	-0.1	0.0	0.0	0.0	0.0	0.2
Ratio_to_super_DEM	0.1	0.0	0.0	-0.1	0.1	0.0	0.0	0.0
Ratio_to_super_WI	0.0	0.0	-0.1	-0.2	-0.2	0.0	0.0	-0.2
Rel__area_to_super_object	0.0	0.0	0.0	0.0	0.0	0.0	0.0	0.1
Standard_deviation_Aspect	0.1	0.0	0.0	-0.2	0.0	-0.1	0.1	-0.1
Standard_deviation_DEM	0.1	0.0	0.0	0.0	0.0	-0.1	-0.1	-0.1
Standard_deviation_Entropy	-0.1	0.3	0.1	-0.1	0.0	0.4	0.4	0.0
Standard_deviation_Photo	0.4	-0.7	0.2	0.6	0.2	-0.4	-0.8	0.2
Standard_deviation_TWI	0.0	0.0	0.0	-0.1	0.0	0.1	0.1	0.0
StdDev_Ratio_to_super_Asp	0.2	0.0	0.0	-0.1	0.0	-0.2	0.0	-0.1
StdDev_Ratio_to_super_Cor	0.8	-0.3	0.8	0.7	0.8	-0.3	-0.3	0.8
StdDev_Ratio_to_super_DEM	0.0	0.0	0.0	0.1	0.1	-0.1	-0.1	0.0
StdDev_Ratio_to_super_Ent	0.0	0.3	0.4	0.0	0.5	0.6	0.2	0.2
StdDev_Ratio_to_super_Pho	0.8	-0.4	0.8	0.7	0.8	-0.6	-0.4	0.5
StdDev_Ratio_to_super_TWI	-0.1	-0.1	-0.1	0.2	0.1	0.1	0.0	0.0
StdDev__to_neighbor_Asp	0.1	-0.1	0.0	0.0	0.1	-0.1	0.0	0.0
StdDev__to_neighbor_Corre	-0.2	0.0	-0.1	-0.1	-0.1	-0.1	0.0	0.0
StdDev__to_neighbor_Entro	0.2	-0.2	-0.1	0.1	-0.2	-0.2	0.1	0.0
StdDev__to_neighbor_Photo	0.1	0.0	0.0	0.1	0.0	0.0	0.0	0.0
StdDev__to_neighbor_Varia	-0.1	0.0	0.0	0.0	0.0	0.1	0.0	0.0
Stddev_Curvature_main	0.0	0.0	-0.1	-0.2	0.2	-0.1	0.0	-0.1

Texture variability cluster Factor Rank	Riparian Landscapes					Upland Landscapes				
	3	3	14	7	14	5	2	13	3	7
Area	-0.1	0.0	-0.1	0.0	0.0	0.1	-0.2	-0.1	0.0	-0.1
Area_of_sub_objects__mean	-0.2	0.0	-0.3	0.0	-0.1	0.2	-0.2	0.0	0.0	-0.1
Area_of_sub_objects__stddev	-0.1	0.1	0.0	0.0	-0.1	0.1	-0.1	0.1	0.0	-0.1
Asymmetry_of_sub_mean	0.1	0.2	0.2	0.0	0.1	-0.1	0.1	0.0	0.0	0.1
Asymmetry_of_sub_stddev	-0.1	0.0	-0.1	0.0	-0.1	0.0	0.0	0.0	0.1	-0.1
Avrg__area_segment	-0.5	-0.2	0.0	-0.2	0.0	-0.2	-0.3	-0.1	-0.1	0.0
Border_length	0.2	0.2	-0.2	0.0	0.0	0.2	0.0	0.1	0.1	-0.1
Compactness	0.1	-0.1	-0.2	-0.1	0.0	-0.1	0.0	0.0	0.0	0.1
Compactness__polygon	-0.5	-0.3	0.0	-0.1	0.1	-0.2	-0.2	-0.2	-0.2	0.1
Contrast_to_neig_pix_Asp	0.1	-0.1	0.0	0.0	0.0	0.1	0.0	0.1	0.0	-0.2

Contrast_to_neig_pix_DEM	-0.1	-0.1	0.1	0.0	-0.1	-0.4	0.1	0.2	0.2	-0.1
Contrast_to_neig_pix_Hom	0.0	0.1	0.1	0.0	0.2	0.0	-0.1	0.0	-0.1	-0.1
Contrast_to_neig_pix_Photo	0.0	0.0	0.0	0.0	-0.1	-0.1	0.0	-0.1	-0.1	0.1
Curvature_length	0.2	0.0	-0.1	0.0	0.0	-0.1	0.1	0.0	0.0	-0.1
Density_of_sub_stddev	0.0	0.1	0.1	0.0	0.0	0.0	0.1	0.1	0.0	0.0
Direction_of_sub_mean	0.0	0.2	0.0	0.1	-0.1	-0.1	0.0	-0.1	0.1	0.1
Direction_of_sub_stddev	0.0	-0.1	-0.1	0.0	-0.1	0.0	0.0	0.1	0.1	0.0
Distance_to_super_obj	0.1	0.0	-0.1	-0.1	0.1	0.2	0.0	0.1	-0.1	0.0
Elliptic_distance_to_super	0.0	0.0	0.1	0.0	0.3	0.0	0.0	0.0	0.0	0.0
Is_center_of_super_object	0.0	-0.1	0.0	0.0	0.0	0.0	0.0	0.0	0.0	0.0
Is_end_of_super_object	0.0	0.0	0.1	0.0	0.0	-0.1	-0.1	0.0	0.0	0.0
Length_of_longest_edge	-0.3	-0.2	0.0	-0.2	0.0	-0.3	-0.2	-0.1	-0.1	0.1
Length_Width	0.0	0.1	0.1	0.0	0.1	-0.1	0.0	-0.1	0.0	0.0
Main_direction	0.1	0.0	0.0	0.1	0.0	-0.1	0.0	-0.1	0.0	0.0
Mean_Aspect	-0.1	-0.2	-0.1	-0.2	-0.1	0.1	0.4	0.0	0.1	0.0
Mean_DEM	-0.1	-0.1	-0.1	-0.1	0.1	0.0	0.7	-0.1	0.8	-0.1
Mean_Diff__to_neig_DEM	0.1	0.0	0.0	-0.2	-0.2	0.0	0.1	-0.1	0.1	0.0
Mean_Diff__to_neig_Photo	0.0	0.0	0.1	0.1	0.1	-0.1	0.1	0.0	0.0	0.1
Mean_Photo	0.4	0.6	0.2	0.5	0.2	0.3	-0.3	0.0	0.0	0.3
Mean_TWI	0.0	-0.1	0.2	0.0	0.2	-0.1	-0.2	-0.2	-0.1	0.2
Mean_diff_to_bri_neigh_asp	0.0	0.0	0.0	-0.1	0.0	-0.1	0.0	0.1	0.0	0.0
Mean_diff_to_bri_neigh_DEM	0.0	-0.2	-0.1	0.2	0.1	0.3	-0.1	-0.1	0.1	-0.1
Mean_diff_to_bri_neigh_hom	0.1	0.0	0.3	0.1	0.3	0.0	0.3	0.0	0.0	0.4
Mean_diff_to_bri_neigh_pho	0.2	0.2	0.1	0.0	0.1	0.0	0.2	0.1	0.1	0.2
Mean_diff_to_bri_neigh_TWI	0.1	0.0	0.1	0.1	0.1	0.2	0.0	-0.3	0.0	0.0
Mean_diff_to_bri_neigh_var	0.0	0.0	0.2	0.1	0.4	-0.1	0.2	0.0	0.0	0.2
Mean_diff__to_super_Asp	0.0	0.0	0.0	0.0	0.0	0.0	0.1	0.0	0.0	0.0
Mean_diff__to_super_Photo	0.0	0.0	0.1	0.0	-0.1	0.0	0.0	-0.1	0.0	0.0
Mean_of_sub_stddev_Hom	0.2	0.3	0.4	0.1	0.4	0.0	0.1	-0.1	0.0	0.2
Mean_of_sub_stddev_Photo	0.3	0.3	0.2	0.2	0.2	0.0	0.3	0.1	0.2	0.1
Mean_of_sub_stddev_TWI	0.0	0.0	0.0	0.1	0.4	0.0	0.0	-0.3	0.0	0.1
Ratio_to_super_Aspect	0.0	0.2	0.1	0.1	0.0	0.0	0.0	0.0	0.0	0.1
Ratio_to_super_DEM	0.0	0.0	0.0	-0.1	0.0	0.1	0.0	0.0	0.1	-0.1
Ratio_to_super_WI	0.0	0.0	0.1	0.0	0.0	0.0	0.0	0.0	0.0	0.0
Rel__area_to_super_object	0.0	0.1	0.0	0.0	0.1	0.0	0.0	0.0	0.0	0.1
Standard_deviation_Aspect	0.1	0.0	-0.2	0.1	-0.1	-0.1	0.2	0.1	0.0	-0.1
Standard_deviation_DEM	-0.1	-0.1	-0.1	0.1	0.1	0.2	0.1	0.0	0.2	0.0
Standard_deviation_Entropy	-0.1	-0.1	0.7	-0.4	0.6	-0.6	-0.7	-0.1	-0.8	0.6
Standard_deviation_Photo	0.6	0.6	0.0	0.6	-0.1	0.5	0.8	0.4	0.6	-0.4
Standard_deviation_TWI	0.0	0.0	0.0	0.0	0.3	0.1	-0.2	-0.2	-0.1	0.1
StdDev_Ratio_to_super_Asp	0.0	0.0	-0.2	0.0	0.0	0.1	-0.1	0.0	0.0	0.0
StdDev_Ratio_to_super_Cor	0.0	0.0	0.0	0.0	0.1	0.0	0.0	0.1	0.0	0.0
StdDev_Ratio_to_super_DEM	0.0	0.1	0.0	-0.1	0.2	0.0	0.0	0.0	0.0	0.0
StdDev_Ratio_to_super_Ent	0.0	0.1	0.3	0.0	0.1	-0.1	-0.1	0.0	-0.1	-0.2
StdDev_Ratio_to_super_Photo	-0.1	0.0	0.0	0.0	0.1	0.0	0.0	0.1	0.1	-0.1
StdDev_Ratio_to_super_TWI	0.0	0.0	-0.1	0.0	0.0	-0.3	0.0	0.0	-0.1	-0.1
StdDev__to_neighbor_Aspec	0.0	0.1	0.0	-0.2	-0.1	-0.1	0.2	0.2	0.0	0.1
StdDev__to_neighbor_Corre	0.9	0.9	-0.1	0.8	0.0	0.8	0.3	0.2	0.1	0.0
StdDev__to_neighbor_Entro	-0.1	-0.2	0.7	-0.3	0.4	-0.3	-0.7	0.0	-0.8	0.8
StdDev__to_neighbor_Photo	0.8	0.7	0.0	0.6	0.1	0.4	0.8	0.9	0.8	0.0
StdDev__to_neighbor_Varia	0.9	0.8	-0.1	0.9	-0.1	0.9	0.9	0.7	0.9	-0.8
Stddev_Curvature_main	0.0	-0.2	-0.1	0.1	0.0	0.1	0.0	0.1	0.0	0.3

Aspect cluster	Riparian Landscapes				Upland Landscapes				
	9	2	15	11	9	12	4	6	8
Area	0.0	-0.2	0.0	0.0	0.1	-0.1	0.2	0.0	0.0
Area_of_sub_objects__mean	-0.1	-0.2	-0.2	-0.2	0.0	-0.1	0.1	-0.1	-0.2
Area_of_sub_objects__stddev	0.0	-0.1	0.0	0.1	0.1	-0.1	0.2	0.1	0.0
Asymmetry_of_sub_mean	0.2	0.1	-0.1	0.0	0.2	0.2	0.1	0.0	0.1
Asymmetry_of_sub_stddev	0.0	0.0	0.1	0.1	-0.1	0.0	-0.1	0.0	0.1
Avrg__area_segment	0.1	0.1	0.1	0.1	0.3	-0.1	0.3	0.2	0.0
Border_length	0.0	-0.2	0.1	0.0	0.0	-0.1	0.0	-0.1	0.1
Compactness	0.1	0.1	0.1	0.2	0.0	0.0	0.0	0.1	0.2
Compactness__polygon	0.1	0.0	0.0	0.0	0.1	0.1	0.1	0.2	-0.1
Contrast_to_neig_pix_Asp	0.0	0.1	0.1	0.2	0.1	0.1	0.3	0.0	-0.1
Contrast_to_neig_pix_DEM	0.0	0.1	0.2	0.1	-0.1	0.0	0.0	0.1	-0.1
Contrast_to_neig_pix_Hom	0.0	0.0	0.1	-0.2	-0.2	0.0	0.0	-0.1	0.0
Contrast_to_neig_pix_Photo	-0.1	0.0	-0.3	-0.1	0.0	0.0	0.0	0.1	-0.1
Curvature_length	-0.1	0.1	-0.1	0.1	-0.2	-0.2	-0.1	0.0	0.1
Density_of_sub_stddev	0.1	0.1	0.0	0.0	0.0	0.2	0.0	0.0	0.0
Direction_of_sub_mean	-0.1	-0.1	0.0	0.0	-0.1	0.0	0.1	-0.1	0.0
Direction_of_sub_stddev	0.0	0.0	0.2	0.1	0.0	-0.3	0.1	0.1	0.2
Distance_to_super_obj	-0.1	0.0	0.0	-0.1	0.1	-0.1	0.1	-0.1	0.0
Elliptic_distance_to_super	-0.1	0.2	0.1	0.0	0.0	-0.2	0.1	0.1	0.0
Is_center_of_super_object	-0.1	0.0	-0.1	-0.1	0.0	0.0	0.0	-0.1	-0.1
Is_end_of_super_object	0.1	0.0	0.1	0.1	0.0	0.1	0.0	0.2	0.1
Length_of_longest_edge	0.4	0.3	0.1	0.2	0.8	0.0	0.7	0.7	0.2
Length_Width	0.1	0.2	0.0	0.0	0.3	0.2	0.2	0.0	0.1
Main_direction	0.0	-0.1	0.0	0.0	0.0	0.1	0.1	-0.1	0.0
Mean_Aspect	0.2	0.1	0.1	0.1	0.1	-0.2	-0.1	0.1	0.2
Mean_DEM	0.1	-0.4	0.3	0.2	0.0	0.1	-0.3	-0.1	0.0
Mean_Diff__to_neig_DEM	0.3	0.1	0.4	0.2	0.0	-0.1	0.1	0.2	0.1
Mean_Diff__to_neig_Photo	0.0	0.1	0.0	0.0	0.0	-0.1	0.0	-0.1	0.0
Mean_Photo	-0.1	0.0	0.1	0.0	-0.1	0.1	0.2	-0.2	-0.1
Mean_TWI	0.1	0.7	0.1	0.0	0.0	-0.2	0.4	0.2	0.0
Mean_diff_to_bri_neigh_asp	0.5	0.4	0.1	0.2	0.3	-0.1	0.5	0.4	0.5
Mean_diff_to_bri_neigh_DEM	-0.4	-0.8	-0.1	-0.3	-0.3	0.7	-0.8	-0.7	-0.3
Mean_diff_to_bri_neigh_hom	0.0	0.2	0.0	0.3	0.2	0.1	0.0	0.1	-0.1
Mean_diff_to_bri_neigh_pho	0.0	0.1	0.0	0.1	0.2	0.2	0.1	0.1	0.1
Mean_diff_to_bri_neigh_TWI	-0.1	0.0	-0.2	-0.1	0.1	0.0	0.5	-0.1	-0.1
Mean_diff_to_bri_neigh_var	-0.1	0.1	0.1	-0.1	0.2	0.2	-0.1	0.0	0.0
Mean_diff__to_super_Asp	0.0	0.1	-0.1	0.0	0.0	-0.1	0.0	0.2	0.1
Mean_diff__to_super_Photo	0.0	0.1	0.1	0.1	0.1	0.0	-0.1	-0.1	0.0
Mean_of_sub_stddev_Hom	-0.1	0.0	-0.1	-0.2	0.0	0.1	-0.1	0.1	0.0
Mean_of_sub_stddev_Photo	0.0	0.0	0.0	-0.2	0.0	0.1	0.0	0.1	0.0
Mean_of_sub_stddev_TWI	0.1	0.1	0.1	0.1	0.1	0.2	0.4	0.1	0.1
Ratio_to_super_Aspect	-0.1	0.0	-0.1	-0.1	0.0	0.0	0.1	0.0	0.1
Ratio_to_super_DEM	-0.1	-0.1	0.1	-0.1	0.0	0.0	-0.1	0.0	-0.1
Ratio_to_super_WI	0.0	0.1	0.1	0.2	-0.1	0.0	0.0	0.1	0.0
Rel__area_to_super_object	0.2	-0.1	0.1	0.1	0.0	0.1	0.1	0.1	0.1
Standard_deviation_Aspect	0.6	0.8	0.5	0.7	0.5	-0.2	0.7	0.8	0.8
Standard_deviation_DEM	-0.3	-0.8	0.1	-0.1	0.0	0.6	-0.7	-0.6	-0.1
Standard_deviation_Entropy	-0.1	0.0	0.0	0.0	0.0	0.1	-0.1	0.0	-0.1
Standard_deviation_Photo	0.0	0.2	-0.2	0.0	0.0	0.0	0.0	0.0	-0.1
Standard_deviation_TWI	0.1	0.2	0.1	0.1	0.1	-0.1	0.5	0.2	0.2
StdDev_Ratio_to_super_Asp	0.6	0.2	0.7	0.7	0.2	0.0	0.2	0.6	0.7

StdDev_Ratio_to_super_Cor	0.1	-0.1	0.1	0.1	0.0	-0.1	0.0	0.0	-0.1
StdDev_Ratio_to_super_DEM	-0.1	-0.1	0.0	-0.1	0.0	0.1	-0.1	0.0	-0.1
StdDev_Ratio_to_super_Ent	0.1	-0.1	-0.1	0.1	-0.2	-0.1	0.1	0.1	-0.2
StdDev_Ratio_to_super_Photo	0.1	-0.1	0.0	-0.1	-0.1	-0.1	0.0	0.1	-0.2
StdDev_Ratio_to_super_TWI	-0.1	-0.1	0.2	0.1	0.1	0.0	0.0	0.1	0.2
StdDev__to_neighbor_Aspec	0.7	0.7	0.3	0.5	0.7	-0.2	0.8	0.7	0.7
StdDev__to_neighbor_Corre	0.1	-0.1	0.1	0.0	-0.2	0.0	0.0	-0.1	0.0
StdDev__to_neighbor_Entro	-0.2	0.2	-0.1	0.1	0.3	0.2	-0.1	0.0	0.0
StdDev__to_neighbor_Photo	0.0	0.3	0.0	0.1	0.3	0.1	0.2	0.0	0.1
StdDev__to_neighbor_Varia	0.0	0.2	0.0	-0.1	0.0	0.0	-0.1	-0.1	0.0
Stddev_Curvature_main	0.1	0.0	0.2	-0.1	0.0	0.0	0.1	-0.1	0.0

Compactness cluster Factor Rank	Riparian Landscapes				Upland Landscapes				
	10	9	4	9	4	10	9	12	5
Area	-0.1	-0.1	-0.1	-0.1	-0.2	-0.4	-0.1	0.0	-0.1
Area_of_sub_objects__mean	-0.2	-0.2	-0.2	-0.2	-0.3	-0.3	-0.1	-0.2	-0.1
Area_of_sub_objects__stddev	-0.1	-0.1	0.0	0.0	0.0	-0.3	0.0	-0.1	0.0
Asymmetry_of_sub_mean	0.7	0.8	0.8	0.8	0.6	0.7	0.8	0.1	0.8
Asymmetry_of_sub_stddev	0.0	-0.1	-0.1	-0.2	-0.1	-0.1	-0.1	0.3	-0.2
Avrg__area_segment	-0.4	-0.3	-0.3	-0.2	-0.5	-0.4	-0.2	-0.2	-0.3
Border_length	0.2	0.3	0.4	0.2	0.2	-0.1	0.1	0.2	0.3
Compactness	0.5	0.6	0.5	0.1	0.8	0.2	0.2	0.7	0.4
Compactness__polygon	-0.6	-0.6	-0.7	-0.5	-0.9	-0.4	-0.4	-0.5	-0.7
Contrast_to_neig_pix_Asp	0.1	0.1	0.0	-0.1	-0.1	-0.1	0.1	0.0	0.1
Contrast_to_neig_pix_DEM	-0.1	-0.4	-0.3	-0.2	0.0	0.0	-0.2	-0.2	-0.1
Contrast_to_neig_pix_Hom	0.0	-0.1	0.0	0.3	0.0	0.0	0.1	0.0	0.0
Contrast_to_neig_pix_Phot	-0.1	0.0	-0.3	0.0	0.0	-0.1	0.1	0.1	-0.2
Curvature_length	0.0	0.0	0.1	0.0	0.2	0.1	-0.2	0.2	0.2
Density_of_sub_stddev	0.2	0.2	0.2	0.1	0.1	0.1	0.2	0.2	0.2
Direction_of_sub_mean	0.0	0.0	0.0	0.1	0.1	0.0	0.1	0.0	0.0
Direction_of_sub_stddev	-0.1	-0.2	-0.2	-0.3	-0.1	-0.3	-0.4	0.0	-0.4
Distance_to_super_obj	0.0	0.1	0.2	0.1	0.0	-0.2	0.0	0.0	0.0
Elliptic_distance_to_super	0.0	0.1	0.0	0.0	0.1	0.0	0.0	0.0	0.2
Is_center_of_super_object	-0.1	0.1	0.0	0.0	0.0	0.1	0.0	0.1	0.0
Is_end_of_super_object	0.0	0.0	0.0	0.1	-0.1	0.0	0.0	0.0	0.0
Length_of_longest_edge	0.1	0.1	0.1	0.2	0.0	0.0	0.1	0.0	0.2
Length_Width	0.8	0.8	0.9	0.8	0.8	0.8	0.8	0.2	0.8
Main_direction	0.0	0.1	0.0	0.1	0.0	-0.1	0.1	0.0	0.1
Mean_Aspect	-0.1	0.0	0.1	0.0	0.0	0.1	0.0	0.1	0.0
Mean_DEM	0.0	0.0	-0.2	-0.1	0.0	-0.1	0.0	0.0	-0.1
Mean_Diff__to_neig_DEM	0.0	-0.1	-0.2	-0.1	0.0	-0.1	0.0	-0.1	-0.1
Mean_Diff__to_neig_Photo	0.1	0.1	0.1	0.1	-0.1	-0.1	-0.1	0.2	0.0
Mean_Photo	0.2	0.1	0.0	0.0	-0.1	-0.1	-0.1	0.0	-0.1
Mean_TWI	0.1	0.1	0.1	0.2	0.0	0.1	0.0	0.0	0.0
Mean_diff_to_bri_neigh_asp	0.0	0.0	0.0	0.0	0.2	0.0	0.1	0.3	0.1
Mean_diff_to_bri_neigh_DEM	-0.1	0.1	0.0	0.0	0.0	0.0	0.2	0.2	0.0
Mean_diff_to_bri_neigh_hom	0.1	0.1	0.2	-0.1	0.1	0.0	0.0	0.0	0.1
Mean_diff_to_bri_neigh_pho	0.2	0.1	0.1	0.1	0.2	0.2	0.1	-0.1	0.1
Mean_diff_to_bri_neigh_TWI	-0.1	0.0	0.0	-0.1	0.0	0.0	0.0	0.0	0.0
Mean_diff_to_bri_neigh_var	0.2	0.2	0.4	0.3	0.1	-0.1	0.1	0.1	0.1
Mean_diff__to_super_Asp	-0.1	0.1	-0.1	0.0	-0.3	-0.1	0.0	0.0	0.0
Mean_diff__to_super_Photo	0.1	-0.1	0.1	0.0	-0.1	0.1	-0.1	0.0	0.0
Mean_of_sub_stddev_Hom	-0.1	0.2	0.2	0.3	0.4	0.1	0.2	-0.2	0.2

Mean_of_sub_stddev_Phot	-0.1	0.0	0.2	0.2	0.3	0.1	0.2	-0.1	0.1
Mean_of_sub_stddev_TWI	0.0	0.1	0.0	-0.1	0.1	0.0	0.0	0.1	0.1
Ratio_to_super_Aspect	0.0	0.0	0.1	0.0	0.0	-0.1	-0.1	0.0	0.0
Ratio_to_super_DEM	0.0	0.0	-0.1	0.0	-0.1	-0.1	0.1	-0.1	0.0
Ratio_to_super_WI	0.0	0.1	0.0	0.1	-0.1	0.0	0.1	0.0	0.2
Rel_area_to_super_object	-0.1	0.0	0.0	0.1	-0.1	0.0	0.0	0.0	-0.1
Standard_deviation_Aspect	0.1	0.2	0.0	-0.1	0.1	0.3	-0.1	0.0	0.0
Standard_deviation_DEM	0.0	0.0	0.1	-0.2	0.4	0.0	0.1	0.3	0.2
Standard_deviation_Entropy	0.0	0.1	0.1	0.3	0.1	0.1	0.2	0.1	0.1
Standard_deviation_Photo	-0.1	0.0	0.0	-0.1	0.2	0.0	0.1	0.0	-0.1
Standard_deviation_TWI	-0.1	0.1	0.1	-0.1	-0.1	0.0	0.1	0.1	0.1
StdDev_Ratio_to_super_Asp	0.1	0.3	0.0	0.1	0.1	0.2	0.1	0.1	0.0
StdDev_Ratio_to_super_Cor	0.0	0.0	0.0	0.0	0.0	0.0	-0.1	-0.1	0.0
StdDev_Ratio_to_super_DEM	0.0	0.0	0.1	0.0	0.1	0.1	0.0	0.1	0.2
StdDev_Ratio_to_super_Ent	-0.1	-0.1	-0.2	0.0	0.2	0.1	0.1	0.1	-0.1
StdDev_Ratio_to_super_Photo	-0.1	-0.1	0.0	-0.1	-0.1	0.1	0.1	-0.2	-0.1
StdDev_Ratio_to_super_TWI	0.1	0.0	0.1	0.0	0.1	0.1	0.1	0.0	0.0
StdDev__to_neighbor_Asp	0.1	0.2	0.3	0.1	0.1	0.2	0.1	0.2	0.3
StdDev__to_neighbor_Corre	0.1	0.1	-0.1	-0.1	0.0	0.0	-0.1	-0.3	-0.1
StdDev__to_neighbor_Entro	0.1	0.2	0.1	0.1	0.0	0.0	0.1	0.1	0.1
StdDev__to_neighbor_Photo	0.1	0.2	0.2	0.1	0.2	0.0	0.2	0.1	0.1
StdDev__to_neighbor_Varia	0.0	0.1	0.1	0.0	0.2	-0.1	0.1	0.1	0.0
Stddev_Curvature_main	-0.1	0.1	-0.2	-0.1	-0.2	-0.1	-0.1	-0.5	-0.3

Landscape position cluster Factor Rank	Riparian Landscapes				Upland Landscapes			
	12	10	9	8	14	6	5	12
Area	0.0	0.0	0.0	0.0	-0.1	0.0	0.0	-0.1
Area_of_sub_objects__mean	0.1	-0.1	0.0	0.0	-0.2	0.0	0.0	0.1
Area_of_sub_objects__stddev	0.0	0.0	0.0	0.0	0.1	-0.1	0.0	0.0
Asymmetry_of_sub_mean	0.0	0.0	0.1	-0.1	0.2	0.1	0.1	0.2
Asymmetry_of_sub_stddev	0.0	-0.1	0.0	-0.1	0.0	-0.1	0.0	-0.2
Avg__area_segment	0.0	0.0	0.0	0.0	-0.1	0.0	-0.1	0.0
Border_length	0.1	0.0	0.0	-0.1	-0.1	0.0	0.0	-0.2
Compactness	0.2	0.1	0.0	0.0	0.0	0.0	0.2	0.0
Compactness__polygon	-0.1	0.0	0.1	0.1	0.0	0.1	-0.1	0.1
Contrast_to_neig_pix_Asp	0.1	0.0	-0.1	0.0	0.2	-0.2	0.0	0.1
Contrast_to_neig_pix_DEM	0.0	-0.3	-0.1	-0.1	0.1	0.0	-0.2	-0.2
Contrast_to_neig_pix_Hom	-0.1	0.0	-0.1	0.1	0.0	0.1	-0.1	0.1
Contrast_to_neig_pix_Photo	0.0	0.0	0.1	0.0	0.0	-0.2	0.1	0.1
Curvature_length	0.1	0.1	0.0	0.1	0.0	-0.1	0.0	0.1
Density_of_sub_stddev	0.0	0.0	0.0	0.0	0.1	0.0	0.0	0.0
Direction_of_sub_mean	0.0	0.0	0.0	-0.1	0.0	0.1	0.0	-0.1
Direction_of_sub_stddev	0.0	0.1	0.0	0.0	0.0	0.1	0.1	-0.2
Distance_to_super_obj	-0.1	0.0	0.1	0.0	-0.4	-0.2	0.0	0.0
Elliptic_distance_to_super	0.1	-0.1	-0.1	0.0	-0.1	-0.1	0.0	-0.1
Is_center_of_super_object	0.0	-0.1	0.0	0.0	0.0	0.0	-0.1	-0.1
Is_end_of_super_object	0.0	0.0	0.1	0.0	0.1	0.0	0.1	0.1
Length_of_longest_edge	0.0	0.0	0.0	-0.1	0.0	0.0	0.0	0.2
Length_Width	-0.1	0.0	0.1	-0.1	0.1	0.0	0.0	0.0
Main_direction	0.0	0.0	0.0	0.0	0.0	0.0	-0.1	0.0
Mean_Aspect	0.0	0.0	0.1	0.1	0.0	0.0	0.0	0.0
Mean_DEM	0.0	0.0	0.0	0.4	0.0	0.0	-0.1	0.0
Mean_Diff__to_neig_DEM	-0.2	-0.2	-0.3	0.7	0.0	-0.2	-0.6	-0.2

Mean_Diff__to_neig_Photo	0.0	0.0	-0.1	0.0	0.1	0.0	-0.2	0.0
Mean_Photo	0.0	0.0	-0.1	0.0	0.2	0.1	-0.2	0.0
Mean_TWI	0.1	0.1	0.3	-0.2	0.0	0.5	0.5	0.1
Mean_diff_to_bri_neigh_asp	0.0	0.0	0.0	0.0	0.0	0.0	0.1	0.0
Mean_diff_to_bri_neigh_DEM	0.0	0.0	0.0	-0.4	0.0	-0.1	0.2	0.0
Mean_diff_to_bri_neigh_hom	0.2	0.1	0.0	0.0	0.0	0.0	-0.1	0.1
Mean_diff_to_bri_neigh_pho	0.0	0.0	0.0	0.0	0.0	0.0	0.1	0.0
Mean_diff_to_bri_neigh_TWI	-0.1	-0.1	0.0	0.0	-0.1	-0.1	-0.2	-0.1
Mean_diff_to_bri_neigh_var	-0.1	0.0	-0.1	0.0	0.1	0.0	0.0	0.1
Mean_diff__to_super_Asp	0.0	0.0	0.0	0.0	0.2	0.0	0.1	0.1
Mean_diff__to_super_Photo	-0.2	-0.2	-0.3	0.1	0.0	0.0	-0.5	-0.1
Mean_of_sub_stddev_Hom	0.0	0.1	-0.1	0.1	-0.1	0.1	0.0	0.1
Mean_of_sub_stddev_Photo	0.0	0.1	0.0	0.1	0.0	0.0	0.0	0.1
Mean_of_sub_stddev_TWI	0.1	0.0	0.1	-0.1	0.2	0.3	0.1	0.1
Ratio_to_super_Aspect	0.0	-0.1	0.0	0.0	-0.1	-0.1	-0.1	-0.2
Ratio_to_super_DEM	-0.7	-0.7	-0.7	0.7	-0.3	-0.5	-0.7	-0.6
Ratio_to_super_WI	0.8	0.8	0.8	-0.7	0.1	0.9	0.9	0.7
Rel__area_to_super_object	0.0	0.0	0.1	0.0	0.2	0.1	0.0	0.0
Standard_deviation_Aspect	0.0	0.1	0.0	-0.1	0.4	0.1	0.0	0.1
Standard_deviation_DEM	-0.1	-0.1	-0.1	0.4	0.0	-0.1	-0.2	-0.1
Standard_deviation_Entropy	0.0	0.1	-0.1	0.1	0.0	0.0	0.0	0.1
Standard_deviation_Photo	0.1	0.1	0.1	0.0	0.0	-0.1	0.0	0.1
Standard_deviation_TWI	0.2	0.2	0.3	-0.2	0.2	0.5	0.4	0.2
StdDev_Ratio_to_super_Asp	0.1	0.3	0.2	-0.2	0.6	0.2	0.2	0.1
StdDev_Ratio_to_super_Cor	-0.3	-0.1	-0.3	0.1	-0.1	-0.1	-0.3	-0.1
StdDev_Ratio_to_super_DEM	-0.4	-0.4	-0.3	0.3	0.1	-0.3	-0.2	-0.1
StdDev_Ratio_to_super_Ent	0.1	0.4	0.1	-0.1	0.0	0.1	0.2	0.4
StdDev_Ratio_to_super_Photo	-0.1	0.1	0.2	0.1	0.1	-0.1	0.0	0.0
StdDev_Ratio_to_super_TWI	0.3	0.6	0.8	-0.4	0.7	0.9	0.8	0.7
StdDev__to_neighbor_Aspect	0.0	-0.1	0.0	0.2	0.1	-0.1	0.0	0.1
StdDev__to_neighbor_Correlation	-0.1	0.0	0.0	0.1	0.1	-0.1	0.0	0.0
StdDev__to_neighbor_Entropy	0.0	-0.1	0.0	0.0	0.0	0.0	0.1	0.0
StdDev__to_neighbor_Photo	0.0	-0.1	0.0	0.1	0.0	0.0	0.0	0.0
StdDev__to_neighbor_Variation	0.0	0.0	0.1	0.0	0.0	-0.1	-0.1	0.1
Stddev_Curvature_main	0.1	0.0	0.0	0.0	0.1	-0.1	0.1	0.1

Position within super-object cluster

	Riparian Landscapes				Upland Landscapes			
Factor Rank	11	13	11	10	11	11	13	13
Area	0.0	0.0	0.0	0.0	0.0	0.1	0.0	0.0
Area_of_sub_objects__mean	0.0	0.0	0.0	-0.1	0.2	-0.1	-0.1	0.0
Area_of_sub_objects__stddev	0.0	0.0	0.0	-0.1	0.0	0.0	0.0	0.0
Asymmetry_of_sub_mean	0.0	-0.1	0.0	0.0	0.2	-0.1	0.0	0.0
Asymmetry_of_sub_stddev	-0.1	-0.1	0.0	0.0	0.0	0.1	-0.1	0.0
Avrg__area_segment	0.1	0.0	-0.1	0.0	0.0	0.0	0.0	0.0
Border_length	0.0	0.0	0.0	-0.1	0.0	0.0	0.0	0.0
Compactness	0.0	-0.1	-0.1	0.0	0.0	-0.1	0.0	0.0
Compactness__polygon	0.0	0.0	0.0	0.1	0.0	0.0	0.0	0.0
Contrast_to_neig_pix_Asp	0.0	0.1	-0.1	0.0	0.0	0.1	0.0	0.0
Contrast_to_neig_pix_DEM	0.0	0.0	0.0	-0.2	-0.1	0.0	0.1	0.0
Contrast_to_neig_pix_Hom	0.1	0.0	0.1	0.1	0.0	0.0	0.0	0.0
Contrast_to_neig_pix_Photo	0.0	-0.1	0.0	0.0	0.0	-0.1	-0.1	0.1
Curvature_length	0.0	-0.1	-0.1	0.1	0.0	-0.1	-0.2	-0.1

Density_of_sub_stddev	0.0	0.0	0.0	0.0	0.1	-0.1	-0.1	0.0
Direction_of_sub_mean	0.0	-0.1	0.0	0.1	0.0	0.0	0.1	-0.1
Direction_of_sub_stddev	-0.1	0.0	0.0	0.0	-0.1	0.1	0.1	0.0
Distance_to_super_obj	0.2	0.2	0.3	0.1	-0.2	0.2	0.2	-0.2
Elliptic_distance_to_super	0.1	0.2	0.0	0.2	-0.1	0.1	0.1	-0.1
Is_center_of_super_object	-0.9	-0.9	-0.9	-0.9	0.9	-0.8	-0.9	0.9
Is_end_of_super_object	0.9	0.8	0.9	0.9	-0.9	0.8	0.8	-0.9
Length_of_longest_edge	0.1	0.0	-0.1	0.0	0.0	0.1	0.0	-0.1
Length_Width	0.1	0.0	0.0	0.1	0.0	0.0	0.0	0.0
Main_direction	0.1	0.0	0.0	0.0	0.0	0.0	0.0	0.0
Mean_Aspect	0.0	0.0	0.1	0.0	0.1	0.0	0.1	0.0
Mean_DEM	0.0	0.1	0.0	0.0	0.0	0.1	0.0	0.0
Mean_Diff_to_neig_DEM	0.0	0.1	0.0	-0.1	0.0	-0.1	-0.1	-0.1
Mean_Diff_to_neig_Photo	0.0	0.0	0.0	0.0	-0.1	0.0	0.1	0.0
Mean_Photo	0.0	0.0	0.0	0.0	-0.1	0.0	0.1	0.0
Mean_TWI	0.0	-0.1	0.0	0.1	-0.1	0.0	0.0	-0.1
Mean_diff_to_bri_neigh_asp	0.1	0.0	0.1	0.0	0.0	0.1	0.1	0.0
Mean_diff_to_bri_neigh_DEM	0.0	0.1	0.0	0.0	-0.1	0.1	0.1	0.1
Mean_diff_to_bri_neigh_hom	0.0	0.1	0.0	0.0	0.0	0.0	0.0	0.0
Mean_diff_to_bri_neigh_pho	0.0	0.1	0.0	0.1	0.0	0.0	0.0	-0.1
Mean_diff_to_bri_neigh_TWI	0.0	0.0	0.0	-0.1	0.0	-0.1	0.0	0.1
Mean_diff_to_bri_neigh_var	0.1	0.1	0.1	0.1	-0.1	0.0	0.0	0.0
Mean_diff_to_super_Asp	0.0	0.0	-0.1	-0.1	-0.1	0.0	0.0	-0.1
Mean_diff_to_super_Photo	0.0	0.1	-0.1	-0.1	-0.1	0.1	0.2	0.0
Mean_of_sub_stddev_Hom	0.0	-0.1	0.0	0.1	0.1	0.0	-0.1	0.1
Mean_of_sub_stddev_Photo	0.0	-0.1	0.0	0.2	0.1	0.0	-0.1	0.0
Mean_of_sub_stddev_TWI	0.0	0.0	0.0	0.0	0.0	0.0	0.0	-0.1
Ratio_to_super_Aspect	-0.1	-0.2	0.1	0.2	0.0	-0.2	0.0	-0.1
Ratio_to_super_DEM	0.0	0.0	0.0	0.1	0.0	0.1	-0.1	0.0
Ratio_to_super_WI	0.1	0.0	0.0	0.1	-0.1	0.0	0.0	-0.1
Rel_area_to_super_object	0.3	0.3	0.3	0.3	-0.2	0.3	0.3	-0.2
Standard_deviation_Aspect	0.1	0.1	0.0	0.0	0.1	0.2	0.1	0.0
Standard_deviation_DEM	0.0	0.1	0.0	0.0	0.0	0.2	0.1	0.0
Standard_deviation_Entropy	-0.1	0.0	-0.1	0.1	0.0	-0.1	0.0	0.1
Standard_deviation_Photo	-0.1	0.0	0.0	0.0	0.1	0.0	0.0	0.1
Standard_deviation_TWI	0.0	0.0	0.0	-0.1	0.0	0.0	0.0	0.0
StdDev_Ratio_to_super_Asp	0.1	0.4	0.2	0.3	0.0	0.5	0.2	-0.2
StdDev_Ratio_to_super_Cor	0.0	0.1	-0.1	0.0	0.1	0.1	0.1	0.0
StdDev_Ratio_to_super_DEM	0.3	0.2	0.2	0.3	-0.2	0.3	0.2	-0.1
StdDev_Ratio_to_super_Ent	0.0	0.0	0.1	0.0	0.0	0.0	0.0	0.0
StdDev_Ratio_to_super_Photo	0.1	0.1	0.1	0.2	0.0	0.2	0.0	-0.1
StdDev_Ratio_to_super_TWI	0.2	0.1	0.1	0.2	-0.1	0.1	0.1	-0.1
StdDev__to_neighbor_Aspec	0.1	0.2	0.1	-0.1	0.0	0.1	0.1	0.0
StdDev__to_neighbor_Corre	0.0	0.0	0.0	-0.1	0.0	0.0	0.0	0.0
StdDev__to_neighbor_Entro	0.0	0.1	-0.1	0.1	0.0	0.0	0.0	0.0
StdDev__to_neighbor_Photo	0.0	0.2	0.0	0.1	0.0	0.0	0.0	0.0
StdDev__to_neighbor_Varia	0.0	0.0	0.0	0.0	0.0	0.0	0.0	0.1
Stddev_Curvature_main	0.0	0.1	0.0	-0.2	0.0	-0.1	0.2	0.3

Object orientation cluster	Riparian Landscapes				Upland Landscapes			
Factor Rank	15	15	12	14	13	12	14	16
Area	0.0	0.1	0.1	0.0	0.0	-0.2	0.0	0.0
Area_of_sub_objects__mean	0.0	0.0	0.1	0.1	0.0	-0.1	0.0	-0.1

Area_of_sub_objects_stddev	0.0	0.1	0.1	0.0	0.0	0.0	0.1	0.0
Asymmetry_of_sub_mean	0.1	0.0	0.1	0.0	0.2	-0.1	0.1	0.1
Asymmetry_of_sub_stddev	0.0	0.0	0.1	0.0	0.0	-0.1	0.1	0.0
Avrg_area_segment	0.0	0.0	0.0	0.0	0.0	-0.1	0.0	0.0
Border_length	0.0	0.2	0.1	0.1	0.0	-0.3	-0.1	-0.1
Compactness	0.1	0.1	-0.2	0.0	0.0	-0.1	0.0	0.0
Compactness_polygon	0.0	-0.1	0.0	-0.1	0.0	0.1	0.1	0.0
Contrast_to_neig_pix_Asp	0.0	0.1	-0.1	0.1	-0.3	0.3	-0.1	-0.2
Contrast_to_neig_pix_DEM	0.2	0.2	0.2	-0.1	0.2	0.0	0.1	0.1
Contrast_to_neig_pix_Hom	0.0	0.0	0.0	0.1	0.0	0.1	0.0	0.0
Contrast_to_neig_pix_Photo	0.0	0.0	0.0	0.0	0.0	-0.1	0.0	0.0
Curvature_length	0.1	0.0	-0.1	-0.1	0.0	0.0	0.1	0.0
Density_of_sub_stddev	0.0	0.0	0.0	0.0	0.1	-0.1	0.1	0.0
Direction_of_sub_mean	0.8	0.8	0.8	0.8	0.8	0.9	0.8	0.8
Direction_of_sub_stddev	0.0	0.0	-0.1	0.1	-0.1	0.0	-0.2	-0.2
Distance_to_super_obj	0.0	0.1	0.1	0.0	0.0	-0.1	-0.1	0.0
Elliptic_distance_to_super	0.0	-0.1	0.0	0.1	0.0	0.1	0.0	0.0
Is_center_of_super_object	0.0	0.0	0.0	0.0	0.0	0.0	0.0	-0.1
Is_end_of_super_object	0.0	-0.1	0.0	0.1	0.0	0.1	0.1	0.0
Length_of_longest_edge	-0.1	-0.2	-0.1	-0.1	0.0	0.0	0.0	0.0
Length_Width	-0.1	0.1	-0.1	0.1	0.0	-0.1	0.1	0.0
Main_direction	0.8	0.9	0.9	0.8	0.8	0.9	0.8	0.8
Mean_Aspect	0.0	-0.1	0.0	0.1	0.1	0.1	0.1	-0.1
Mean_DEM	-0.1	0.0	0.1	0.0	-0.1	-0.1	0.1	0.0
Mean_Diff_to_neig_DEM	0.0	0.1	0.0	0.0	-0.2	-0.1	0.1	-0.1
Mean_Diff_to_neig_Photo	0.0	0.0	-0.1	0.0	0.0	0.1	0.1	0.0
Mean_Photo	0.0	0.0	0.0	0.0	-0.1	0.1	0.0	0.0
Mean_TWI	-0.1	-0.1	0.0	0.1	0.1	0.0	-0.1	-0.2
Mean_diff_to_bri_neigh_asp	0.1	-0.1	-0.1	0.0	0.0	0.0	-0.1	-0.1
Mean_diff_to_bri_neigh_DEM	0.0	-0.1	0.2	0.0	0.1	-0.1	0.0	0.1
Mean_diff_to_bri_neigh_hom	-0.1	0.0	-0.1	0.0	0.1	0.0	0.1	0.1
Mean_diff_to_bri_neigh_pho	0.0	0.0	0.0	0.1	0.0	0.0	-0.1	0.1
Mean_diff_to_bri_neigh_TWI	0.0	0.0	-0.1	-0.1	0.1	0.0	0.0	0.0
Mean_diff_to_bri_neigh_var	-0.1	0.1	-0.2	0.2	0.0	0.0	0.1	0.1
Mean_diff_to_super_Asp	0.0	0.0	0.0	0.0	0.1	0.0	0.0	0.0
Mean_diff_to_super_Photo	-0.1	-0.1	-0.1	-0.1	0.0	0.1	0.0	0.0
Mean_of_sub_stddev_Hom	0.0	0.0	-0.1	-0.1	0.0	0.0	0.0	0.0
Mean_of_sub_stddev_Photo	0.0	0.0	0.0	-0.1	0.0	0.0	0.0	0.1
Mean_of_sub_stddev_TWI	0.0	0.0	0.0	0.0	0.1	0.0	0.0	-0.1
Ratio_to_super_Aspect	0.0	0.0	0.0	0.0	-0.1	-0.2	0.1	0.0
Ratio_to_super_DEM	0.0	0.0	0.1	0.0	0.0	-0.1	0.0	0.0
Ratio_to_super_WI	-0.1	0.0	0.2	0.1	0.1	0.0	0.0	-0.1
Rel_area_to_super_object	0.0	0.0	0.0	0.0	0.0	0.0	0.0	0.1
Standard_deviation_Aspect	0.0	-0.1	0.0	-0.1	-0.1	0.0	-0.1	0.0
Standard_deviation_DEM	0.0	0.0	0.1	0.1	0.1	-0.1	0.0	0.2
Standard_deviation_Entropy	-0.1	-0.1	0.0	0.1	0.0	0.0	0.1	0.1
Standard_deviation_Photo	0.1	0.0	0.1	-0.1	0.0	0.0	-0.1	0.1
Standard_deviation_TWI	0.0	0.0	0.0	-0.1	0.1	0.0	-0.1	-0.1
StdDev_Ratio_to_super_Asp	-0.1	-0.1	0.0	0.0	-0.1	-0.2	-0.1	0.1
StdDev_Ratio_to_super_Cor	0.0	0.0	0.0	0.0	0.0	0.0	-0.1	-0.1
StdDev_Ratio_to_super_DEM	0.1	0.1	0.0	0.1	0.1	0.0	0.0	0.0
StdDev_Ratio_to_super_Ent	0.1	0.0	0.2	0.0	0.0	0.0	0.2	0.0
StdDev_Ratio_to_super_Photo	0.0	0.0	-0.1	-0.1	-0.1	0.0	-0.2	-0.1
StdDev_Ratio_to_super_TWI	0.0	0.1	-0.1	0.1	0.1	0.0	-0.1	0.0
StdDev_to_neighbor_Aspect	0.0	-0.1	0.0	0.1	-0.2	0.1	-0.1	-0.1

StdDev__to_neighbor_Corre	0.1	0.0	0.2	-0.2	-0.1	-0.1	-0.1	0.1
StdDev__to_neighbor_Entro	-0.1	0.1	-0.1	0.2	0.0	-0.1	0.0	0.1
StdDev__to_neighbor_Photo	0.0	0.0	-0.1	0.0	0.0	-0.1	0.1	0.1
StdDev__to_neighbor_Varia	0.0	0.1	0.0	-0.1	0.1	-0.1	0.1	0.1
Stddev_Curvature_main	0.1	-0.1	-0.3	0.1	0.1	0.0	-0.2	0.1

Slope orientation cluster	Riparian Landscapes					Upland Landscapes								
	Factor Rank	16	18	12	13	13	16	8	17	14	11	15	17	18
Area		0.0	0.0	0.0	0.1	-0.1	0.1	0.0	0.0	0.0	0.0	0.0	0.0	-0.1
Area_sub_mean		0.0	0.1	-0.1	0.1	-0.2	0.1	0.0	0.0	-0.1	-0.1	0.1	0.0	-0.1
Area_sub_stddev		0.1	-0.1	0.0	0.0	0.0	-0.1	-0.1	0.0	-0.1	-0.1	0.0	0.0	-0.1
Asym_of_sub_mean		-0.1	-0.1	0.1	0.0	0.0	0.1	0.2	0.1	-0.2	0.0	-0.1	0.0	0.1
Asym_of_sub_stddev		0.0	0.0	0.0	-0.1	0.1	0.0	0.0	-0.1	0.1	-0.1	0.1	-0.1	0.0
Avrg_area_segment		0.0	0.2	0.0	-0.1	-0.1	0.0	0.0	0.1	-0.1	0.1	0.0	0.0	0.1
Border_length		0.0	0.0	-0.1	0.1	-0.1	0.1	-0.1	0.0	0.0	-0.1	0.0	0.0	-0.2
Compactness		0.0	0.1	-0.1	0.0	0.0	0.0	0.1	-0.1	-0.1	-0.1	0.0	-0.1	-0.1
Compactness_poly		0.1	0.1	0.0	0.0	0.0	0.0	0.1	0.1	-0.1	0.2	0.1	-0.1	0.2
Con_neig_pix_Asp		0.1	-0.1	0.1	0.1	0.0	0.0	-0.2	-0.2	0.2	0.0	0.1	0.1	0.0
Con_neig_pix_DEM		0.2	-0.1	0.1	-0.1	0.0	0.0	0.0	0.1	-0.1	-0.1	-0.1	0.0	0.0
Cont_neig_pix_Hom		0.1	-0.1	0.0	0.0	-0.1	-0.2	0.1	0.1	-0.1	0.0	0.0	0.0	0.0
Cont_neig_pix_Phot		-0.1	0.1	-0.1	-0.1	0.0	0.0	0.0	0.0	0.0	0.1	-0.1	0.0	0.0
Curvature_length		0.1	0.0	-0.1	-0.1	0.0	0.0	0.0	-0.1	0.1	0.1	-0.2	0.0	0.1
Density_sub_stddev		0.0	0.0	0.0	0.0	0.0	0.1	0.1	0.0	0.0	0.0	0.1	-0.1	0.0
Direction_sub_mean		0.0	-0.1	0.0	0.1	0.1	0.0	-0.1	0.0	0.0	0.1	0.1	0.0	0.0
Direction_sub_stddev		0.1	0.0	0.0	0.0	0.1	0.0	-0.1	-0.1	0.1	0.0	0.0	0.1	-0.1
Distance_super_obj		0.0	-0.1	0.0	0.0	0.1	0.0	-0.2	0.0	0.0	0.0	0.0	0.0	-0.1
Elliptic_dist_to_super		0.0	0.0	-0.1	0.1	-0.1	0.0	0.0	0.0	-0.1	0.0	0.0	0.0	0.2
Is_center_super_obj		0.0	0.0	0.0	0.0	0.1	-0.1	-0.1	0.1	0.1	0.0	0.0	0.0	0.0
Is_end_super_object		0.0	0.0	-0.1	0.0	0.0	0.0	0.0	0.1	-0.1	0.0	0.0	0.0	0.1
Length_longest_edge		-0.2	0.2	-0.1	-0.2	-0.1	0.0	0.0	0.0	-0.2	0.0	0.1	-0.1	0.1
Length_Width		-0.1	0.0	0.1	0.0	0.0	-0.1	0.1	0.0	0.0	0.0	-0.1	0.0	0.1
Main_direction		0.0	0.0	0.0	0.1	0.0	0.0	0.0	-0.1	-0.1	0.1	0.0	0.0	0.0
Mean_Aspect		0.8	0.2	0.8	0.8	0.9	0.1	-0.7	0.1	0.3	0.8	0.1	0.8	0.2
Mean_DEM		0.0	0.0	0.0	0.0	-0.1	0.0	0.0	-0.1	0.0	0.0	0.0	-0.1	0.0
Mean_Dif_neig_DEM		0.0	0.1	0.0	0.1	-0.1	0.1	0.1	0.0	0.0	-0.1	-0.1	0.0	-0.1
Mean_Dif_neig_Photo		-0.1	0.0	0.0	-0.1	-0.1	0.0	0.2	0.0	-0.2	-0.3	0.0	-0.1	0.1
Mean_Photo		-0.2	0.0	-0.2	-0.2	0.0	-0.1	0.6	0.1	-0.1	-0.4	0.1	-0.4	0.0
Mean_TWI		0.0	0.0	-0.1	0.0	0.0	0.0	0.1	0.0	0.0	0.0	-0.1	-0.1	0.1
Mn_dif_bri_nei_asp		-0.7	-0.2	-0.7	-0.8	-0.8	-0.1	0.7	-0.1	-0.4	-0.6	-0.1	-0.7	-0.1
Mn_dif_bri_nei_DEM		0.0	0.0	0.1	0.1	0.2	-0.1	0.0	0.0	0.0	0.3	0.0	-0.1	0.1
Mn_dif_bri_nei_hom		-0.2	0.1	0.1	0.0	0.1	0.1	-0.2	-0.2	0.0	0.0	0.0	0.1	-0.1
Mn_dif_bri_nei_pho		-0.1	0.0	-0.1	0.0	0.0	0.0	-0.2	-0.1	0.2	0.1	0.0	0.0	-0.1
Mn_dif_bri_nei_TWI		0.0	0.0	0.1	0.0	0.1	0.0	-0.1	0.1	0.0	0.1	0.0	0.1	0.0
Mn_dif_bri_nei_var		0.0	0.0	0.0	0.0	0.1	-0.2	-0.1	-0.1	-0.1	-0.1	-0.1	0.0	0.0
Mn_diff_super_Asp		0.2	0.8	0.7	0.6	0.3	0.8	-0.2	0.5	0.8	0.4	0.7	0.2	0.8
Mn_diff_super_Photo		0.2	-0.2	0.0	0.1	0.0	0.0	0.0	-0.2	-0.2	-0.2	0.0	0.1	-0.2
Mn_sub_stddev_Hom		-0.1	0.0	-0.1	0.0	0.0	0.1	-0.1	0.0	-0.1	0.1	-0.2	0.2	0.0
Mn_sub_stddev_Phot		-0.1	0.0	0.0	0.0	0.1	0.0	-0.1	0.1	0.0	0.1	-0.1	0.0	0.0
Mn_sub_stddev_TWI		0.0	0.0	0.0	0.0	0.0	0.0	0.1	0.2	0.1	0.0	-0.1	0.0	-0.1
Ratio_super_Aspect		0.0	0.8	0.3	0.2	0.0	0.8	-0.1	0.7	0.5	0.0	0.8	0.0	0.7
Ratio_super_DEM		0.1	0.0	0.1	0.0	0.1	0.1	0.1	0.2	0.1	0.1	-0.1	0.0	0.0
Ratio_super_WI		0.1	0.0	0.1	0.0	-0.1	0.2	0.1	-0.1	0.0	0.0	0.0	0.1	-0.1
Rel_area_to_super		-0.1	0.0	0.0	0.0	0.1	0.0	0.1	0.0	0.0	0.0	0.0	0.0	-0.1
Stddev_Aspect		0.0	-0.1	0.1	-0.1	-0.1	0.0	0.4	0.0	0.1	0.2	0.0	0.0	0.1

Stddev_DEM	0.0	0.0	0.1	0.0	0.0	0.0	0.0	-0.1	0.0	0.3	0.0	-0.1	0.0
Stddev_Entropy	-0.1	0.0	-0.1	-0.1	-0.1	-0.1	-0.1	0.0	0.0	0.1	-0.1	0.3	0.0
Stddev_Photo	-0.1	0.0	-0.1	0.0	0.1	0.0	-0.1	0.1	0.1	0.2	-0.1	0.0	0.0
Stddev_TWI	0.0	0.0	0.0	0.0	-0.1	0.1	0.1	0.1	-0.1	0.0	-0.1	0.0	0.0
StD_Ratio_sup_Asp	0.1	-0.1	0.0	-0.1	0.1	-0.1	0.1	0.0	0.2	0.2	0.1	0.0	0.0
StD_Ratio_sup_Cor	0.1	-0.1	-0.1	0.0	0.0	-0.1	0.1	-0.1	0.1	0.0	0.0	-0.1	0.0
StD_Ratio_sup_DEM	-0.1	0.0	0.0	0.0	0.0	0.0	0.2	0.0	-0.1	-0.1	0.0	-0.1	0.0
StD_Ratio_sup_Ent	0.0	0.1	0.0	-0.1	-0.1	-0.1	0.0	0.0	0.1	0.0	-0.2	0.2	0.0
StD_Ratio_sup_Photo	0.1	0.0	-0.1	0.0	0.0	0.0	0.2	0.2	0.1	0.2	0.0	-0.1	0.2
StD_Ratio_sup_TWI	0.1	0.0	-0.1	0.1	-0.1	0.3	0.1	0.0	0.0	-0.1	-0.1	-0.1	0.0
StdDev_to_nei_Asp	-0.1	0.1	0.0	-0.2	-0.4	0.1	0.3	0.0	0.0	-0.2	0.0	0.0	0.0
StdDev_to_nei_Cor	-0.1	0.0	-0.1	-0.2	0.0	0.0	0.3	0.0	-0.1	-0.3	0.1	-0.3	0.0
StdDev_to_nei_Ent	-0.2	0.1	-0.1	0.0	0.0	0.0	-0.3	-0.2	0.0	0.0	0.0	0.0	0.0
StdDev_to_nei_Photo	0.0	0.0	-0.1	0.0	0.0	0.0	-0.2	0.0	0.0	0.0	0.0	-0.1	0.0
StdDev_to_nei_Var	0.0	0.0	0.0	0.0	0.1	0.0	-0.1	0.0	0.0	0.1	0.0	0.1	0.0
Stddev_Curv_main	0.0	-0.1	-0.1	0.1	-0.2	0.2	-0.1	0.0	0.0	-0.3	0.2	0.0	0.0

Texture context cluster	Riparian Landscapes			Upland Landscapes						
	Factor Rank	13	16	15	15	18	2	9	10	9
Area		0.0	0.0	-0.1	0.1	-0.1	-0.1	0.1	0.0	-0.1
Area_of_sub_objects__mean		-0.1	0.1	0.0	-0.1	0.1	-0.2	0.1	0.0	-0.1
Area_of_sub_objects__stddev		0.0	0.0	-0.1	-0.1	-0.1	0.0	0.1	0.0	0.0
Asymmetry_of_sub_mean		0.1	-0.1	0.0	0.0	0.1	0.1	0.1	0.0	0.1
Asymmetry_of_sub_stddev		0.0	0.0	0.0	0.1	-0.1	0.0	0.0	0.0	-0.1
Avg_area_segment		0.0	0.1	-0.1	0.0	0.0	-0.2	0.0	0.0	0.0
Border_length		-0.1	0.0	-0.1	0.1	0.0	0.2	0.1	0.0	0.0
Compactness		-0.1	-0.1	-0.3	-0.1	0.0	0.1	0.2	0.0	0.3
Compactness__polygon		0.1	-0.1	0.0	-0.1	0.0	-0.3	-0.2	0.0	0.0
Contrast_to_neig_pix_Asp		0.0	0.0	0.0	0.1	0.1	-0.1	-0.1	0.1	-0.1
Contrast_to_neig_pix_DEM		-0.1	0.2	-0.1	0.0	-0.1	0.1	0.0	-0.1	0.0
Contrast_to_neig_pix_Hom		0.4	0.3	0.4	-0.1	0.0	-0.2	0.3	0.5	-0.2
Contrast_to_neig_pix_Photo		-0.2	-0.3	0.0	0.0	0.0	0.0	0.5	0.1	-0.1
Curvature_length		0.0	0.0	-0.1	0.0	0.3	0.2	0.1	0.1	0.1
Density_of_sub_stddev		0.0	0.0	0.0	0.0	0.1	0.0	0.0	0.0	0.0
Direction_of_sub_mean		0.1	0.1	0.0	0.0	0.0	0.0	0.0	0.0	0.0
Direction_of_sub_stddev		0.0	0.1	0.1	0.1	-0.1	0.1	0.1	-0.1	0.0
Distance_to_super_obj		-0.1	0.1	0.1	0.0	-0.1	0.1	0.0	0.0	0.0
Elliptic_distance_to_super		0.0	0.0	0.1	-0.1	-0.1	0.0	0.1	0.0	0.0
Is_center_of_super_object		0.1	-0.1	0.0	0.0	0.0	0.0	0.0	0.0	0.0
Is_end_of_super_object		0.0	0.0	0.0	0.0	-0.1	0.0	0.0	0.1	0.0
Length_of_longest_edge		0.0	0.1	-0.1	-0.1	0.0	-0.1	0.0	-0.2	0.1
Length_Width		-0.1	-0.1	0.0	0.1	0.2	0.1	0.0	0.0	0.1
Main_direction		0.0	0.1	-0.1	0.0	0.0	-0.1	0.0	-0.1	0.1
Mean_Aspect		0.0	0.1	0.0	0.0	0.0	0.8	-0.1	-0.1	0.1
Mean_DEM		0.0	-0.1	0.0	0.1	0.1	0.2	-0.1	-0.1	0.3
Mean_Diff__to_neig_DEM		0.0	0.0	0.0	0.0	0.1	0.0	-0.1	0.0	-0.1
Mean_Diff__to_neig_Photo		-0.1	0.0	0.2	0.1	-0.1	0.0	-0.2	-0.1	0.1
Mean_Photo		0.0	-0.3	0.1	0.0	0.0	-0.5	0.0	0.3	-0.1
Mean_TWI		0.0	-0.3	0.0	-0.1	0.0	-0.1	0.0	0.0	0.5
Mean_diff_to_bri_neigh_asp		0.0	0.1	0.0	0.0	0.0	-0.4	0.1	-0.1	0.0
Mean_diff_to_bri_neigh_DEM		0.0	-0.1	0.0	0.0	-0.1	-0.2	0.0	0.0	0.0
Mean_diff_to_bri_neigh_hom		-0.2	-0.3	-0.3	0.3	0.2	0.7	-0.1	-0.6	0.4
Mean_diff_to_bri_neigh_phot		0.0	-0.1	-0.1	0.0	0.1	0.1	0.1	-0.2	0.3

Mean_diff_to_bri_neigh_TWI	0.0	-0.1	-0.1	0.9	-0.1	-0.1	0.0	-0.2	0.1
Mean_diff_to_bri_neigh_var	0.4	0.1	0.4	0.1	0.0	0.1	0.0	0.1	0.3
Mean_diff_to_super_Asp	0.0	-0.2	0.0	0.0	0.0	0.1	0.1	0.2	0.0
Mean_diff_to_super_Ph0	0.3	0.1	0.7	0.0	-0.1	0.0	-0.3	-0.2	0.1
Mean_of_sub_stddev_Hom	0.2	0.1	0.0	0.1	0.5	0.5	0.2	0.0	0.0
Mean_of_sub_stddev_Ph0t	0.0	0.0	-0.1	0.0	0.3	0.1	0.1	0.0	0.1
Mean_of_sub_stddev_TWI	0.0	0.0	0.0	0.0	0.0	0.0	0.0	0.0	0.0
Ratio_to_super_Aspect	0.1	-0.1	-0.1	0.1	0.0	0.0	0.1	-0.2	0.0
Ratio_to_super_DEM	0.0	0.0	0.2	0.0	0.0	0.0	-0.2	0.0	0.0
Ratio_to_super_WI	0.1	0.0	0.1	0.0	0.2	0.0	-0.1	0.0	0.1
Rel_area_to_super_object	0.0	0.0	0.0	0.0	0.0	0.0	0.0	0.0	0.0
Standard_deviation_Aspect	-0.1	0.0	0.0	0.0	-0.1	-0.3	0.0	0.1	0.0
Standard_deviation_DEM	0.0	0.0	0.0	0.0	0.1	-0.1	0.0	0.0	0.1
Standard_deviation_Entropy	0.7	0.2	0.2	0.1	0.3	0.7	0.6	0.1	-0.1
Standard_deviation_Ph0t0	-0.2	0.0	-0.3	0.0	0.2	0.0	0.1	0.0	0.0
Standard_deviation_TWI	0.0	-0.1	0.0	0.0	0.0	-0.1	-0.1	0.0	0.0
StdDev_Ratio_to_super_Asp	0.1	0.0	0.1	0.0	-0.2	0.0	0.0	0.1	-0.1
StdDev_Ratio_to_super_Cor	0.1	0.2	0.0	-0.2	0.4	-0.2	0.8	-0.2	0.0
StdDev_Ratio_to_super_DEM	-0.2	0.0	0.0	0.0	0.1	-0.1	0.0	0.0	0.1
StdDev_Ratio_to_super_Ent	0.8	0.7	0.6	-0.1	0.4	-0.1	0.9	0.6	-0.1
StdDev_Ratio_to_super_Ph0	0.1	0.2	-0.1	-0.1	0.3	0.0	0.0	0.0	-0.1
StdDev_Ratio_to_super_TWI	0.0	0.1	0.3	0.0	0.1	0.0	-0.1	0.1	-0.1
StdDev_to_neighbor_Aspec	0.0	0.0	0.1	0.2	-0.1	-0.2	0.0	-0.2	0.2
StdDev_to_neighbor_Corre	0.0	-0.1	0.0	0.7	0.1	0.9	-0.1	0.7	-0.8
StdDev_to_neighbor_Entro	0.0	-0.3	0.0	0.3	0.1	0.9	-0.2	-0.5	0.3
StdDev_to_neighbor_Ph0t0	-0.1	0.0	0.1	0.2	0.0	-0.1	0.0	-0.2	0.8
StdDev_to_neighbor_Varia	0.0	0.1	0.0	0.1	0.0	0.5	0.1	0.1	0.3
Stddev_Curvature_main	0.0	-0.2	-0.1	0.0	0.0	0.1	0.0	0.0	0.2

Landscape context cluster Factor Rank	Riparian Landscapes					Upland Landscapes					
	8	17	8	16	7	7	8	8	16	10	14
Area	0.0	0.0	0.0	-0.1	0.2	-0.2	-0.1	0.0	0.0	0.1	-0.2
Area_of_sub_objects__mean	0.0	-0.1	0.0	-0.1	0.0	-0.2	-0.1	0.0	-0.2	-0.1	-0.1
Area_of_sub_objects__stdd	0.0	-0.1	0.0	0.0	0.1	-0.1	-0.2	0.0	0.1	0.0	-0.2
Asymmetry_of_sub_mean	-0.1	-0.2	0.1	0.1	-0.1	-0.1	-0.1	-0.1	0.0	0.1	-0.1
Asymmetry_of_sub_stddev	0.1	0.0	0.1	-0.1	0.0	0.0	0.0	0.0	-0.1	0.0	0.0
Avrg__area_segment	0.0	-0.2	0.0	-0.1	0.0	-0.2	-0.1	-0.1	0.0	0.1	-0.1
Border_length	0.1	0.1	0.1	-0.2	0.2	-0.2	-0.1	0.1	-0.1	0.0	-0.3
Compactness	0.1	0.1	0.1	-0.1	-0.1	0.0	-0.1	0.1	-0.1	-0.1	-0.2
Compactness__polygon	-0.1	-0.2	0.0	0.1	0.0	0.0	0.0	-0.2	0.1	0.0	0.2
Contrast_to_neig_pix_Asp	0.0	0.1	-0.2	-0.2	0.0	0.0	0.0	0.2	0.6	0.1	0.2
Contrast_to_neig_pix_DEM	-0.2	0.4	-0.5	0.2	-0.2	0.7	0.7	-0.2	0.6	-0.2	0.7
Contrast_to_neig_pix_Hom	0.0	-0.2	0.0	0.0	-0.3	-0.1	-0.1	0.1	-0.1	0.0	0.0
Contrast_to_neig_pix_Ph0t0	0.0	0.1	0.0	0.1	0.0	0.1	0.1	-0.4	0.1	0.0	0.2
Curvature_length	0.0	0.1	0.0	-0.1	0.0	0.2	0.1	0.0	0.1	0.0	-0.1
Density_of_sub_stddev	0.1	-0.1	0.1	-0.1	0.0	0.0	-0.1	0.1	-0.1	0.1	-0.1
Direction_of_sub_mean	0.1	0.0	-0.1	0.1	-0.2	0.0	-0.1	0.0	0.0	-0.1	0.0
Direction_of_sub_stddev	0.0	0.2	0.1	0.1	0.1	0.0	0.1	0.1	0.1	0.0	-0.2
Distance_to_super_obj	0.1	0.0	0.0	-0.1	-0.2	-0.1	-0.2	0.0	0.1	0.1	-0.1
Elliptic_distance_to_super	0.0	0.0	0.0	-0.1	0.0	0.0	-0.1	-0.1	0.0	0.0	0.0
Is_center_of_super_object	0.0	0.0	0.0	-0.1	0.1	0.0	0.0	0.0	0.0	0.0	0.0
Is_end_of_super_object	0.0	0.0	0.0	0.0	-0.1	0.1	0.0	0.0	0.0	0.0	0.0
Length_of_longest_edge	0.0	-0.2	0.1	0.0	-0.1	0.0	-0.1	0.1	0.0	0.3	0.1

Length_Width	-0.1	0.0	0.0	-0.1	-0.1	-0.1	-0.1	0.1	0.0	0.1	-0.1
Main_direction	0.0	0.0	0.0	0.0	-0.1	0.0	0.0	0.0	0.0	0.0	0.1
Mean_Aspect	0.0	0.0	0.0	0.0	0.1	0.0	0.0	0.1	0.0	0.0	0.0
Mean_DEM	-0.3	0.3	-0.3	0.7	0.1	0.5	0.7	0.0	0.1	-0.2	0.4
Mean_Diff__to_neig_DEM	-0.3	0.6	-0.3	0.7	-0.1	0.8	0.8	-0.2	0.4	-0.2	0.7
Mean_Diff__to_neig_Photo	0.0	0.1	0.0	0.0	0.1	0.0	0.0	0.0	0.1	0.0	0.0
Mean_Photo	0.0	0.2	-0.1	0.0	0.1	0.0	-0.1	-0.1	0.1	0.1	0.0
Mean_TWI	-0.1	-0.1	0.0	-0.3	-0.1	-0.6	-0.5	0.6	-0.2	0.1	-0.2
Mean_diff_to_bri_neigh_asp	0.0	0.0	0.1	0.1	0.0	0.0	0.1	-0.2	0.1	-0.1	0.1
Mean_diff_to_bri_neigh_DEM	0.0	-0.2	0.0	-0.2	0.4	-0.2	-0.1	-0.1	-0.1	-0.1	-0.3
Mean_diff_to_bri_neigh_hom	0.1	0.4	0.1	0.0	0.4	0.1	0.1	0.1	0.0	0.3	0.1
Mean_diff_to_bri_neigh_pho	0.0	0.2	0.2	0.1	0.0	0.1	0.0	0.0	-0.1	0.1	0.0
Mean_diff_to_bri_neigh_TWI	0.9	0.0	0.8	-0.1	0.7	0.0	-0.3	0.7	0.2	0.8	0.0
Mean_diff_to_bri_neigh_var	0.0	0.1	0.1	-0.1	-0.1	0.0	0.0	0.3	0.0	0.0	0.0
Mean_diff__to_super_Asp	0.0	0.0	0.0	0.1	0.0	0.0	0.0	0.0	0.2	-0.1	0.0
Mean_diff__to_super_Photo	0.0	0.0	0.0	0.0	0.0	0.0	-0.1	0.2	-0.2	0.0	0.0
Mean_of_sub_stddev_Hom	0.0	-0.1	0.1	0.1	0.2	0.1	0.1	0.1	-0.1	0.2	0.0
Mean_of_sub_stddev_Photo	0.0	0.0	0.1	0.1	0.2	0.0	-0.1	0.0	0.0	0.2	0.0
Mean_of_sub_stddev_TWI	0.8	0.0	0.8	0.0	0.8	-0.2	-0.2	0.7	0.0	0.8	-0.2
Ratio_to_super_Aspect	0.0	0.0	0.0	0.2	0.1	0.1	-0.1	-0.1	0.0	0.0	-0.1
Ratio_to_super_DEM	0.0	0.0	0.0	0.2	-0.1	0.5	0.1	0.0	0.1	0.0	0.3
Ratio_to_super_WI	0.1	-0.1	0.0	0.0	0.2	-0.4	-0.1	0.0	0.0	0.0	-0.1
Rel__area_to_super_object	0.0	0.0	0.1	0.0	0.0	0.0	0.0	0.1	0.0	0.0	0.0
Standard_deviation_Aspect	0.0	0.0	0.1	0.0	-0.1	0.0	0.0	-0.1	0.0	0.1	0.0
Standard_deviation_DEM	-0.1	0.1	-0.1	0.2	0.4	0.2	0.2	-0.2	0.1	-0.2	0.1
Standard_deviation_Entropy	0.0	0.1	0.0	0.0	0.1	-0.1	0.0	0.0	-0.1	0.1	0.0
Standard_deviation_Photo	0.0	0.0	0.1	0.0	0.2	0.0	0.0	-0.2	0.0	0.0	0.1
Standard_deviation_TWI	0.9	-0.1	0.9	-0.1	0.9	-0.5	-0.4	0.7	-0.1	0.8	-0.3
StdDev_Ratio_to_super_Asp	0.0	0.1	0.0	0.1	0.1	0.1	0.1	0.0	0.1	0.1	0.0
StdDev_Ratio_to_super_Cor	0.0	0.0	0.0	0.1	0.0	0.0	0.0	0.1	-0.1	0.0	0.0
StdDev_Ratio_to_super_DEM	0.0	0.1	0.1	-0.1	0.0	0.0	0.0	0.1	0.0	0.1	0.1
StdDev_Ratio_to_super_Ent	-0.1	-0.1	0.1	0.2	0.1	0.0	-0.1	0.0	0.1	0.1	0.1
StdDev_Ratio_to_super_Photo	0.0	-0.1	0.0	0.1	0.1	-0.2	0.0	0.1	-0.1	0.0	0.0
StdDev_Ratio_to_super_TWI	0.2	0.0	0.2	0.1	0.3	-0.3	0.0	0.1	0.0	0.2	-0.1
StdDev__to_neighbor_Aspec	0.1	0.1	0.2	0.1	0.2	0.0	0.0	0.1	0.0	0.1	0.0
StdDev__to_neighbor_Corre	0.0	0.0	-0.1	0.1	0.1	0.0	0.1	0.0	-0.1	-0.1	0.0
StdDev__to_neighbor_Entro	0.1	0.3	0.0	-0.2	0.2	0.0	0.1	0.1	0.0	0.2	0.0
StdDev__to_neighbor_Photo	0.1	0.1	0.1	-0.1	0.3	0.1	0.0	0.0	0.0	0.1	0.0
StdDev__to_neighbor_Varia	0.0	-0.1	0.1	-0.1	0.1	0.1	0.2	0.0	0.0	0.0	0.1
Stddev_Curvature_main	0.0	0.0	-0.1	0.0	0.1	0.0	0.0	0.0	0.1	-0.2	0.0

Dissimilarity to super-object cluster

Factor Rank

	Riparian Landscapes					Upland Landscapes				
	5	7	7	8	6	1	3	2	7	4
Area	0.9	-0.2	-0.3	-0.3	0.4	0.8	0.6	0.9	-0.2	0.3
Area_of_sub_objects__mean	0.4	-0.1	-0.1	-0.1	0.3	0.4	0.2	0.3	-0.1	0.0
Area_of_sub_objects__stddev	0.6	-0.1	-0.2	-0.2	0.3	0.6	0.5	0.7	-0.1	0.1
Asymmetry_of_sub_mean	-0.1	0.0	0.1	0.1	0.0	0.0	0.0	0.0	0.1	-0.1
Asymmetry_of_sub_stddev	0.3	-0.1	-0.1	-0.2	0.1	0.3	0.2	0.3	-0.1	0.2
Avrg__area_segment	0.4	-0.1	-0.3	0.0	0.3	0.6	0.5	0.8	-0.2	0.2
Border_length	0.8	-0.2	-0.2	-0.3	0.5	0.8	0.6	0.8	-0.3	0.4
Compactness	-0.2	0.0	0.0	0.0	0.2	-0.1	-0.1	-0.2	0.1	0.1
Compactness__polygon	-0.1	-0.1	-0.1	0.0	-0.1	0.0	0.1	0.0	0.0	-0.1

Contrast_to_neig_pix_Asp	0.0	0.0	0.0	0.0	0.0	0.0	0.1	0.1	0.2	0.0
Contrast_to_neig_pix_DEM	0.2	0.1	0.0	0.0	0.0	-0.1	0.0	-0.1	-0.1	0.1
Contrast_to_neig_pix_Hom	0.0	0.0	0.0	-0.1	-0.1	0.0	0.0	-0.1	0.0	0.0
Contrast_to_neig_pix_Photo	0.1	0.1	0.1	0.2	0.0	0.0	0.0	0.1	0.1	0.0
Curvature_length	-0.5	0.0	0.2	0.0	-0.1	-0.4	-0.3	-0.5	0.2	-0.1
Density_of_sub_stddev	0.2	-0.1	-0.1	0.0	0.0	0.2	0.2	0.3	0.0	0.1
Direction_of_sub_mean	0.1	0.0	0.0	0.1	0.0	0.1	-0.1	0.0	0.0	0.1
Direction_of_sub_stddev	0.3	-0.1	-0.1	-0.1	0.1	0.3	0.4	0.3	-0.1	0.3
Distance_to_super_obj	0.1	0.8	0.8	0.7	0.1	-0.7	-0.7	0.0	0.8	-0.8
Elliptic_distance_to_super	-0.4	0.8	0.7	0.6	-0.9	-0.8	-0.8	-0.3	0.8	-0.7
ls_center_of_super_object	0.0	-0.1	-0.2	-0.1	0.0	0.0	0.1	0.0	-0.1	0.1
ls_end_of_super_object	0.0	-0.1	-0.2	-0.1	0.2	0.2	0.3	0.0	-0.2	0.1
Length_of_longest_edge	0.1	0.0	0.0	0.2	0.2	0.1	0.2	0.3	0.0	-0.1
Length_Width	0.0	0.0	0.0	0.1	0.1	0.0	0.0	-0.1	0.0	0.0
Main_direction	-0.1	0.0	0.0	0.0	0.0	0.0	-0.1	0.0	0.0	0.0
Mean_Aspect	0.0	0.0	0.1	0.0	0.1	-0.2	0.0	-0.1	0.0	-0.1
Mean_DEM	0.0	-0.1	0.0	-0.1	0.0	-0.1	0.1	-0.1	0.0	0.0
Mean_Diff__to_neig_DEM	-0.2	-0.1	-0.1	-0.1	0.0	-0.1	0.0	-0.1	-0.2	0.1
Mean_Diff__to_neig_Photo	-0.1	0.0	0.0	-0.1	0.0	0.0	0.0	0.0	0.0	0.0
Mean_Photo	-0.1	0.0	0.0	-0.1	0.0	0.1	0.1	0.0	-0.1	0.1
Mean_TWI	0.0	0.0	0.0	0.0	0.0	0.1	-0.2	0.1	0.1	0.1
Mean_diff_to_bri_neigh_asp	0.0	-0.1	0.0	0.0	0.0	0.0	0.1	0.1	0.0	0.0
Mean_diff_to_bri_neigh_DEM	0.1	0.0	-0.1	-0.1	0.0	0.1	0.0	0.2	0.0	0.1
Mean_diff_to_bri_neigh_hom	-0.1	0.1	0.0	0.0	0.1	0.0	-0.1	-0.1	0.0	0.1
Mean_diff_to_bri_neigh_pho	0.0	0.0	-0.1	0.0	0.0	0.0	-0.1	-0.1	0.0	0.1
Mean_diff_to_bri_neigh_TWI	0.0	0.1	0.0	-0.1	0.0	0.1	-0.1	-0.1	-0.1	0.0
Mean_diff_to_bri_neigh_var	-0.1	-0.1	0.0	-0.2	0.0	-0.1	0.0	-0.2	0.0	0.1
Mean_diff__to_super_Asp	-0.1	0.0	0.0	0.1	0.1	0.0	0.0	0.0	0.1	-0.1
Mean_diff__to_super_Photo	0.0	0.0	0.0	0.0	0.0	0.0	0.1	-0.1	0.0	0.0
Mean_of_sub_stddev_Hom	0.0	0.0	0.0	0.0	0.0	0.0	0.2	0.2	-0.1	0.0
Mean_of_sub_stddev_Photo	0.1	0.0	-0.1	0.1	0.0	0.0	0.2	0.3	-0.1	0.1
Mean_of_sub_stddev_TWI	0.1	0.0	-0.1	0.0	0.1	0.2	0.1	0.3	-0.1	0.0
Ratio_to_super_Aspect	0.0	-0.1	-0.1	0.0	-0.1	0.0	0.0	0.1	-0.1	0.0
Ratio_to_super_DEM	-0.2	0.0	-0.1	0.0	0.1	0.1	0.0	0.1	0.0	0.1
Ratio_to_super_WI	0.0	0.1	0.1	0.1	-0.2	0.0	-0.1	-0.1	0.1	-0.1
Rel__area_to_super_object	0.4	-0.8	-0.8	-0.7	0.8	0.9	0.8	0.4	-0.8	0.8
Standard_deviation_Aspect	-0.1	-0.1	0.0	0.1	0.0	-0.1	0.0	-0.1	0.0	0.0
Standard_deviation_DEM	0.1	-0.1	-0.2	-0.2	0.1	0.3	0.3	0.3	-0.2	0.3
Standard_deviation_Entropy	-0.1	0.1	0.0	0.2	-0.1	0.0	-0.1	-0.1	0.1	0.0
Standard_deviation_Photo	0.0	0.1	0.0	0.2	-0.1	0.0	0.0	0.2	0.0	0.0
Standard_deviation_TWI	0.0	0.0	0.0	0.0	0.0	0.1	-0.1	0.1	0.0	0.0
StdDev_Ratio_to_super_Asp	0.1	-0.1	-0.3	0.0	0.1	0.3	0.1	0.1	-0.2	0.2
StdDev_Ratio_to_super_Cor	0.0	-0.1	0.0	-0.1	0.0	0.1	0.0	0.0	-0.1	0.1
StdDev_Ratio_to_super_DEM	0.2	-0.6	-0.6	-0.5	0.8	0.8	0.8	0.3	-0.7	0.8
StdDev_Ratio_to_super_Ent	0.0	0.0	0.0	0.0	-0.1	0.1	0.0	0.0	0.0	0.1
StdDev_Ratio_to_super_Photo	0.1	-0.1	-0.2	-0.2	0.1	0.2	0.2	0.2	-0.2	0.3
StdDev_Ratio_to_super_TWI	-0.1	-0.4	-0.2	0.0	0.4	0.2	0.2	0.0	-0.1	0.2
StdDev__to_neighbor_Aspec	0.1	-0.1	0.0	0.0	0.0	0.1	0.1	0.2	-0.1	-0.1
StdDev__to_neighbor_Corre	-0.1	0.0	0.0	0.0	-0.1	0.0	0.0	-0.1	-0.1	0.1
StdDev__to_neighbor_Entro	0.0	-0.1	-0.1	0.0	0.1	0.0	0.0	0.0	0.0	0.1
StdDev__to_neighbor_Photo	0.0	0.0	-0.1	0.0	0.1	0.0	0.0	0.0	-0.1	0.1
StdDev__to_neighbor_Varia	0.0	0.1	-0.1	0.0	0.0	-0.1	-0.1	0.0	0.0	0.0
Stddev_Curvature_main	0.0	0.1	-0.1	0.3	0.1	0.0	0.0	0.1	0.0	0.0

Curvature cluster Factor Rank Metric #	Riparian Landscapes						Upland Landscapes		
	14	19	17	10	17	17	18	16	15
Area	0.1	0.1	-0.1	-0.1	0.0	-0.3	-0.2	0.2	-0.1
Area_of_sub_objects__mean	0.1	0.0	0.0	0.0	-0.1	-0.3	0.0	0.2	-0.1
Area_of_sub_objects__stddev	0.1	0.0	-0.1	0.0	0.0	-0.2	-0.2	0.1	-0.1
Asymmetry_of_sub_mean	0.0	0.2	-0.1	0.1	0.0	0.0	0.0	-0.2	-0.1
Asymmetry_of_sub_stddev	-0.1	-0.1	0.0	-0.1	0.0	-0.1	-0.1	0.0	0.1
Avrg__area_segment	0.2	0.3	0.0	0.1	0.1	0.0	-0.2	0.2	0.0
Border_length	0.0	-0.1	0.0	-0.3	-0.1	-0.4	-0.2	0.2	-0.2
Compactness	-0.2	-0.3	0.3	-0.5	0.0	0.0	-0.1	0.0	0.0
Compactness__polygon	0.2	0.3	0.1	0.3	0.1	0.1	0.1	0.0	0.2
Contrast_to_neig_pix_Asp	-0.1	0.8	0.2	0.0	0.8	0.7	-0.1	0.1	0.0
Contrast_to_neig_pix_DEM	-0.1	0.1	-0.1	0.7	-0.1	-0.2	0.5	0.1	-0.3
Contrast_to_neig_pix_Hom	0.1	-0.1	0.0	0.1	0.0	0.1	0.0	-0.1	0.1
Contrast_to_neig_pix_Photo	0.0	0.0	0.0	0.0	0.1	0.0	0.1	0.0	-0.1
Curvature_length	-0.7	-0.1	0.6	-0.2	0.2	0.0	0.1	-0.2	-0.1
Density_of_sub_stddev	0.0	0.0	0.0	-0.1	0.0	-0.1	0.0	0.0	0.0
Direction_of_sub_mean	-0.1	0.1	0.1	0.1	0.0	0.1	0.0	0.0	0.0
Direction_of_sub_stddev	0.1	-0.1	0.1	0.0	0.0	0.1	-0.1	0.0	0.1
Distance_to_super_obj	0.1	-0.1	0.0	-0.1	0.0	0.0	0.6	0.2	-0.2
Elliptic_distance_to_super	-0.1	0.0	0.1	0.0	0.1	0.0	0.0	0.2	0.1
Is_center_of_super_object	0.0	0.0	0.1	-0.1	0.0	0.0	0.0	0.0	0.2
Is_end_of_super_object	0.1	0.0	-0.1	0.1	-0.1	0.0	0.0	0.0	0.1
Length_of_longest_edge	0.1	0.4	0.0	0.0	0.2	0.0	0.0	0.0	0.2
Length_Width	0.1	0.1	0.0	-0.1	0.0	-0.1	0.0	-0.1	-0.2
Main_direction	0.1	-0.2	0.0	0.1	-0.1	0.0	-0.1	0.1	0.0
Mean_Aspect	0.0	0.1	-0.1	0.0	0.0	0.0	0.1	0.1	0.0
Mean_DEM	0.1	0.0	0.0	0.1	0.0	0.1	0.1	-0.2	0.3
Mean_Diff__to_neig_DEM	0.0	0.1	0.0	0.2	-0.1	-0.1	0.2	0.0	0.0
Mean_Diff__to_neig_Photo	0.0	-0.1	0.1	0.0	0.0	0.0	0.0	0.0	0.0
Mean_Photo	0.0	0.0	0.1	-0.1	0.0	0.1	0.1	0.0	0.0
Mean_TWI	0.0	0.0	-0.1	-0.1	0.0	-0.1	0.1	0.1	-0.2
Mean_diff_to_bri_neigh_asp	0.1	0.0	0.1	0.0	0.0	0.0	0.0	0.0	0.1
Mean_diff_to_bri_neigh_DEM	0.0	0.0	0.1	-0.1	0.0	-0.1	0.0	0.0	0.0
Mean_diff_to_bri_neigh_hom	-0.1	0.1	0.1	-0.1	0.0	-0.1	0.1	-0.1	0.0
Mean_diff_to_bri_neigh_pho	0.0	0.0	0.1	-0.1	-0.1	0.0	0.1	-0.1	-0.1
Mean_diff_to_bri_neigh_TWI	-0.1	-0.1	0.0	-0.1	-0.1	-0.1	-0.1	0.0	-0.3
Mean_diff_to_bri_neigh_var	0.0	-0.1	0.0	0.1	-0.1	0.1	0.2	-0.3	0.1
Mean_diff__to_super_Asp	-0.1	0.0	0.3	0.2	0.3	0.1	0.0	-0.3	0.0
Mean_diff__to_super_Photo	-0.1	0.0	0.0	-0.1	-0.3	-0.2	-0.1	0.0	0.0
Mean_of_sub_stddev_Hom	0.0	0.1	0.0	0.0	-0.1	0.1	0.2	0.0	0.0
Mean_of_sub_stddev_Photo	0.0	0.1	-0.1	0.2	0.1	0.2	0.2	0.0	0.0
Mean_of_sub_stddev_TWI	0.0	0.0	0.0	-0.3	0.0	0.0	0.0	0.1	-0.2
Ratio_to_super_Aspect	0.0	-0.1	0.4	0.8	0.1	-0.1	0.0	0.1	0.5
Ratio_to_super_DEM	0.1	0.0	0.0	0.0	0.1	0.0	-0.3	0.1	0.1
Ratio_to_super_WI	0.2	0.0	0.1	0.0	0.0	0.0	0.1	0.1	0.0
Rel__area_to_super_object	0.0	0.0	-0.1	0.0	0.0	0.0	0.0	-0.1	0.0
Standard_deviation_Aspect	0.0	0.0	0.1	-0.1	0.2	0.4	0.0	0.0	0.1
Standard_deviation_DEM	0.0	0.0	0.0	0.0	0.0	-0.2	0.1	0.1	0.0
Standard_deviation_Entropy	0.0	0.0	0.1	0.0	0.0	0.1	0.1	-0.2	0.0
Standard_deviation_Photo	0.0	0.1	-0.1	0.0	0.1	0.1	0.1	0.1	-0.1

Standard_deviation_TWI	0.1	0.1	0.1	-0.2	0.1	0.1	-0.1	0.1	-0.2
StdDev_Ratio_to_super_Asp	0.0	-0.1	0.1	0.0	0.0	-0.1	0.0	0.0	0.0
StdDev_Ratio_to_super_Cor	0.0	-0.1	0.1	-0.1	-0.2	-0.1	0.1	0.0	0.1
StdDev_Ratio_to_super_DEM	0.1	0.0	0.0	-0.2	0.3	0.0	0.1	0.0	0.0
StdDev_Ratio_to_super_Ent	0.0	0.0	-0.2	0.0	0.0	0.1	0.1	0.1	0.0
StdDev_Ratio_to_super_Ph	0.0	0.0	0.0	0.2	0.0	0.1	-0.1	0.0	0.1
StdDev_Ratio_to_super_TWI	0.5	0.1	-0.1	-0.1	0.0	0.1	0.1	0.2	0.0
StdDev__to_neighbor_Aspec	0.1	0.1	0.1	0.0	0.1	0.1	-0.1	0.0	0.0
StdDev__to_neighbor_Corre	0.0	0.0	0.1	0.0	0.0	0.1	0.0	0.0	0.1
StdDev__to_neighbor_Entro	0.0	0.0	0.2	0.0	0.0	0.0	0.0	-0.1	0.1
StdDev__to_neighbor_Photo	0.0	0.0	0.1	-0.1	0.0	0.0	0.1	-0.1	0.0
StdDev__to_neighbor_Varia	0.0	0.0	0.0	0.1	0.0	0.0	0.1	-0.1	0.1
Stddev_Curvature_main	0.8	-0.2	-0.6	0.1	-0.4	0.5	0.2	0.8	0.7

Size cluster Factor Rank	Riparian Landscapes			Upland Landscapes	
	5	5	4	7	2
Metric #					
Area	0.7	0.7	0.5	-0.3	0.7
Area_of_sub_objects__mean	0.4	0.6	0.4	-0.4	0.5
Area_of_sub_objects__stddev	0.4	0.3	0.4	-0.2	0.5
Asymmetry_of_sub_mean	0.0	-0.1	0.0	0.1	0.0
Asymmetry_of_sub_stddev	0.0	0.1	0.0	0.0	0.2
Avrg__area_segment	0.8	0.8	0.7	-0.5	0.8
Border_length	0.4	0.4	0.0	0.2	0.4
Compactness	-0.3	-0.4	-0.7	0.7	-0.5
Compactness__polygon	0.2	0.3	0.6	-0.7	0.4
Contrast_to_neig_pix_Asp	0.2	0.0	0.0	0.1	0.2
Contrast_to_neig_pix_DEM	-0.1	-0.1	0.0	-0.1	-0.1
Contrast_to_neig_pix_Hom	0.0	0.0	0.2	0.2	0.0
Contrast_to_neig_pix_Ph	0.1	0.0	-0.1	0.0	0.0
Curvature_length	-0.5	-0.6	-0.8	0.6	-0.6
Density_of_sub_stddev	0.1	0.1	0.0	-0.1	0.1
Direction_of_sub_mean	0.0	0.1	0.0	0.0	-0.1
Direction_of_sub_stddev	0.1	0.0	0.0	0.2	0.0
Distance_to_super_obj	-0.1	0.2	-0.2	0.0	0.1
Elliptic_distance_to_super	-0.2	-0.3	-0.1	0.1	-0.3
Is_center_of_super_object	0.0	0.1	0.0	-0.1	0.0
Is_end_of_super_object	0.0	0.0	0.0	-0.1	-0.1
Length_of_longest_edge	0.7	0.5	0.6	-0.1	0.5
Length_Width	-0.1	-0.1	-0.2	0.2	-0.2
Main_direction	0.0	0.1	0.0	-0.1	0.0
Mean_Aspect	0.0	0.0	0.0	0.1	0.1
Mean_DEM	0.0	-0.1	0.2	0.1	-0.3
Mean_Diff__to_neig_DEM	-0.2	-0.3	0.1	0.1	-0.1
Mean_Diff__to_neig_Photo	-0.1	-0.1	-0.1	0.1	-0.1
Mean_Photo	-0.2	-0.3	-0.1	0.0	-0.1
Mean_TWI	0.0	-0.1	-0.2	0.1	0.0
Mean_diff_to_bri_neigh_asp	0.1	0.0	0.1	0.0	0.1
Mean_diff_to_bri_neigh_DEM	0.1	0.0	-0.1	0.0	-0.2
Mean_diff_to_bri_neigh_hom	-0.1	-0.2	-0.3	-0.1	-0.3
Mean_diff_to_bri_neigh_ph	-0.1	-0.1	-0.2	0.0	-0.2
Mean_diff_to_bri_neigh_TWI	0.0	0.0	0.0	0.1	0.1

Mean_diff_to_bri_neigh_var	-0.2	-0.1	0.0	0.4	-0.2
Mean_diff_to_super_Asp	0.1	0.0	0.0	0.0	-0.2
Mean_diff_to_super_Ph0	-0.1	0.1	0.1	0.0	0.0
Mean_of_sub_stddev_Hom	0.1	0.0	0.0	-0.1	0.0
Mean_of_sub_stddev_Ph0t	0.1	0.0	0.1	-0.1	0.0
Mean_of_sub_stddev_TWI	0.0	0.1	0.1	0.2	0.1
Ratio_to_super_Aspect	0.2	0.1	0.0	0.0	0.1
Ratio_to_super_DEM	0.0	0.0	-0.1	0.1	-0.1
Ratio_to_super_WI	-0.1	-0.1	0.1	0.0	-0.1
Rel_area_to_super_object	0.2	0.2	0.2	-0.1	0.2
Standard_deviation_Aspect	0.0	0.1	-0.1	-0.1	-0.1
Standard_deviation_DEM	0.0	0.0	0.0	0.0	-0.2
Standard_deviation_Entropy	-0.1	0.0	0.2	0.1	-0.1
Standard_deviation_Ph0t	0.0	0.0	-0.1	-0.3	0.0
Standard_deviation_TWI	0.0	-0.1	0.1	0.1	0.0
StdDev_Ratio_to_super_Asp	0.1	0.1	0.0	-0.1	0.0
StdDev_Ratio_to_super_Cor	0.0	-0.1	-0.1	0.1	0.0
StdDev_Ratio_to_super_DEM	0.1	0.1	0.0	0.0	0.1
StdDev_Ratio_to_super_Ent	0.1	0.1	0.2	0.1	0.0
StdDev_Ratio_to_super_Ph0	0.1	0.1	0.0	-0.4	0.1
StdDev_Ratio_to_super_TWI	0.0	0.1	0.0	0.0	-0.1
StdDev_to_neighbor_Aspec	0.3	0.2	0.1	-0.1	0.2
StdDev_to_neighbor_Corre	-0.1	-0.1	0.1	0.2	0.0
StdDev_to_neighbor_Entro	-0.1	-0.1	0.0	0.1	-0.1
StdDev_to_neighbor_Ph0t	-0.1	-0.2	-0.3	0.0	-0.1
StdDev_to_neighbor_Varia	-0.1	-0.1	0.0	0.2	-0.1
Stddev_Curvature_main	0.0	0.2	0.2	-0.1	0.1

Site cluster Factor Rank	Riparian Landscapes			Upland Landscapes	
	2	1	3	11	
Area	-0.1	-0.1	-0.1		-0.1
Area_of_sub_objects__mean	0.0	-0.1	-0.2		-0.2
Area_of_sub_objects__stddev	0.0	0.0	0.0		-0.1
Asymmetry_of_sub_mean	0.1	0.1	0.2		0.0
Asymmetry_of_sub_stddev	-0.1	0.0	0.0		0.1
Avrg__area_segment	0.1	0.1	-0.2		-0.1
Border_length	-0.1	-0.1	0.0		-0.1
Compactness	0.1	0.2	0.1		-0.2
Compactness__polygon	0.1	0.0	0.0		0.0
Contrast_to_neig_pix_Asp	0.0	0.1	-0.1		0.3
Contrast_to_neig_pix_DEM	0.1	-0.2	-0.1		0.0
Contrast_to_neig_pix_Hom	-0.1	0.0	-0.1		-0.1
Contrast_to_neig_pix_Ph0t	0.0	0.1	-0.1		-0.1
Curvature_length	0.0	0.1	0.1		0.0
Density_of_sub_stddev	0.0	0.1	0.1		0.0
Direction_of_sub_mean	-0.1	-0.3	0.1		0.0
Direction_of_sub_stddev	-0.1	0.0	-0.1		0.1
Distance_to_super_obj	0.0	0.1	0.1		0.0
Elliptic_distance_to_super	0.0	0.3	0.0		-0.1
Is_center_of_super_object	0.0	0.0	-0.1		0.0
Is_end_of_super_object	-0.1	0.0	0.1		0.0
Length_of_longest_edge	0.1	0.4	-0.1		-0.1

Length_Width	0.1	0.1	0.2	0.1
Main_direction	-0.1	-0.2	0.1	0.1
Mean_Aspect	0.0	0.0	0.0	-0.1
Mean_DEM	-0.7	-0.7	-0.7	0.5
Mean_Diff__to_neig_DEM	-0.2	-0.2	-0.3	0.1
Mean_Diff__to_neig_Photo	0.1	0.1	0.1	0.0
Mean_Photo	0.2	0.1	-0.1	0.0
Mean_TWI	0.8	0.7	0.8	-0.6
Mean_diff_to_bri_neigh_asp	0.1	0.2	-0.1	0.0
Mean_diff_to_bri_neigh_DEM	-0.7	-0.7	-0.4	0.6
Mean_diff_to_bri_neigh_hom	0.3	0.4	0.4	0.1
Mean_diff_to_bri_neigh_pho	0.3	0.3	0.3	0.1
Mean_diff_to_bri_neigh_TWI	0.0	0.6	-0.2	0.0
Mean_diff_to_bri_neigh_var	0.1	0.3	0.5	0.0
Mean_diff__to_super_Asp	0.0	0.0	0.0	-0.2
Mean_diff__to_super_Pho	0.0	0.0	0.0	0.0
Mean_of_sub_stddev_Hom	0.2	0.2	0.0	0.0
Mean_of_sub_stddev_Photo	0.0	0.1	0.0	0.0
Mean_of_sub_stddev_TWI	0.0	0.5	0.1	-0.1
Ratio_to_super_Aspect	0.0	0.0	0.0	0.2
Ratio_to_super_DEM	0.0	-0.1	-0.1	-0.1
Ratio_to_super_WI	0.2	0.2	0.1	-0.1
Rel__area_to_super_object	0.0	0.0	0.2	0.1
Standard_deviation_Aspect	0.5	0.7	0.0	-0.3
Standard_deviation_DEM	-0.8	-0.8	-0.6	0.7
Standard_deviation_Entropy	0.5	0.1	0.4	-0.1
Standard_deviation_Photo	0.0	0.0	-0.2	0.0
Standard_deviation_TWI	0.1	0.8	0.0	-0.3
StdDev_Ratio_to_super_Asp	-0.1	0.0	0.1	0.1
StdDev_Ratio_to_super_Cor	0.0	0.0	-0.1	0.0
StdDev_Ratio_to_super_DEM	0.0	-0.1	0.0	0.1
StdDev_Ratio_to_super_Ent	-0.1	-0.1	0.0	-0.4
StdDev_Ratio_to_super_Photo	-0.1	-0.1	0.0	-0.2
StdDev_Ratio_to_super_TWI	-0.1	0.0	0.0	0.0
StdDev__to_neighbor_Aspec	0.3	0.6	-0.2	-0.1
StdDev__to_neighbor_Corre	-0.2	-0.4	-0.4	0.1
StdDev__to_neighbor_Entro	0.7	0.6	0.7	0.1
StdDev__to_neighbor_Photo	0.3	0.5	0.6	0.1
StdDev__to_neighbor_Varia	0.0	0.0	0.0	0.2
Stddev_Curvature_main	0.0	-0.1	-0.1	0.1